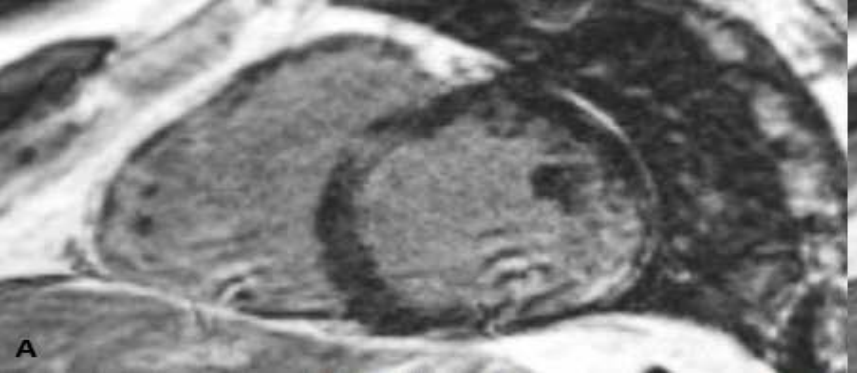

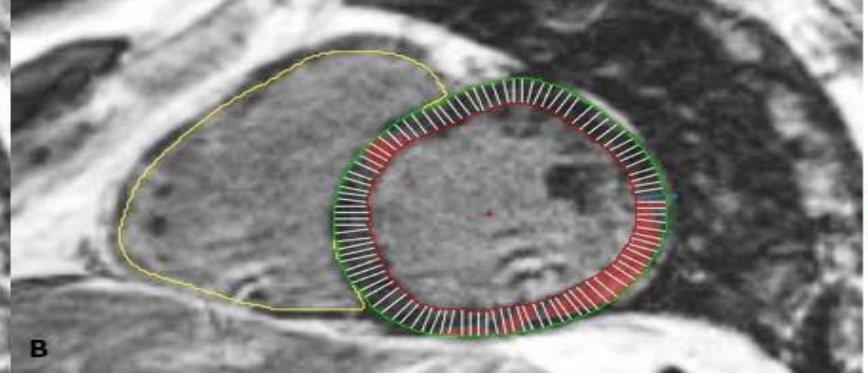

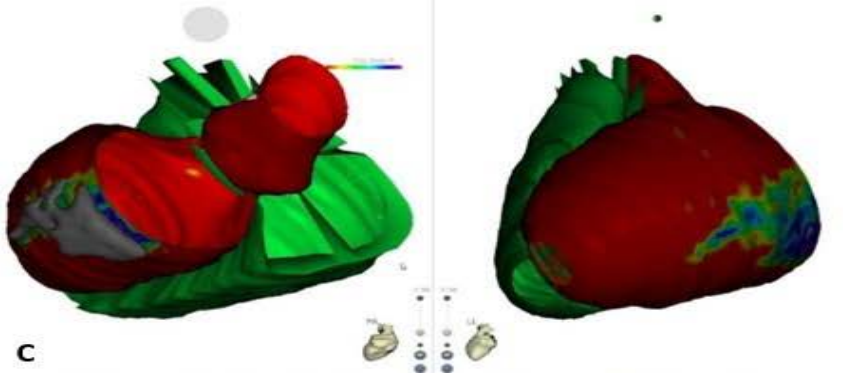

MRI image integration in VT substrate ablation

Mediplex Sejong Hospital
Jaeseok Park, MD.

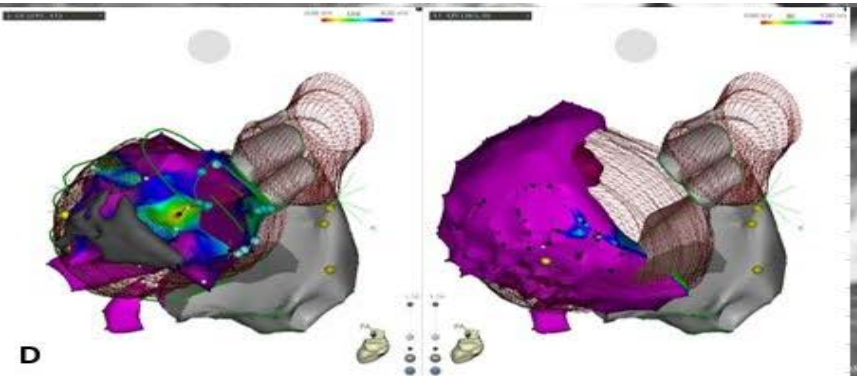

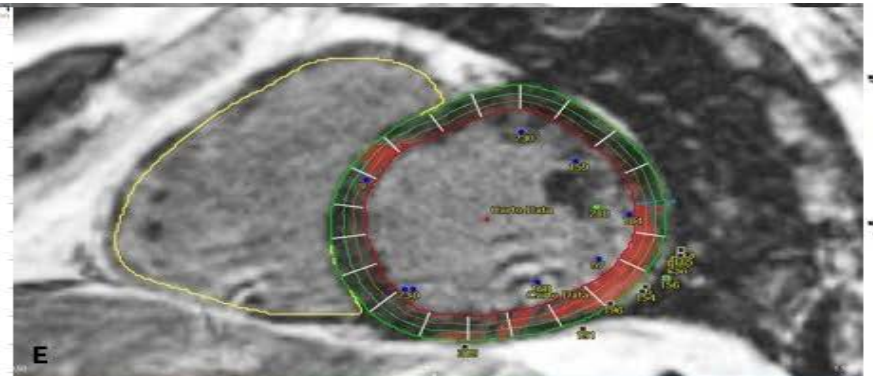

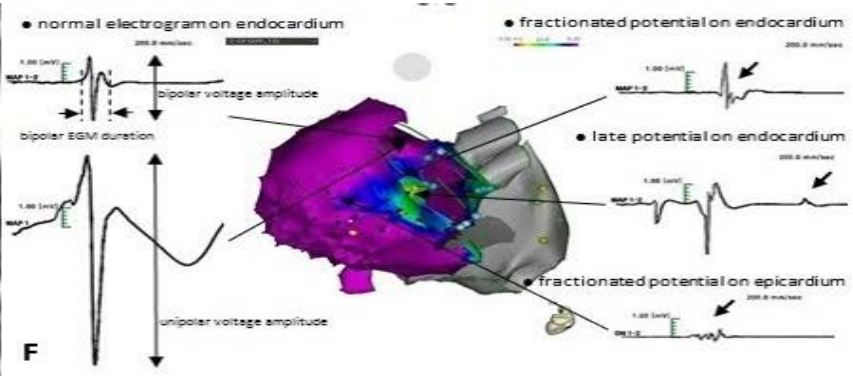

Outcome & survival benefit of VT ablation

Freedom from recurrent ventricular tachycardia after catheter ablation is associated with improved survival in patients with structural heart disease: An International VT Ablation Center Collaborative Group study

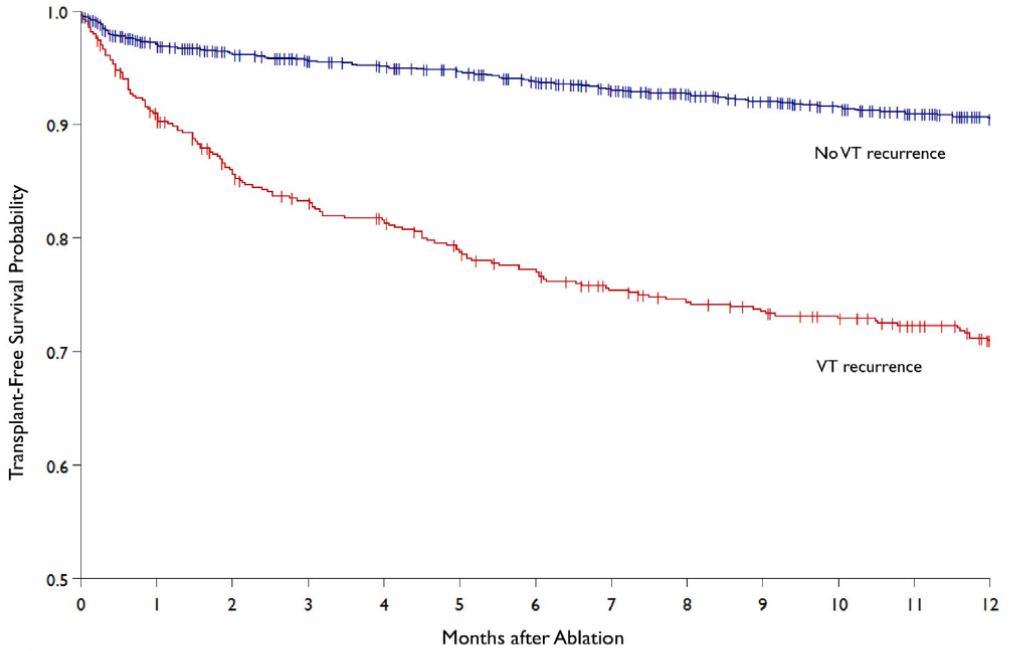

Kaplan–Meier display of transplant-free survival between patients with and without ventricular tachycardia (VT) recurrence.

- 2061 patients with structural heart disease
- 12 international centers
- One-year freedom from VT recurrence was 70% (72%in ischemic & 68% in NICM)
- At 1 year, the estimated rate of transplant and/or mortality was 15%.
- Transplant-free survival was significantly higher in patients without VT recurrence than in those with recurrence (90% vs 71%, P<.001).
- In multivariable analysis, the recurrence of VT after ablation showed the highest risk for transplant and/or mortality [hazard ratio 6.9].

Heart Rhythm 2015;12:1997-2007

Acute Hemodynamic Decompensation During Catheter Ablation of Scar-Related Ventricular Tachycardia

Incidence, Predictors, and Impact on Mortality

Pasquale Santangeli, MD; Daniele Muser, MD; Erica S. Zado, PA-C; Silvia Magnani, MD; Sumun Khetpal, MS; Mathew D. Hutchinson, MD; Gregory Supple, MD; David S. Frankel, MD; Fermin C. Garcia, MD; Rupa Bala, MD; Michael P. Riley, MD, PhD; David Lin, MD; J. Eduardo Rame, MD; Robert Schaller, DO; Sanjay Dixit, MD; Francis E. Marchlinski, MD; David J. Callans, MD

- 193 patients undergoing RFCA of scar-related VT
- AHD occurred in 22 (11%) patients
- At 21±7 months, higher mortality rate in the AHD group compared with the rest (50% vs. 11%, log-rank P<0.001)

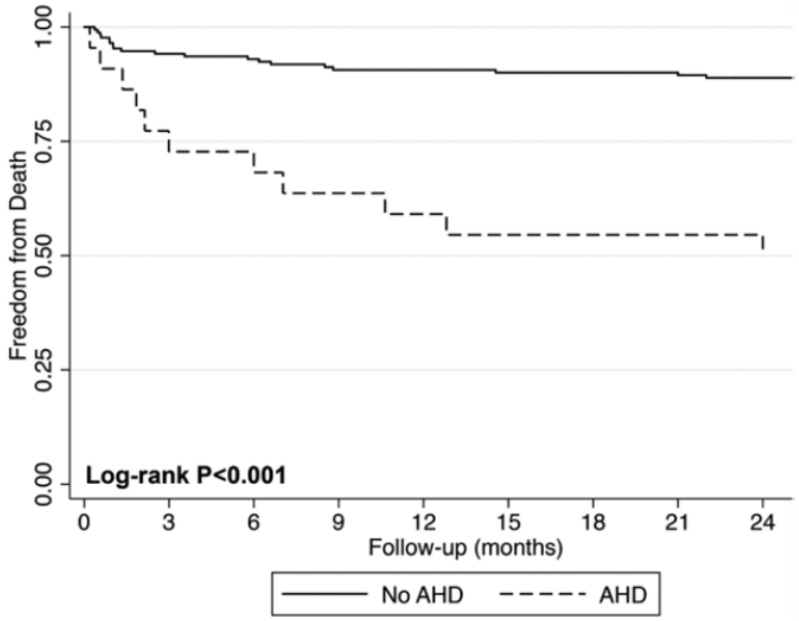

Figure 1. Kaplan–Meier survival curve showing freedom from death in patients experiencing periprocedural acute hemodynamic decompensation (AHD) compared with the rest of the population.

Table 3. Predictors of Periprocedural Acute Hemodynamic Decompensation (AHD) at Univariate Logistic Regression Analysis

Variable	OR	95% CI	*P* Value
Clinical data			
Age >60 y	3.24	1.07–9.82	0.037
Male sex	3.71	0.48–28.50	0.208
Diabetes mellitus	2.81	1.15–6.90	0.024
COPD*	5.46	2.24–13.33	<0.001
OSAS	0.51	0.07–4.00	0.521
PAD	0.58	0.07–4.62	0.609
Creatinine ≥1.5 mg/dL	0.98	0.37–2.58	0.961
BUN, mmol/L	1.01	0.97–1.05	0.705
Systolic blood pressure, mm Hg	0.99	0.96–1.03	0.737
Ischemic cardiomyopathy	6.26	1.81–21.62	0.004
NYHA class III/IV	6.11	2.53–14.75	<0.001
VT storm	5.12	1.84–14.22	0.002
Echocardiographic data			
LVEF <25%	3.00	1.27–7.07	0.012
LVEDD, mm	1.02	0.98–1.07	0.311
RV dysfunction (moderate/severe)	1.34	0.50–3.58	0.558
Therapy			
Beta-blockers	2.87	0.37–22.26	0.312
ACE-I/ARB	2.10	0.69–6.40	0.190
Diuretics	2.05	0.82–5.16	0.125
Spironolactone	0.68	0.24–1.91	0.470
CRT-D	1.12	0.48–2.64	0.791
Procedural data			
General anesthesia	3.56	1.50–8.44	0.004
No. of VT induced	0.99	0.79–1.25	0.929
VT cycle length, ms†	1.00	0.99–1.01	0.228
Radiofrequency time, min	1.00	0.99–1.02	0.735
Procedural time, hours	0.97	0.78–1.22	0.803

Santangeli et al. Circ Arrhythm Electrophysiol 2015;8:68-75

Substrate ablation approaches for unstable VT

Study	Year	No. of patients	Type of substrate	LVEF (%)	End-point assessed (% achieved)	EPI mapping/ ablation	RF duration (lesions or min)	Follow-up (months)	VT recurre
Linear ablation lesions									
Marchlinski et al[26]	2000	16	9 ICM, 7 NICM	32 ± 15				(3–36)	25%
Soejima et al[47]	2001	40	ICM	29 ± 10				± 6	47%
Reddy et al[1]	2007	64	ICM					± 8	12%
Ablation of late potentials									
Arenal et al[9]	2003	24	21 ICM, 2 NICM, 1 ToF	30 ± 9				± 4	21%
Volkmer et al[19]	2006	25	ICM	30 ± 8				±	
Nogami et al[16]	2008	18	ARVC	NR				±	
Garcia et al[14]	2009	13	ARVC	NR				±	
Bai et al[11]	2011	26	ARVC	53 ± 10				±	
Vergara et al[18]	2012	50	36 ICM, 14 NICM	32 ± 9 ICM; 36 ± 10 NICM	Elimination of LPs (84%)	Yes	NR	13 ±	
Arenal et al[10]	2013	59	ICM					±	
Ablation of LAVA									
Jais et al[15]	2012	70	56 ICM, 14 NICM					(14	
Scar homogenization									
Di Biase et al[13]	2012	43	ICM					(19	
Ablation of interconnected channels (scar dechanneling)									
Berruezo et al[12]	2012	11	ARVC					(6-	
Tung et al[17]	2013	21	15 ICM, 2 NICM, 2 ARVC, 1 sarc noncompaction, 1 Chagas					(6-	
Berruezo et al[21]	2015	101	75 ICM, 26 NICM						
Core isolation of critical substrate elements									
Tzou et al[20]	2015	44	32 ICM, 12 NICM					±	

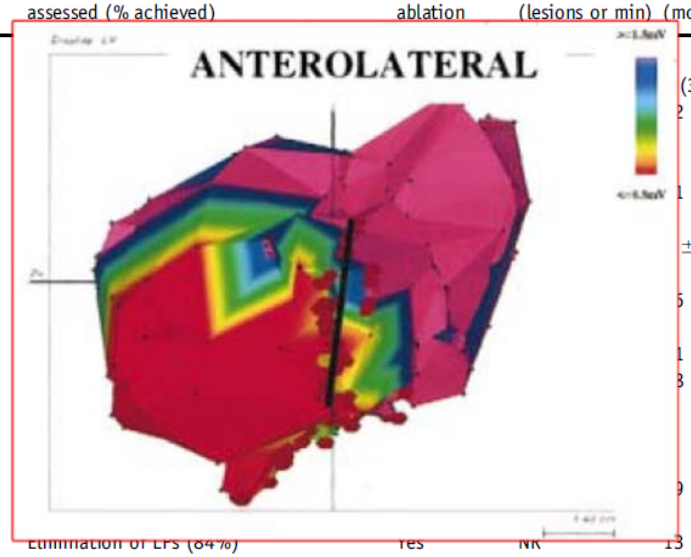

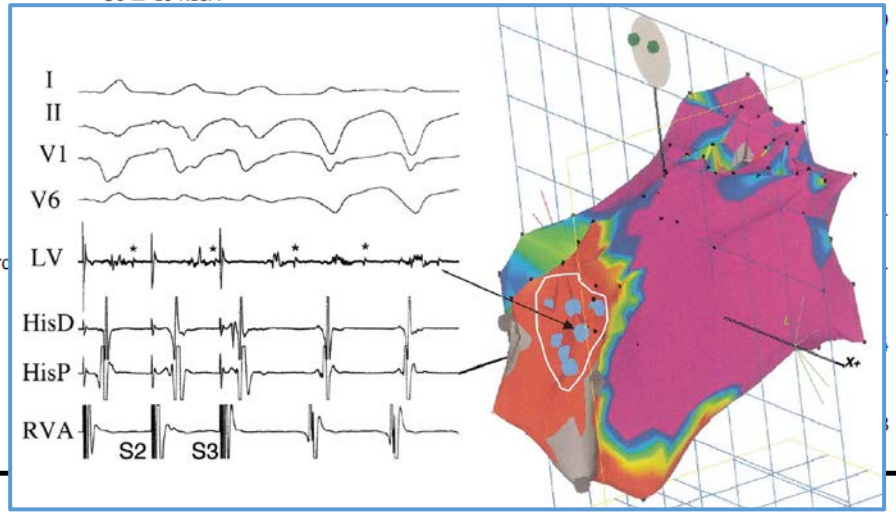

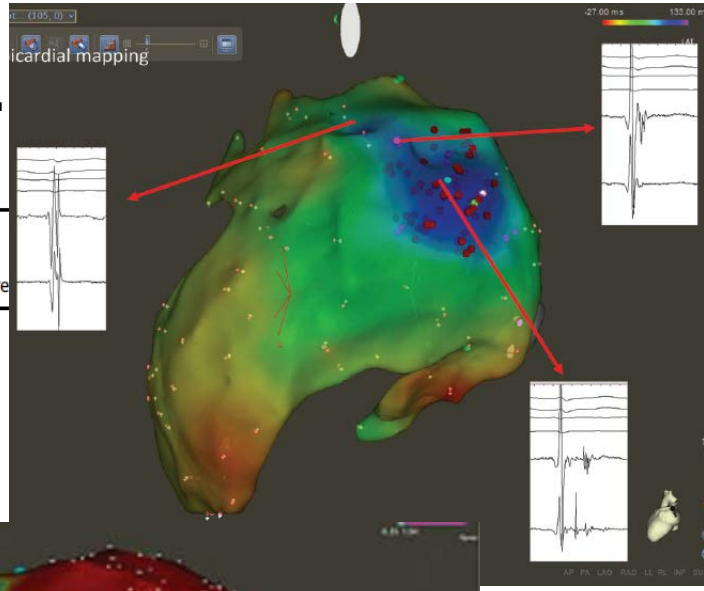

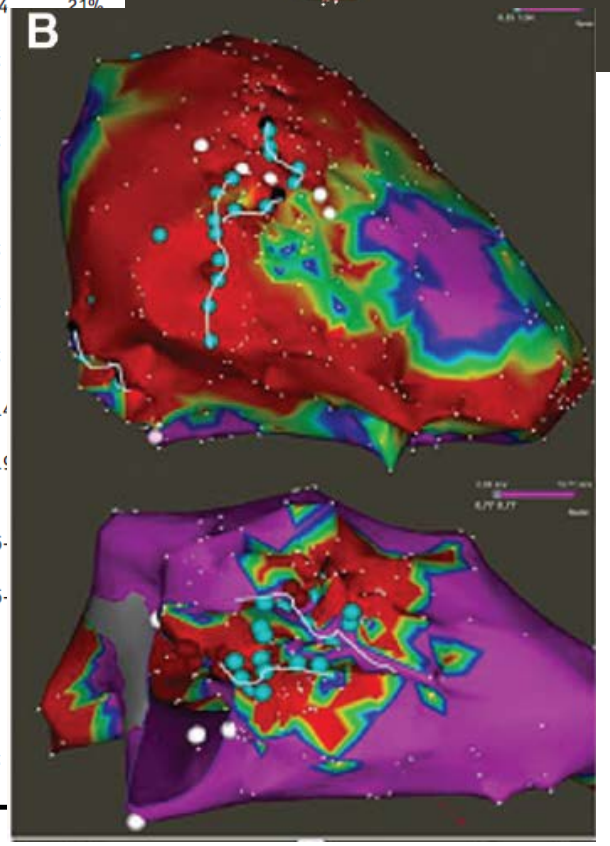

Santangeli et al. Heart Rhythm 2016;569-583

Limitations of 3D-Electroanatomic mapping

- Careful electroanatomic mapping (EAM) to delineate 3D distribution of the substrate (scar area & late potentials) is critical to guide entrainment maneuvers and ablation.
- However, the accuracy of EAM for precise scar delineation is limited due to catheter contact and orientation, or mapping density.
- Therefore, development of techniques to visualize the substrate would be of clinical value.
- The use of late gadolinium enhancement (LGE) CMR to detect myocardial fibrosis and its arrhythmic substrate has been well established.

Differentiation between ischemic & NICM

- The pattern of fibrosis differs greatly from those found in ischemic heart disease, and varies between non-ischemic pathologies.
- Wu et al. were the first to report that LGE-CMR may hold promise in differentiating ischemic from NICM. Nearly all patients with ischemic heart disease & prior MI had LGE.
- LGE was present in 25-71% of NICM patients & in almost all ICM patients shown in a meta-analysis.

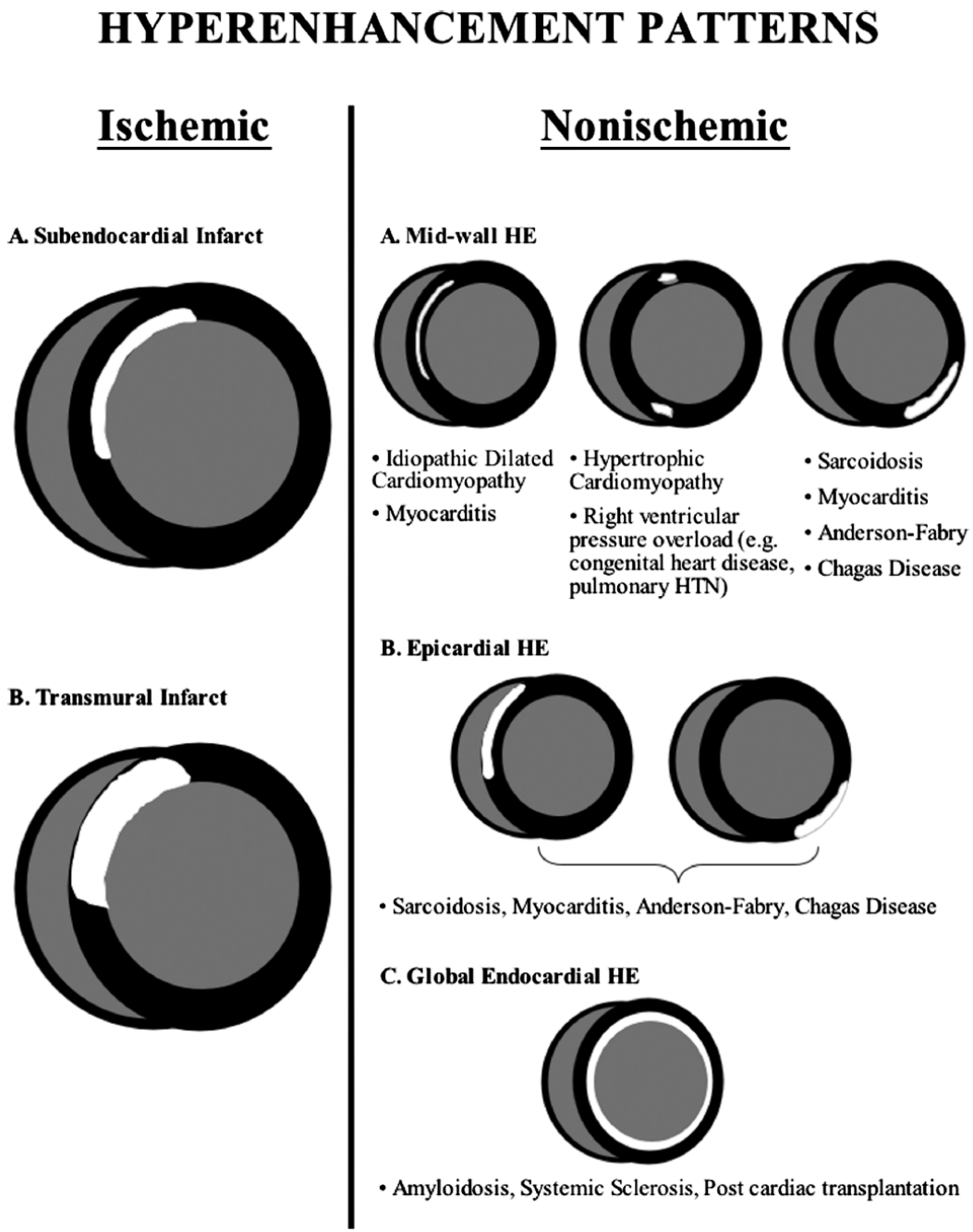

Mahrholdt et al. Eur. Heart J. 2005;26:1461-1474

ORIGINAL ARTICLE

Safety of Magnetic Resonance Imaging in Patients with Cardiac Devices

Saman Nazarian, M.D., Ph.D., Rozann Hansford, R.N., M.P.H., Amir A. Rahsepar, M.D., Valeria Weltin, M.S., Diana McVeigh, B.S., Esra Gucuk Ipek, M.D., Alan Kwan, M.D., Ronald D. Berger, M.D., Ph.D., Hugh Calkins, M.D., Albert C. Lardo, Ph.D., Michael A. Kraut, M.D., Ph.D., Ihab R. Kamel, M.D., Ph.D., Stefan L. Zimmerman, M.D., and Henry R. Halperin, M.D.

METHODS

We performed a prospective, nonrandomized study to assess the safety of MRI at a magnetic field strength of 1.5 Tesla in 1509 patients who had a pacemaker (58%) or an implantable cardioverter–defibrillator (42%) that was not considered to be MRI-conditional (termed a "legacy" device). Overall, the patients underwent 2103 thoracic and nonthoracic MRI examinations that were deemed to be clinically necessary. The pacing mode was changed to asynchronous mode for pacing-dependent patients and to demand mode for other patients. Tachyarrhythmia functions were disabled. Outcome assessments included adverse events and changes in the variables that indicate lead and generator function and interaction with surrounding tissue (device parameters).

RESULTS

No long-term clinically significant adverse events were reported. In nine MRI examinations (0.4%; 95% confidence interval, 0.2 to 0.7), the patient's device reset to a backup mode. The reset was transient in eight of the nine examinations. In one case, a pacemaker with less than 1 month left of battery life reset to ventricular inhibited pacing and could not be reprogrammed; the device was subsequently replaced. The most common notable change in device parameters (>50% change from baseline) immediately after MRI was a decrease in P-wave amplitude, which occurred in 1% of the patients. At long-term follow-up (results of which were available for 63% of the patients), the most common notable changes from baseline were decreases in P-wave amplitude (in 4% of the patients), increases in atrial capture threshold (4%), increases in right ventricular capture threshold (4%), and increases in left ventricular capture threshold (3%). The observed changes in lead parameters were not clinically significant and did not require device revision or reprogramming.

- No long-term significant adverse events.
- No requirement of revision.
- The patient's device reset to a backup mode in 9 MRI examinations (0.4%). The reset was transient in 8 of the 9 examinations. In one case, a pacemaker with less than 1 month left of battery life reset to ventricular inhibited pacing; the device was replaced.
- The m/c change immediately after MRI: decrease in P-wave amplitude (in 1%).
- At long-term follow-up, the m/c changes: decreases in P-wave amplitude (in 4%), increases in atrial capture threshold (in 4%), increases in RV capture threshold (in 4%), increases in LV capture threshold (in 3%).

Nazarian et al. NEJM. 2017;377:2555-2564

THE USE OF CONTRAST-ENHANCED MAGNETIC RESONANCE IMAGING TO IDENTIFY REVERSIBLE MYOCARDIAL DYSFUNCTION

RAYMOND J. KIM, M.D., EDWIN WU, M.D., ALLEN RAFAEL, M.D., ENN-LING CHEN, PH.D., MICHELE A. PARKER, M.S., ORLANDO SIMONETTI, PH.D., FRANCIS J. KLOCKE, M.D., ROBERT O. BONOW, M.D., AND ROBERT M. JUDD, PH.D.

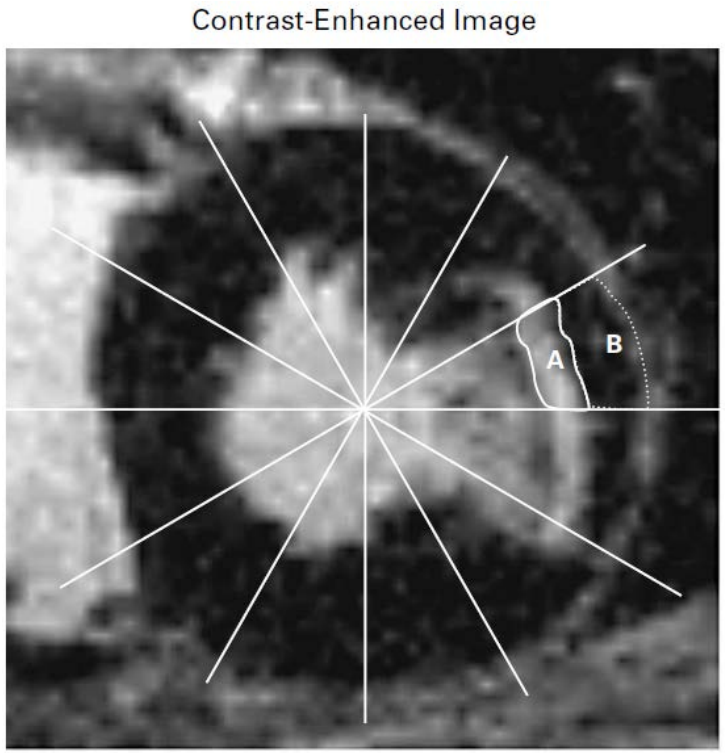

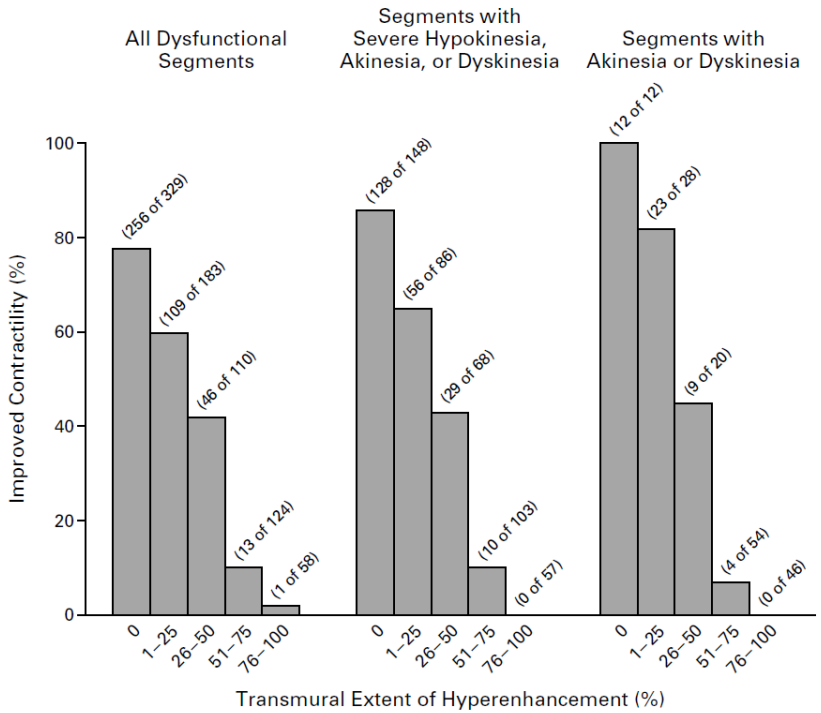

Raymond J. Kim et al. NEJM. 2000;343:1445-53

Impact of Unrecognized Myocardial Scar Detected by Cardiac Magnetic Resonance Imaging on Event-Free Survival in Patients Presenting With Signs or Symptoms of Coronary Artery Disease

Raymond Y. Kwong, MD, MPH; Anna K. Chan, MBBS; Kenneth A. Brown, MD; Carmen W. Chan, MBBS; H. Glenn Reynolds, MSc; Sui Tsang, BS; Roger B. Davis, ScD

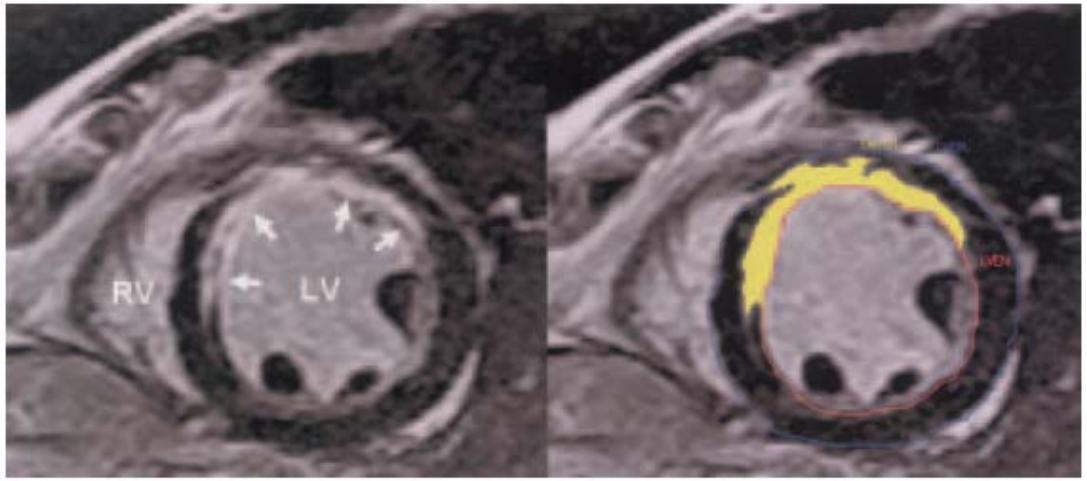

LGE defined as any region with SI > 2SD above a remote normal myocardial region

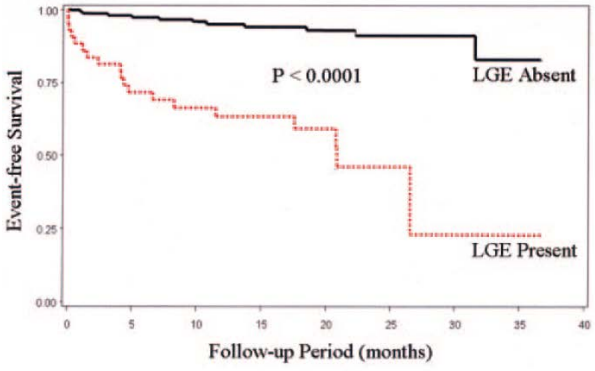

MACE

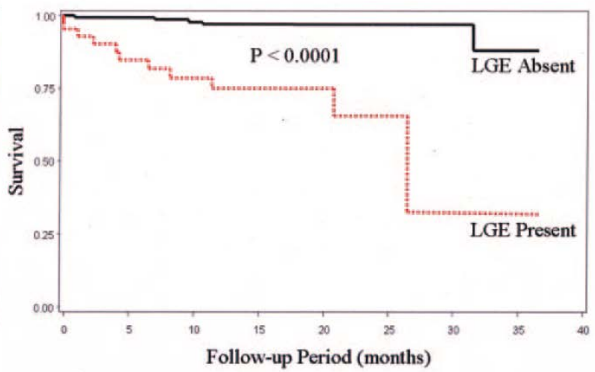

Cardiac mortality

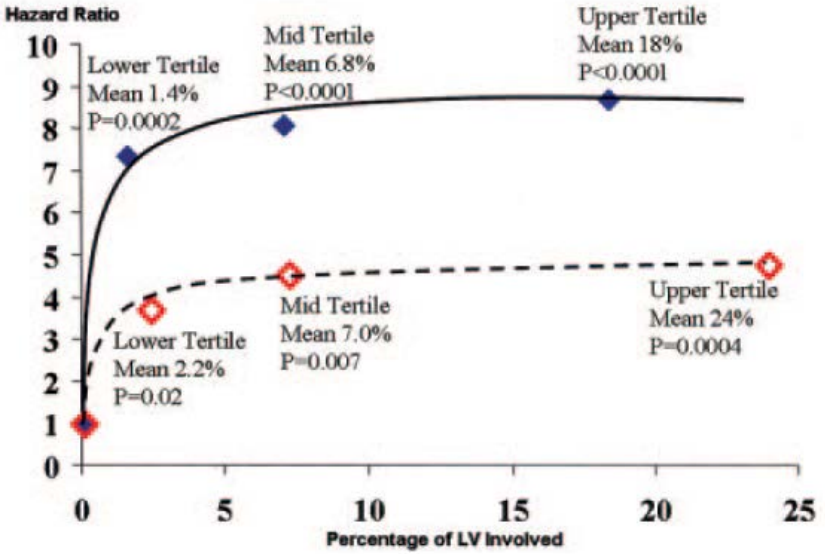

Figure 5. LGE% and WMS% in tertiles and HR for MACE.

TABLE 4. Best Overall Multivariable Cox Proportional-Hazards Regression Models for All MACE and Cardiac Mortality, When All Variables Were Considered

	HR (95% CI)	*P*
MACE (LR χ^2 for model=33.74)		
Presence of LGE	5.98 (2.68-13.3)	<0.0001
Angiographically significant coronary stenosis at study completion*	2.43 (1.11-5.32)	0.03
Cardiac mortality (LR χ^2 for model=21.15)		
Presence of LGE	9.43 (3.15-28.3)	<0.0001
MI by noninvasive stress imaging*	3.00 (0.91-9.90)	0.07

Kwong et al. Circulation. 2006;113:2733-2743

Infarct Tissue Heterogeneity Assessed With Contrast-Enhanced MRI Predicts Spontaneous Ventricular Arrhythmia in Patients With Ischemic Cardiomyopathy and Implantable Cardioverter-Defibrillator

Stijntje D. Roes, MD; C. Jan Willem Borleffs, MD; Rob J. van der Geest, MSc; Jos J.M. Westenberg, PhD; Nina Ajmone Marsan, MD; Theodorus A.M. Kaandorp, MD; Johan H.C. Reiber, PhD; Katja Zeppenfeld, MD; Hildo J. Lamb, MD; Albert de Roos, MD; Martin J. Schalij, MD; Jeroen J. Bax, MD

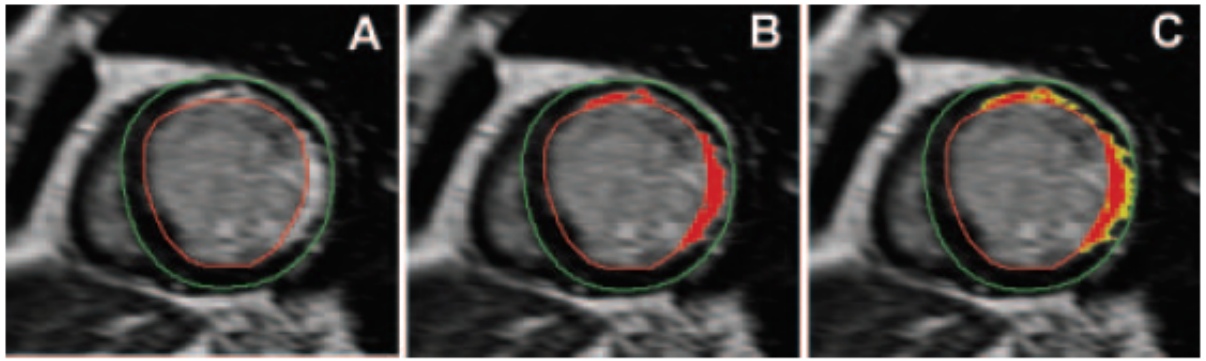

Figure 1. Assessment of the infarct gray zone: Short-axis contrast-enhanced MRI of a patient with a previous MI. A, Endocardial (red) and epicardial (green) borders were outlined manually. Subsequently, the maximum signal intensity (SI) within the infarct region was determined. B, The infarct core was defined as myocardium with SI ≥50% of the maximum SI (red area). C, The infarct gray zone was defined as myocardium with SI ≥35% but with SI <50% of the maximum SI (yellow area).

Table 4. Univariable Analysis of MRI Variables for Prediction of Appropriate ICD Therapy

	HR	95% CI	χ^2	*P* Value
LVEF	0.53/10%	0.27–1.04	3.4	0.06
LV EDV	1.00/10 mL	0.95–1.04	0.0	0.9
LV ESV	1.00/10 mL	0.97–1.05	0.2	0.7
LV mass	0.97/10 g	0.86–1.11	0.2	0.7
Total infarct size (infarct core+gray zone)	1.15/10 g	0.99–1.33	3.4	0.06
Infarct core	1.10/10 g	0.87–1.37	0.6	0.4
Infarct gray zone	1.56/10 g	1.14–2.14	7.6	0.006

Table 5. Multivariable Cox Proportional Hazards Model for Prediction of Appropriate ICD Therapy

	HR	95% CI	χ^2	*P* Value
LVEF	0.72/10%	0.32–1.64	0.6	0.4
Infarct gray zone	1.49/10 g	1.01–2.20	4.0	0.04
Infarct core	0.92/10 g	0.69–1.22	0.3	0.6

Roes et al. Circ CV Img. 2009;2:183-190

Magnetic Resonance Assessment of the Substrate for Inducible Ventricular Tachycardia in Nonischemic Cardiomyopathy

Saman Nazarian, MD; David A. Bluemke, MD, PhD; Albert C. Lardo, PhD; Menekhem M. Zviman, PhD; Stanley P. Watkins, MD, MPH; Timm L. Dickfeld, MD, PhD; Glenn R. Meininger, MD; Ariel Roguin, MD, PhD; Hugh Calkins, MD; Gordon F. Tomaselli, MD; Robert G. Weiss, MD; Ronald D. Berger, MD, PhD; João A.C. Lima, MD; Henry R. Halperin, MD, MA

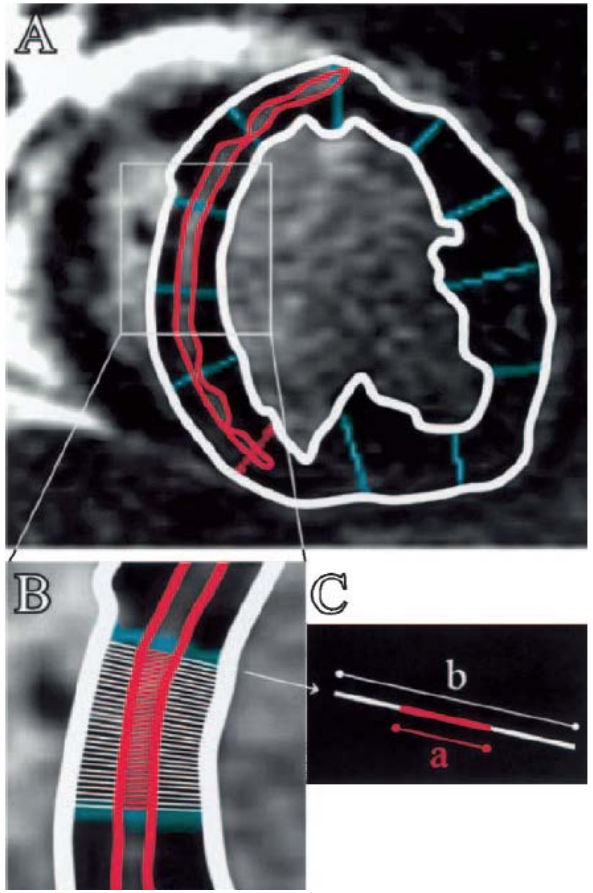

- **Methods:** The transmural extent of scar as percentage of wall thickness was calculated manually after tracing.
- **Results:** Predominance of scar distribution involving 26%-75% of wall thickness was significantly predictive of inducible VT, and remained independently predictive in the multivariable model after adjustment for LVEF (odds ratio, 9.125; *P*=0.020).
- *Conclusions*—MR assessment of scar distribution can identify the substrate for inducible VT and may identify high-risk patients with NICM.

TABLE 2. MRI Parameters and Comparison After Stratification by Inducibility at Electrophysiological Study*

		Electrophysiological Study		
	All Patients (n=26)	Inducible (n=5)	Noninducible (n=21)	*P*
Left ventricular ejection fraction, %	27 (17–43)	16 (13–29)	29 (19–44)	0.18
Left ventricular end-diastolic volume, mL	201 (129–273)	159 (154–273)	205 (129–259)	0.72
Left ventricular mass, g	153 (113–192)	184 (160–197)	144 (113–189)	0.38
Patients with scar, n (%)	17 (65)	5 (100)	12 (57)	0.13
Scar volume, %	4.6 (0.8–7.2)	6.0 (5.7–7.2)	1.5 (0.7–6.3)	0.09
Predominant scar distribution involving 26%–75% of wall thickness, n (%)	6 (23)	5 (100)	1 (5)	<0.001

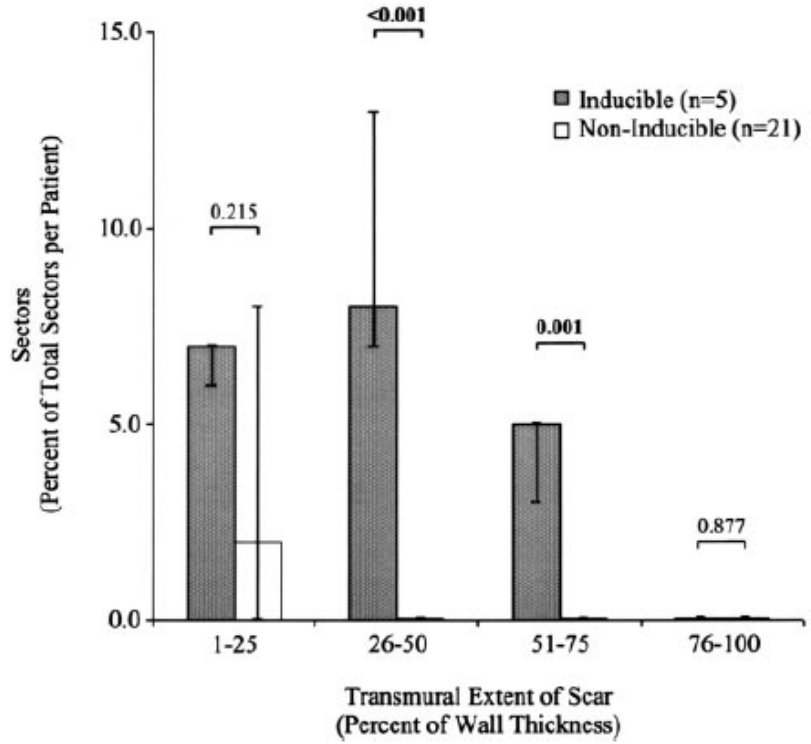

Nazarian et al. Circulation. 2005;112:2821-2825

Late Gadolinium Enhancement by Cardiovascular Magnetic Resonance Heralds an Adverse Prognosis in Nonischemic Cardiomyopathy

Katherine C. Wu, MD, FACC,* Robert G. Weiss, MD,*‡ David R. Thiemann, MD,*§
Kakuya Kitagawa, MD,* André Schmidt, MD,* Darshan Dalal, MD,* Shenghan Lai, MD, PHD,†
David A. Bluemke, MD, PHD,*‡ Gary Gerstenblith, MD, FACC,* Eduardo Marbán, MD, PHD, FACC,*
Gordon F. Tomaselli, MD, FACC, João A. C. Lima, MD, FACC*‡

Baltimore, Maryland

- 65 NICM patients underwent CMR before ICD implantation for primary prevention.

Table 2 Number of Index and Cumulative Events Grouped by Presence or Absence of CMR LGE

Variable	LGE Absent by CMR (n = 38)	LGE Present by CMR (n = 27)
Number of patients who experienced an index composite outcome*	3 (8%)	12 (44%)
HF hospitalization	0	8
Appropriate ICD firing	3	4
Cardiac death	0	0
Cumulative number of events over the follow-up period	3	25
HF hospitalization	0	13
Appropriate ICD firing	3	9
Cardiac death	0	3

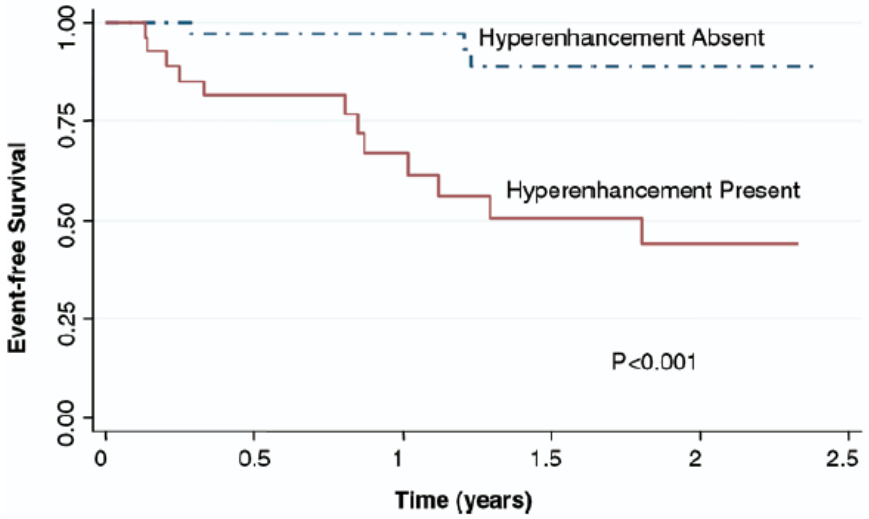

- After adjustment for LV volume index & functional class, patients with LGE had an 8-fold higher risk of adverse composite outcome (HR 8.2).

- CMR LGE in NICM strongly predicted adverse cardiac outcomes.

Wu et al. JACC. 2008;51:2412-21

JACC: CARDIOVASCULAR IMAGING
© 2016 BY THE AMERICAN COLLEGE OF CARDIOLOGY FOUNDATION
PUBLISHED BY ELSEVIER
VOL. 9, NO. 9, 2016
ISSN 1936-878X/$36.00
http://dx.doi.org/10.1016/j.jcmg.2016.01.033

Myocardial Fibrosis Assessment by LGE Is a Powerful Predictor of Ventricular Tachyarrhythmias in Ischemic and Nonischemic LV Dysfunction

A Meta-Analysis

19 studies enrolling 2850 patients with ICM & NICM with 423 arrhythmic events mean follow-up of 2.8 years.
Arrhythmic outcomes (SCD, aborted SCD, VT, VF, and appropriate ICD therapy)

TABLE 3 Tachyarrhythmic Event Rate and Odds Ratio in the Different Subgroups of Studies

	Studies	Patients	% AER	LGE-CMR % of LGE+ AER*	LGE-CMR % LGE− AER*	OR (95% CI)	p Value
Total	19	2,850	5.3	8.6	1.7	5.62 (4.20-7.51)	<0.00001
ICM	5	358	8.9	13.2	3.3	5.05 (2.73-9.36)	<0.00001
NICM	8	1,443	3.7	7.6	1.3	6.27 (4.15-9.47)	<0.00001
Mixed population	6	1,049	6.8	8.8	1.8	4.92 (2.70-8.98)	<0.00001
Mean EF ≤30%	11	1,178	6.6	10.3	1.2	9.56 (5.63-16.23)	<0.00001
Mean EF >30%	8	1,672	4.6	7.4	2.0	4.48 (3.17-6.33)	<0.00001

Values are n or %. *LGE+/− test results based on the criteria reported in Table 1.
AER = annualized event rate; ICM = ischemic cardiomyopathy; NICM = nonischemic cardiomyopathy; OR = odds ratio; other abbreviations as in Table 1.

TABLE 1 Characteristics of the 19 Selected Studies, Subgrouped According to Cardiomyopathy Etiology

First Author (Ref. #)	Year	Patients (n)	Follow-Up (Months)	Arrhythmic Endpoint in the Meta-Analysis	% LGE-CMR Prevalence	LGE-CMR Cutoff in the Meta-Analysis	NOS
Studies including ischemic cardiomyopathy patients							
Roes et al. (8)	2009	91	9 (2-20)	ICD therapy†	100	Gray zone extent = 16.7 g	4,0,2
Boyé et al. (13)	2011	52	41 ± 11	ICD therapy†, CD	100	Relative infarct transmurality = 43%	3,0,3
De Hann et al. (14)	2011	55	24 (11-36)	ICD therapy, VT	100	Peri-infarct zone threshold, g	4,0,2
Alexandre et al. (15)	2013	66	42 (22-52)	ICD therapy†	100	2 segments with scar extent ≥50%	4,0,3
Demirel et al. (16)	2014	94	65 (54-79)	ICD therapy†, VT	100	Peri to core-infarct mass ratio = 0.6	4,0,3
Studies including nonischemic cardiomyopathy patients							
Assomull et al. (17)	2006	101	22 ± 12	Sudden death, VT‡	35	LGE presence in midwall	4,2,2
Iles et al. (18)	2011	61	19 (13-29)	ICD therapy†	51	LGE presence	4,2,2
Leyva et al. (19)	2012	97	35*	Sudden death ‡	26	LGE presence in midwall	4,2,3
Gulati et al. (11)	2013	472	64*	ICD therapy, sudden death, aSD‡	30	LGE presence in midwall	4,2,3
Neilan et al. (20)	2013	162	29 ± 18	ICD therapy†, sudden death‡	50	LGE presence	4,2,2
Muller et al. (21)	2013	185	21*	aSD, ICD therapy‡	51	LGE presence	4,2,3
Perazzolo-Marra et al. (22)	2014	137	36*	ICD therapy†, sudden death, VT/VF	56	LGE presence	4,0,3
Masci et al. (23)	2014	228	23 (13-37)	ICD therapy, aSD, sudden death‡	27	LGE presence	4,2,2
Studies including a mixed population of ischemic and nonischemic cardiomyopathy patients							
Fernandez-Armenta et al. (24)	2012	78 (41/37)	25 (15-34)	ICD therapy†	69	Border zone = 9.5 g	4,0,2
Gao et al. (9)	2012	124 (59/65)	21 ± 9	ICD therapy†, sudden death, aSD	100/71§	LGE extent = 38.7 g/20.8 g§	4,0,2
Klem et al. (10)	2012	137 (73/64)	24 (20-29)	ICD therapy, sudden death‡	96/58§	LGE = 5% LV mass	4,0,2
Wu et al. (25)	2012	235 (137/98)	43*	ICD therapy†	73	Gray zone extent = 8.7 g/0 g§	4,0,3
Mordi et al. (26)	2014	157 (61/96)	31*	ICD therapy†‡	100/25§	LGE percentage = 23%/0%§	4,0,2
Almehmadi et al. (27)	2014	318 (149/169)	16*	ICD therapy†, sudden death	78	LGE presence	4,0,2

TABLE 5 Association Between the Risk of Ventricular Arrhythmias and the Extent of the Total/Heterogeneous Scar, Assessed by LGE-CMR

First Author (Ref. #)	Scar Patterns From LGE-CMR Image Analysis	HR (95% CI)	p Value
Studies including ischemic cardiomyopathy patients			
Roes et al. (8)	Total scar mass (g), HR per 10 g increase	1.15 (0.99-1.33)*	0.06
	Gray zone mass (g), HR per 10 g increase	1.49 (1.01-2.20)†	0.04
Alexandre et al. (15)	Total scar mass (g)	3.15 (1.35-7.33)†	<0.001
Demirel et al. (16)	Total scar mass (g)	1.01 (0.99-1.03)*	0.18
	Peri to core-infarct mass ratio	2.01 (1.17-3.44)†	0.01
Studies including nonischemic cardiomyopathy patients			
Assomull et al. (17)	Total scar extent (% of LV mass)	1.12 (1.03-1.24)†‡	0.02
Gulati et al. (11)	Total scar extent (% of LV mass), HR per 1% increase	1.10 (1.05-1.16)†	<0.001
Neilan et al. (20)	Total scar extent (% of LV mass), HR per 1% increase	1.17 (1.12-1.22)†	<0.0001
Perazzolo Marra et al. (22)	Total scar extent (% of LV mass)	1.04 (0.98-1.09)*	0.18
Masci et al. (23)	Total scar extent (number of segments)	1.24 (1.11-1.38) †§	<0.001
Studies including a mixed population of ischemic and nonischemic cardiomyopathy patients			
Fernandez-Armenta et al. (24)	Total scar extent (% of LV volume), HR per 1% increase	1.10 (1.06-1.15)†	<0.01
	Border zone mass (g), HR per 1 g increase	1.06 (1.04-1.09)†	< 0.01
Gao et al. (9)	Total scar mass (g), HR per 10 g increase	1.38 (1.18-1.62)†	<0.001
	Gray-zone mass (g), HR per 10 g increase‖	1.47 (0.96-2.26)*	0.074
Klem et al. (10)	Total scar extent (% of LV mass)	1.04 (1.00-1.07)*	0.03
Wu et al. (25)	Total scar mass (g, tertiles), HR 3RD tertile versus reference	3.40 (1.60-7.00)*§	0.001
	Gray-zone mass (g, tertiles), HR 3RD tertile versus reference	4.60 (1.40-15.4)†§	0.01
Mordi et al. (26)	Total scar extent (% of LV mass), HR per 1% increase	1.04 (1.01-1.07)†	0.004
Almehmadi et al. (27)	Total scar extent (% of LV mass), HR per 1% increase	1.00 (0.90-1.00)†	0.22

Assessment of myocardial scarring improves risk stratification in patients evaluated for ICD

Whereas the rate of adverse events steadily increased with decreasing LVEF, a sharp step-up was observed for scar size 5% of LV mass (hazard ratio [HR]: 5.2). On multivariable Cox proportional hazards analysis, scar size (as a continuous variable or dichotomized at 5%) was an independent predictor of adverse outcome.

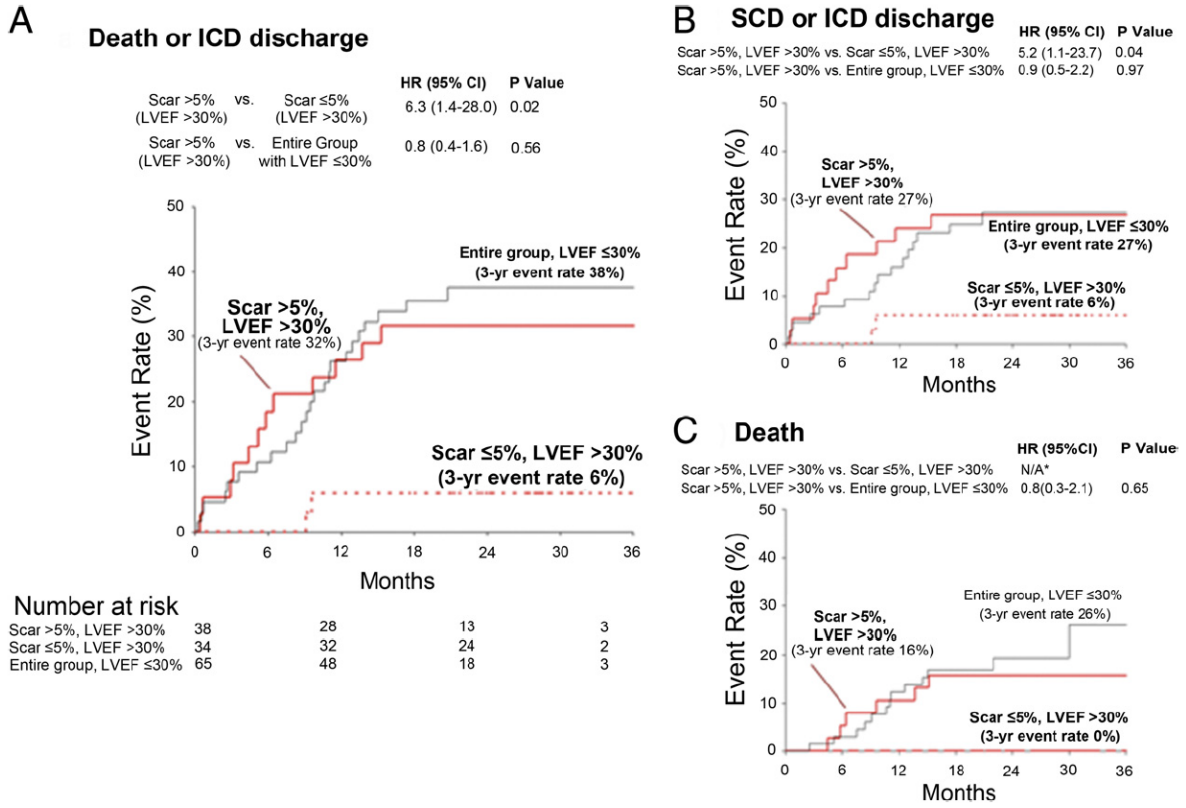

Figure 2 Kaplan-Meier Estimates of Adverse Events in Patients With LVEF >30%

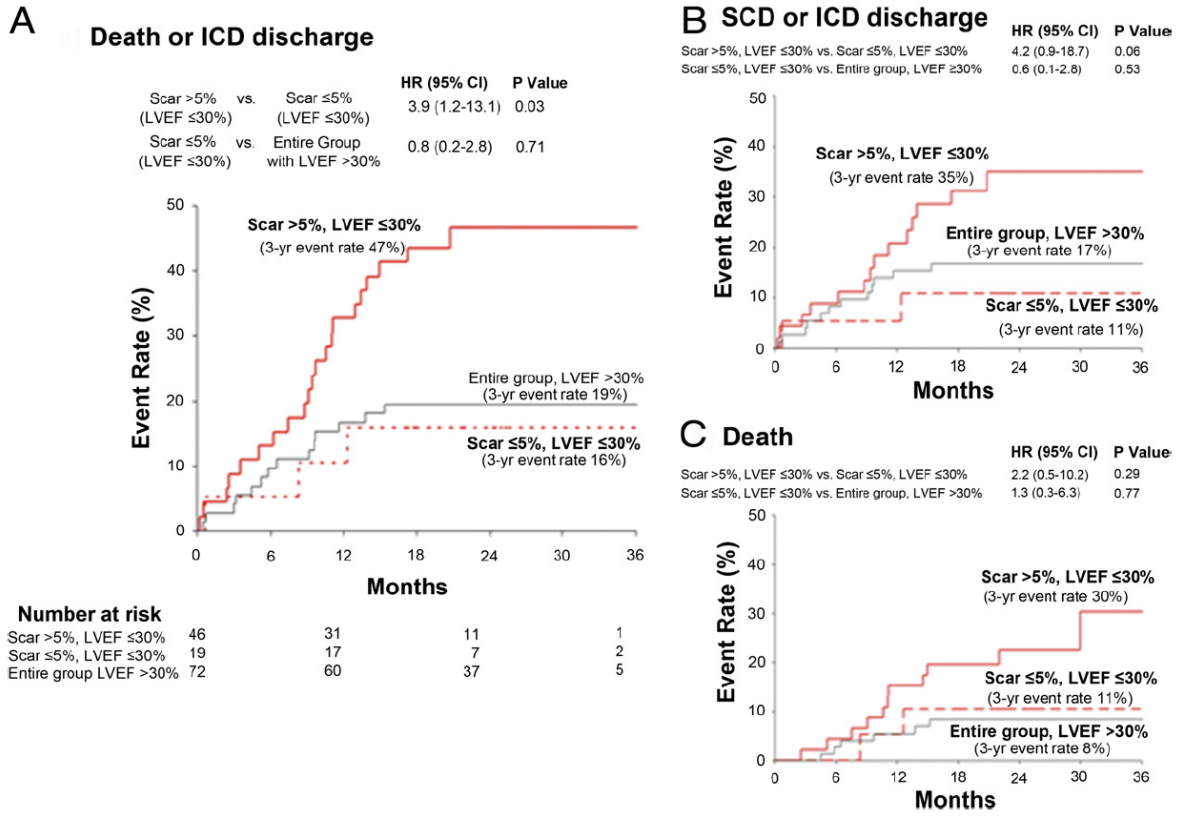

Figure 3 Kaplan-Meier Estimates of Adverse Events in Patients With LVEF ≤30%

Igor Klem & Raymond Kim et al. JACC. 2012;60:408-20

Characterization of the Peri-Infarct Zone by Contrast-Enhanced Cardiac Magnetic Resonance Imaging Is a Powerful Predictor of Post–Myocardial Infarction Mortality

Andrew T. Yan, MD; Adolphe J. Shayne, MD; Kenneth A. Brown, MD; Sandeep N. Gupta, PhD; Carmen W. Chan, MBBS; Tuan M. Luu, BSc; Marcelo F. Di Carli, MD; H. Glenn Reynolds, MSc; William G. Stevenson, MD; Raymond Y. Kwong, MD, MPH

- Peri-infarct regions based on SI threshold of 2-3 SDs above remote normal myocardium).
- In multivariable analysis, LVEF & %MDEperi were strong predictors of all-cause mortality.
- The extent of peri-infact zone provides incremental prognostic value beyond LVEF.

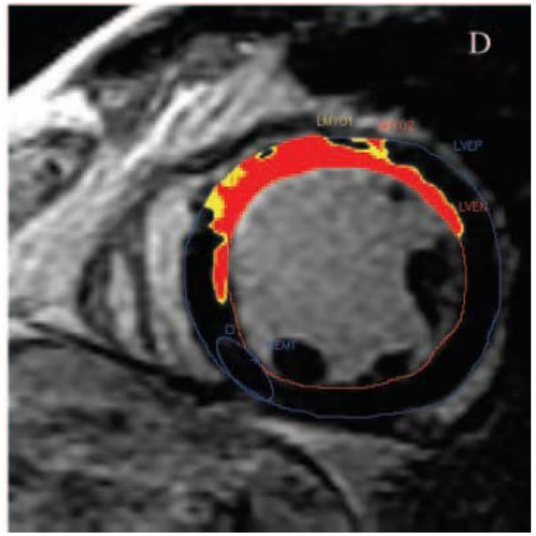

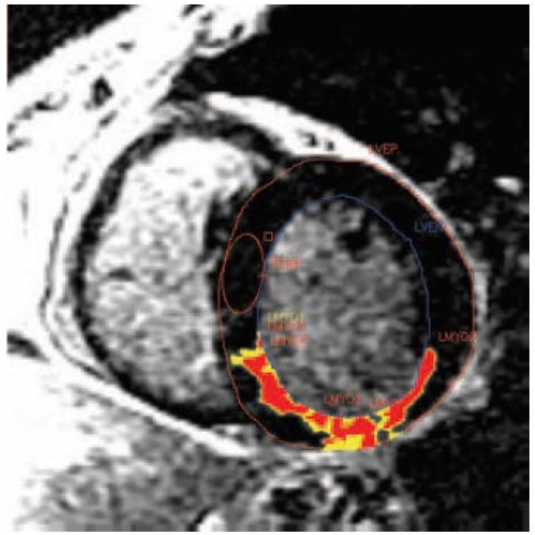

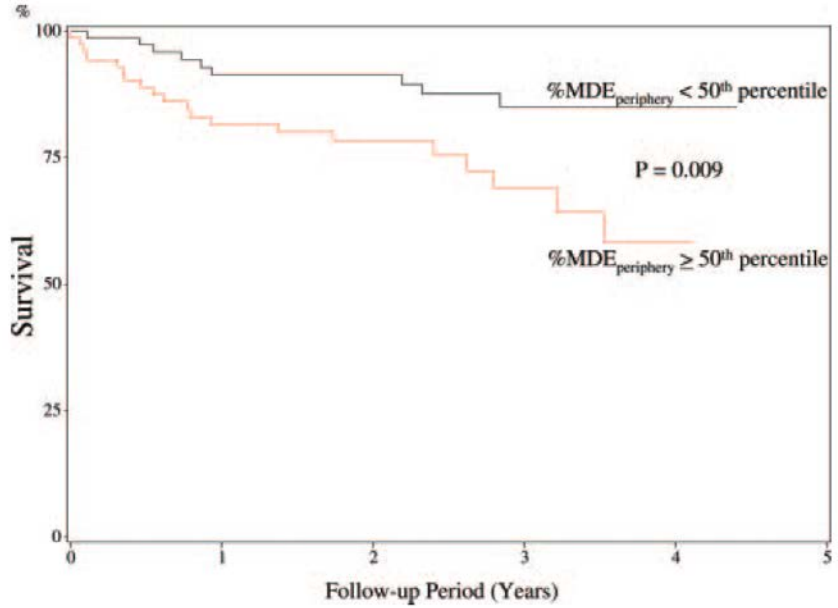

Figure 2. Kaplan-Meier survival curves for all-cause mortality, stratified by median $\%MDE_{Periphery}$.

TABLE 2. Univariable and Multivariable Associations With All-Cause Mortality

	Univariable Analysis		Multivariable Analysis 1		Multivariable Analysis 2	
Variable	Unadjusted HR (95% CI)	P	Adjusted HR (95% CI)	P	Adjusted HR (95% CI)	P
Age*	1.37 (0.96-1.97)	0.09	…	…	1.45 (0.98-2.14)	0.06
Diabetes	2.21 (1.05-4.66)	0.04	…	…	…	…
Previous percutaneous coronary intervention	0.37 (0.16-0.88)	0.02	…	…	…	…
Previous coronary bypass surgery	2.39 (1.08-5.30)	0.03	…	…	…	…
QRS duration >120 ms	2.29 (0.98-5.38)	0.06	…	…	…	…
Left bundle-branch block	3.21 (1.22-8.44)	0.02	…	…	…	…
Corrected QT >440 ms	2.37 (1.14-4.93)	0.02	…	…	…	…
LV end-diastolic volume index†	1.13 (1.04-1.22)	0.004	…	…	…	…
LV end-systolic volume index†	1.13 (1.05-1.23)	0.002	1.16 (1.07-1.26)	<0.001	…	…
LVEF‡	1.36 (1.08-1.72)	0.01	…	…	1.52 (1.19-1.94)	<0.001
$\%MDE_{periphery}$§	1.31 (1.06-1.63)	0.01	1.45 (1.15-1.84)	0.002	1.42 (1.11-1.81)	0.005
$MDE_{periphery}$, g	1.06 (1.00-1.11)	0.035	…	…	…	…

For model 1, predictors on univariable analysis ($P<0.10$) were evaluated in this multivariable model by forward stepwise selection ($P<0.10$ for entry and $P>0.05$ for removal) criteria. For model 2, age, LVEF, and $\%MDE_{periphery}$ were all entered into this multivariable model.

*HR per decade increase.

†HR per 10-mL/m^2 increase.

‡HR per 10% decrease.

§HR per 10% increase.

Yan et al. Circulation. 2006;114:32-39

Scar characterization to predict life-threatening VA & SCD

FIGURE 2 BZ Channel Mass Calculation

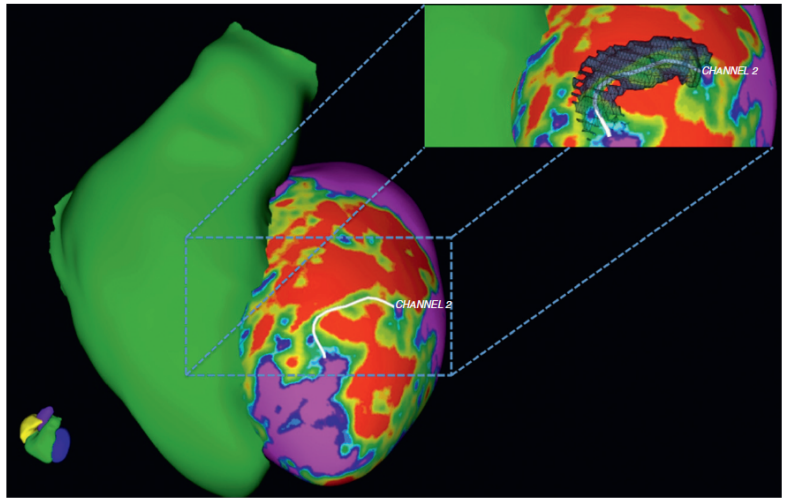

TABLE 3 ce-CMR Scar Parameters

	ICD Therapy/SCD (n = 25)	No ICD Therapy/SCD (n = 186)	p Value*
Scar mass, g	38.7 ± 34.2	17.9 ± 17.2	<0.001
BZ mass, g	20.0 ± 22.5	8.7 ± 10.8	<0.001
BZ mass/scar mass ratio	0.49 ± 0.13	0.4 ± 0.21	0.044
Core mass, g	19.0 ± 14.2	9.3 ± 8.7	<0.001
BZ channel mass, g	3.6 ± 3.0	1.8 ± 3.4	<0.001

TABLE 4 Multivariate Competing Risk Regression Analysis for the Association Between Clinical and ce-CMR Parameters and the Study Endpoint of ICD Therapy or SCD

	HR (95% CI)	p Value
Multivariate model 1		
Scar mass, g	1.04 (1.03–1.05)	**<0.001**
Sex	0.70 (0.19–2.63)	0.602
LVEF, %	0.99 (0.93–1.04)	0.621
NYHA functional class I–II vs. III–IV	0.46 (0.19–1.13)	0.241
Multivariate model 2		
BZ mass, g	1.06 (1.04–1.08)	**<0.001**
Sex	0.57 (0.16–2.06)	0.389
LVEF, %	0.98 (0.93–1.04)	0.583
NYHA functional class I–II vs. III–IV	0.51 (0.20–1.28)	0.153
Multivariate model 3		
BZ channel mass, g	1.21 (1.10–1.32)	**<0.001**
Sex	0.42 (0.12–1.51)	0.185
LVEF, %	1.00 (0.95–1.05)	0.977
NYHA functional class I–II vs. III–IV	0.72 (0.30–1.70)	0.455

Acosta et al. JACC Img. 2018;11:561-572

Postprocessing methods for myocardial scar quantification

- LGE-CMR techniques and diagnostic cutoffs are not uniform, and the assessment of fibrosis extent and heterogeneity, is still a complex and operator dependent procedure.

- Full width at half-maximum criterion has been shown to be the optimal method in several studies, esp. with ICMP. But, a unified statement regarding the best methodology is still lacking.

- Guidelines for LGE cardiac MRI by SCMR recommend to use the same method & software for quantitation - manual planimetry, 'n' standard deviations, or full-width at half-maximum for all studies.

Ambale-Venkatesh, B. & Lima, J. A. C. Nat. Rev. Cardiol. 12, 18–29 (2015)

Accurate and Objective Infarct Sizing by Contrast-Enhanced Magnetic Resonance Imaging in a Canine Myocardial Infarction Model

Luciano C. Amado, MD,* Bernhard L. Gerber, MD,* Sandeep N. Gupta, PHD,‡ Dan W. Rettmann, BS,‡ Gilberto Szarf, MD,† Robert Schock, PHD,§ Khurram Nasir, MD, MPH,* Dara L. Kraitchman, VMD, PHD,† João A. C. Lima, MD*

Baltimore, Maryland; Waukesha, Wisconsin; and Mahwah, New Jersey

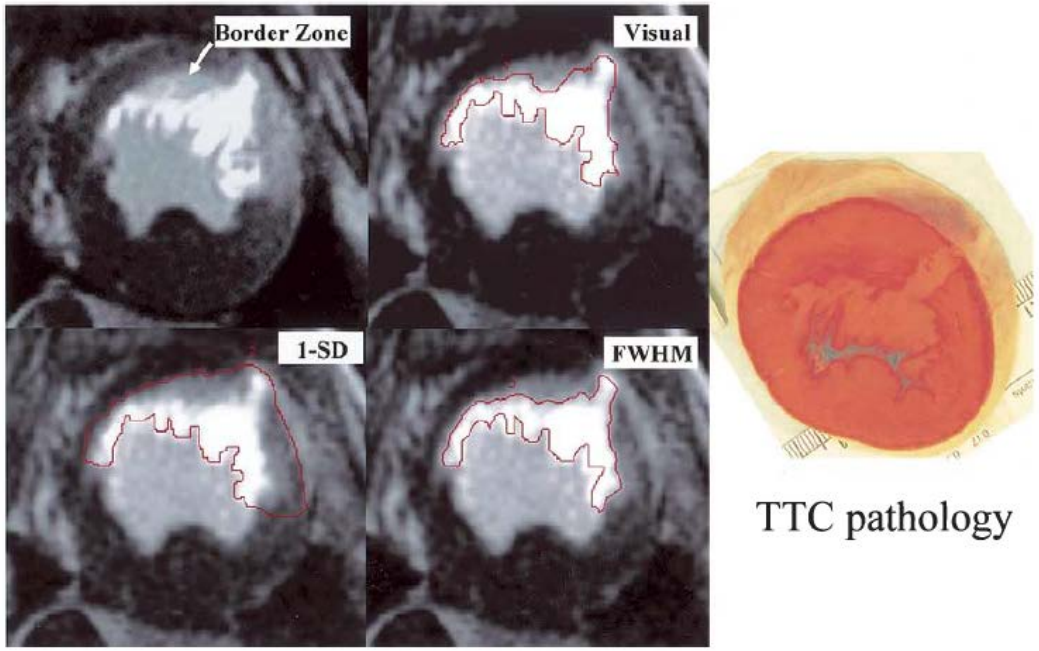

TTC pathology

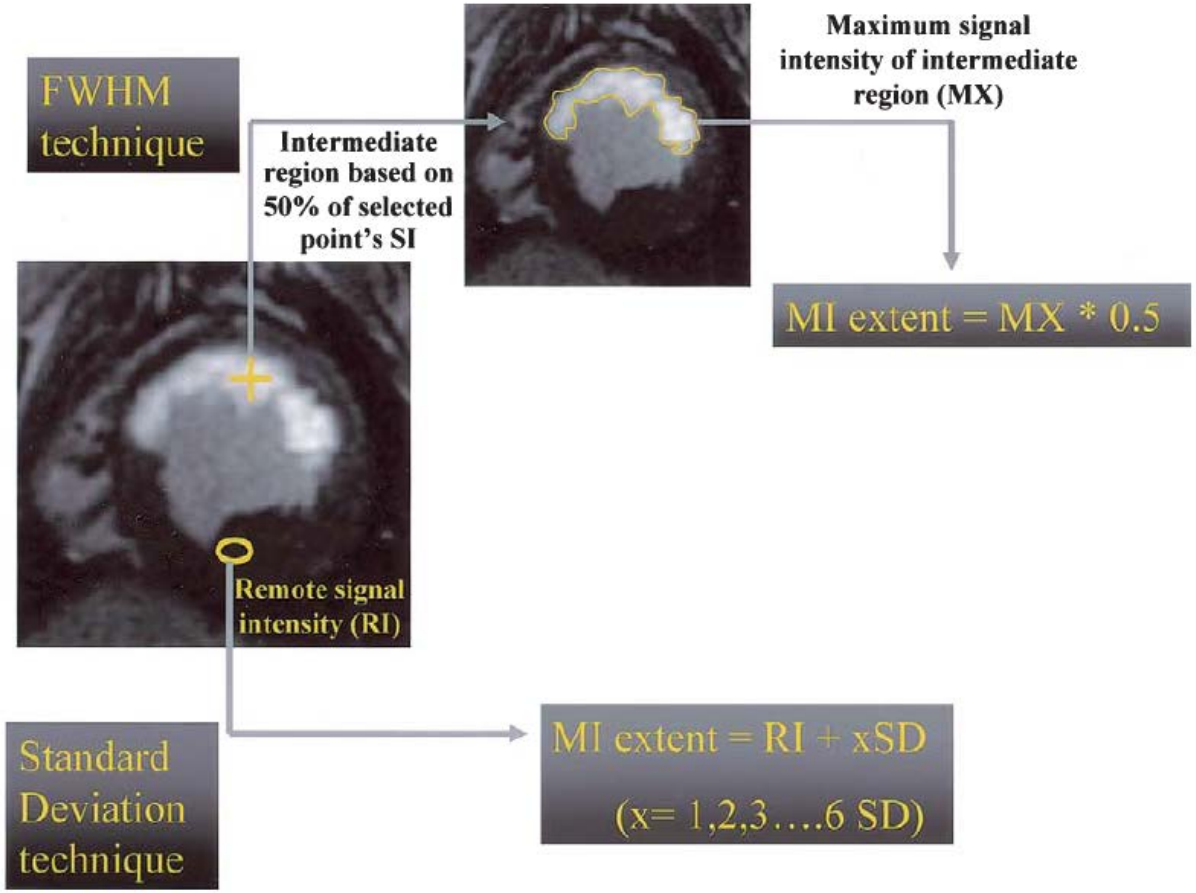

Table 1. Statistical Analysis

	FWHM	1 SD	2 SD	3 SD	4 SD	5 SD	6 SD	Visual
Pearson correlation (r^2)	0.94	0.85	0.79	0.71	0.56	0.42	0.35	0.69
Linear regression (p value)	<0.001*	<0.05*	<0.05*	<0.05*	NS	NS	NS	<0.05*
Bland-Altman plot (bias†)	4.1 ± 1.1%	22.8 ± 3.2%	11.8 ± 2.5%	6.0 ± 2.1%	6.6 ± 1.7%	8.1 ± 1.8%	8.7 ± 2.1%	8.6 ± 1.9%

*Compared with postmortem data. †Bias expressed as percentage of left ventricle (mean ± SD).
FWHM = full-width at half-maximum; NS = not significant; SD = standard deviation.

Amado et al. JACC. 2004;44:2383-9

Contents lists available at ScienceDirect

European Journal of Radiology

journal homepage: www.elsevier.com/locate/ejrad

Comparison of different quantification methods of late gadolinium enhancement in patients with hypertrophic cardiomyopathy

Mateusz Spiewak[a,*], Lukasz A. Malek[a,1], Jolanta Misko[b,2], Lidia Chojnowska[c,1], Barbara Milosz[b,2], Mariusz Klopotowski[c,1], Joanna Petryka[a,1], Maciej Dabrowski[c,1], Cezary Kepka[a,1], Witold Ruzyllo[c,3]

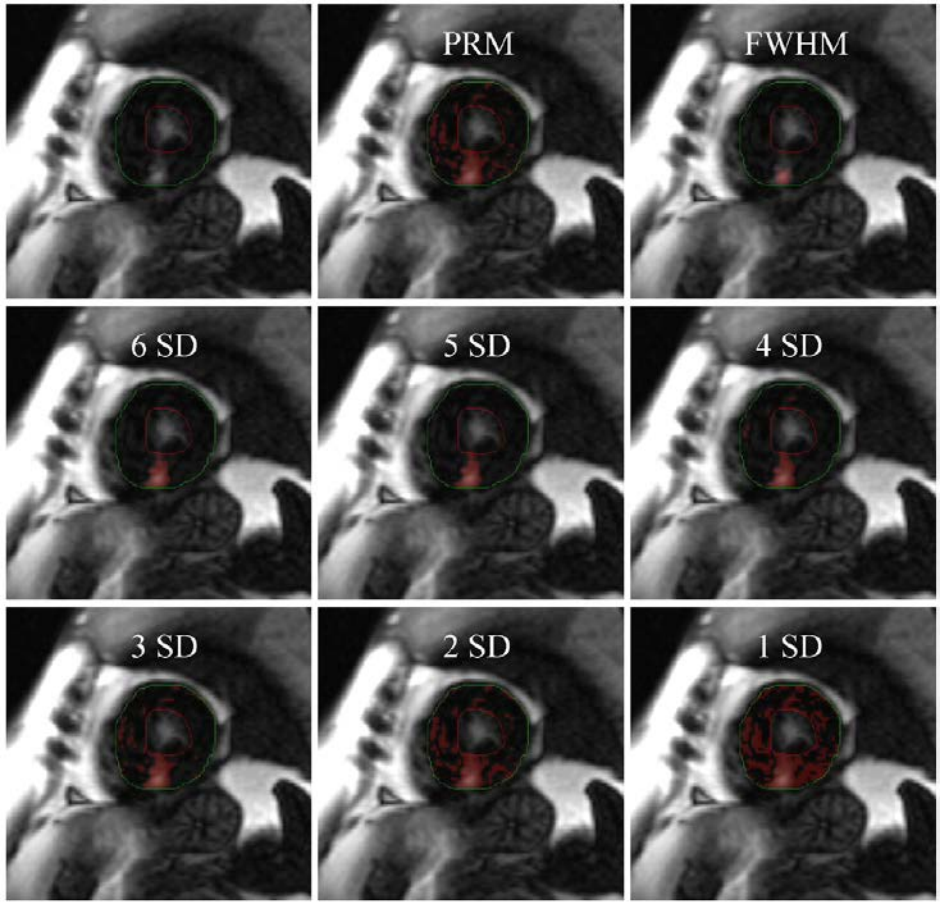

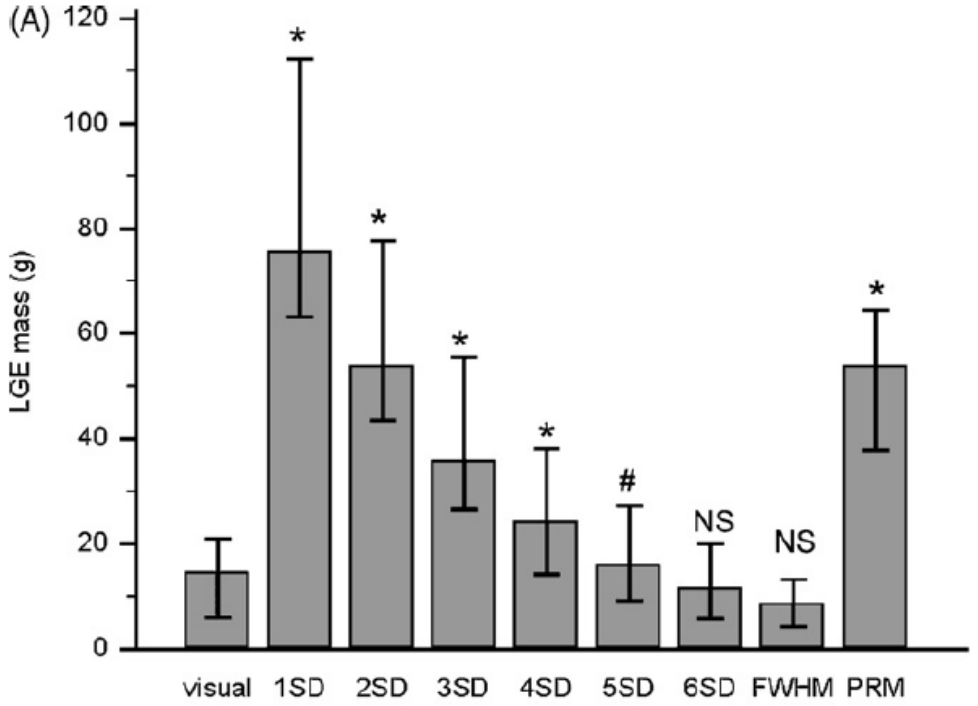

Table 1
Comparison of different thresholding techniques with visual analysis.

	1SD	2SD	3SD	4SD	5SD	6SD	FWHM	PRM
Spearman correlation (rho)	0.602, $p = 0.003$	0.701, $p = 0.0006$	0.831, $p < 0.0001$	0.902, $p < 0.0001$	0.952, $p < 0.0001$	0.956, $p < 0.0001$	0.16, NS	0.743, $p = 0.0009$
Bland–Altman plot (bias)[a]	−74.3 ± 63.2	−48.4 ± 52.6	−29.3 ± 42.1	−15.8 ± 30.1	−6.1 ± 17.2	0.7 ± 7.0	9.0 ± 63.6	−41.8 ± 48.7

[a] Bias expressed as mean late gadolinium enhancement size difference (g) ± 2SD when compared to visual analysis. PRM, peak remote myocardium; FWHM, full-width at half maximum; and SD, standard deviation.

Spiewak et al. Eur J Radiol. 2010;74:e149-53

Histological validation of cardiac magnetic resonance analysis of regional and diffuse interstitial myocardial fibrosis

Leah M. Iles[1,2*], Andris H. Ellims[1,2], Huw Llewellyn[3], James L. Hare[1,2], David M. Kaye[1,2], Catriona A. McLean[3], and Andrew J. Taylor[1,2]

[1]Department of Cardiovascular Medicine, Alfred Hospital, Melbourne, Australia; [2]Baker IDI Heart and Diabetes Institute, Melbourne, Australia; and [3]Department of Anatomical Pathology, Alfred Hospital, Melbourne, Australia

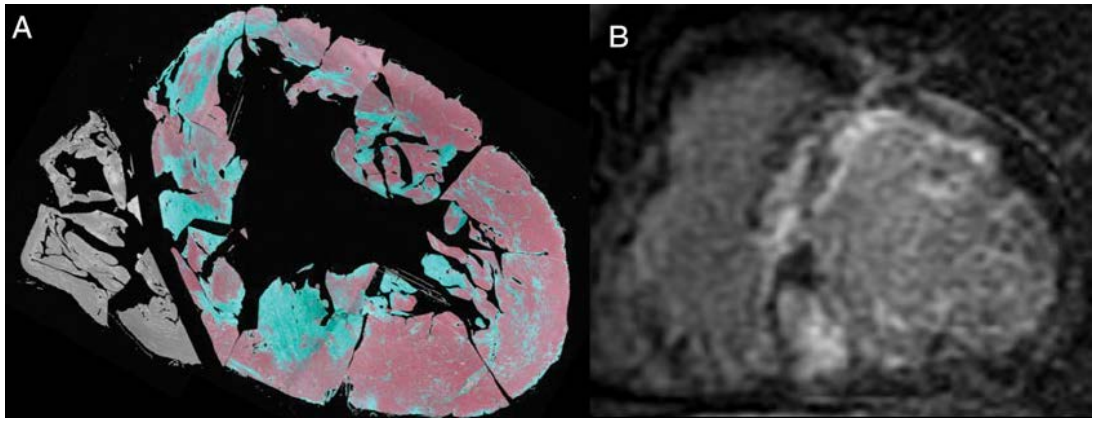

Table 2 Correlations between histological myocardial fibrosis and CMR quantification of LGE at a range of signal intensity thresholds

Quantification	% Global quantification ($n = 11$)	Difference (LGE-histology)	*R*	% Segmental quantification ($n = 66$)	Difference (LGE-histology)	*R*
Masson trichrome	11.3 ± 12.1	–	–	11.8 ± 16.4	–	–
LGE 2 SD	49.6 ± 12.5	38.3	0.70*	49.0 ± 26.5	37.2	0.52§
LGE 3 SD	35.8 ± 12.6	24.5	0.78†	35.9 ± 25.4	24.1	0.59§
LGE 5 SD	17.1 ± 11.7	5.8	0.88‡	18.7 ± 21.7	6.9	0.72§
LGE 6 SD	12.3 ± 11.0	1.0	0.91‡	12.8 ± 18.8	1.0	0.74§
LGE 8 SD	6.6 ± 8.2	−4.7	0.92‡	6.8 ± 13.9	−5.0	0.76§
LGE 10 SD	3.5 ± 5.4	−7.8	0.93§	3.6 ± 9.5	−8.2	0.78§

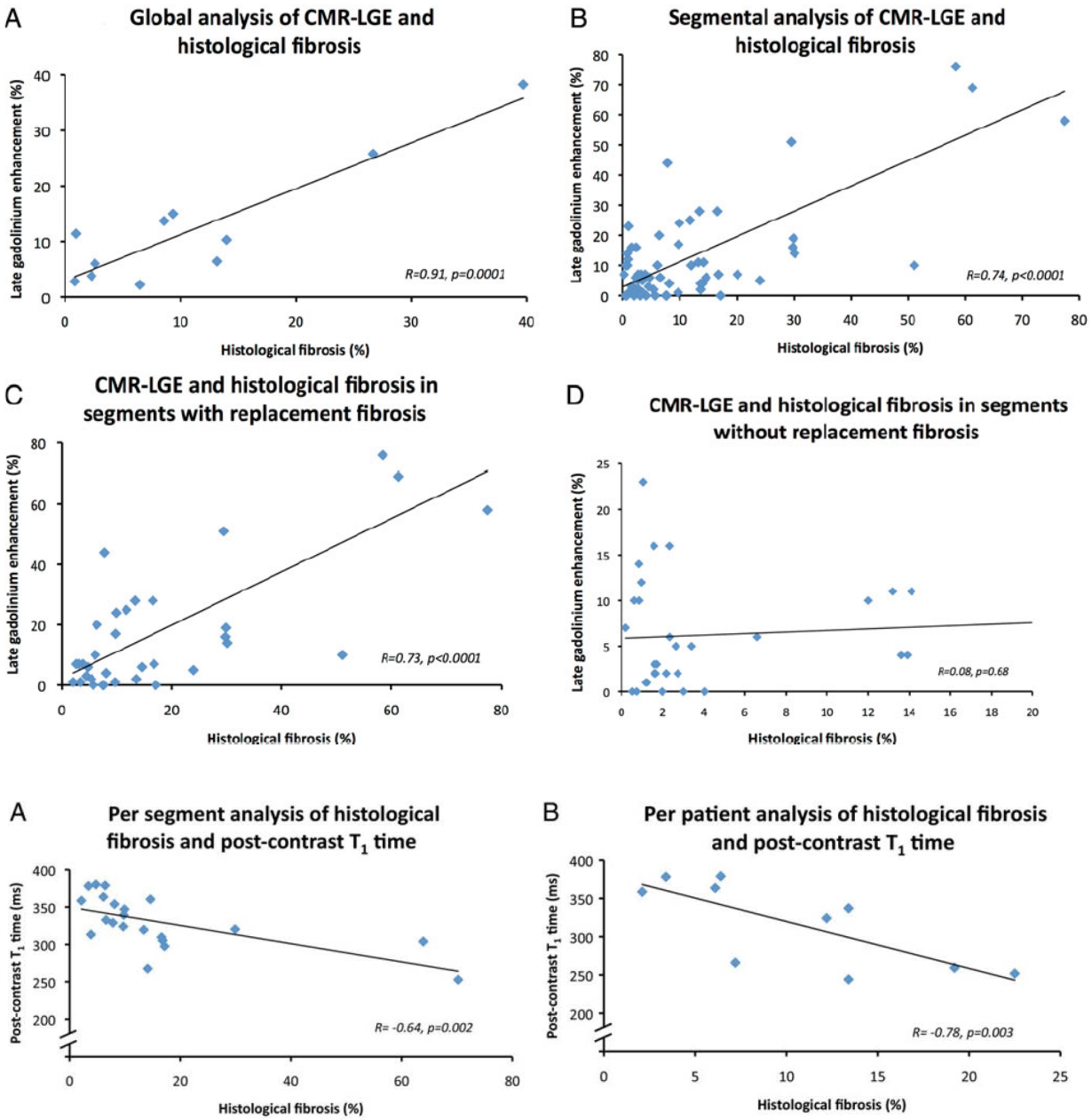

Iles et al. Eur Heart J-CV Img. 2015;16:14-22

Integrative Physiology

Magnetic Resonance–Based Anatomical Analysis of Scar-Related Ventricular Tachycardia

Implications for Catheter Ablation

Hiroshi Ashikaga, Tetsuo Sasano, Jun Dong, M. Muz Zviman, Robert Evers, Bruce Hopenfeld, Valeria Castro, Robert H. Helm, Timm Dickfeld, Saman Nazarian, J. Kevin Donahue, Ronald D. Berger, Hugh Calkins, M. Roselle Abraham, Eduardo Marbán, Albert C. Lardo, Elliot R. McVeigh, Henry R. Halperin

- VT activation sequence map was registered with 3D scar anatomy derived from high-resolution LGE MRI in a swine model of chronic MI.
- The reentry isthmus was characterized by small volume of viable myocardium bound by the infarct border zone or over the infarct.
- In conclusion, CMR revealed a scar with spatially complex structures, particularly at the isthmus (substrate for VT).
- CMR-based visualization of scar morphology would potentially contribute to preprocedural planning for catheter ablation of scar-related, unmappable VT.

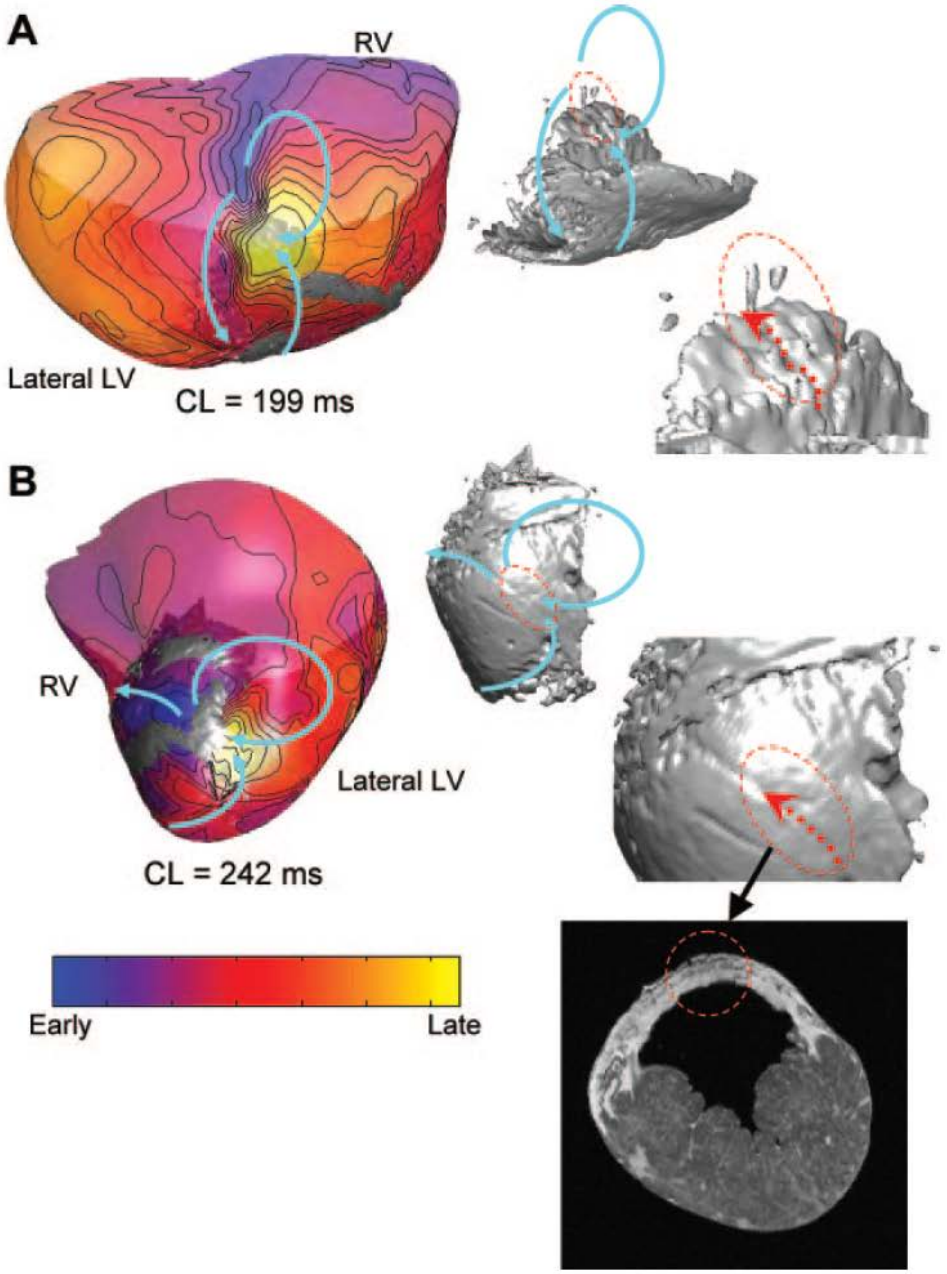

Ashikaga et al. Circ Res. 2007;939-947

Journal of the American College of Cardiology
© 2011 by the American College of Cardiology Foundation
Published by Elsevier Inc.

Vol. 57, No. 2, 2011
ISSN 0735-1097/$36.00
doi:10.1016/j.jacc.2010.07.043

Cardiac Imaging

Noninvasive Identification of Ventricular Tachycardia-Related Conducting Channels Using Contrast-Enhanced Magnetic Resonance Imaging in Patients With Chronic Myocardial Infarction

Comparison of Signal Intensity Scar Mapping and Endocardial Voltage Mapping

Esther Perez-David, MD,* Ángel Arenal, MD,* José L. Rubio-Guivernau, PHD,†
Roberto del Castillo, MD,* Leonardo Atea, MD,* Elena Arbelo, MD, PHD,‡
Eduardo Caballero, MD, PHD,‡ Verónica Celorrio, MD,* Tomas Datino, MD, PHD,*
Esteban Gonzalez-Torrecilla, MD, PHD,* Felipe Atienza, MD,* Maria J. Ledesma-Carbayo, PHD,†
Javier Bermejo, MD,* Alfonso Medina, MD, PHD,‡ Francisco Fernández-Avilés, MD, PHD*
Madrid and Las Palmas de Gran Canaria, Spain

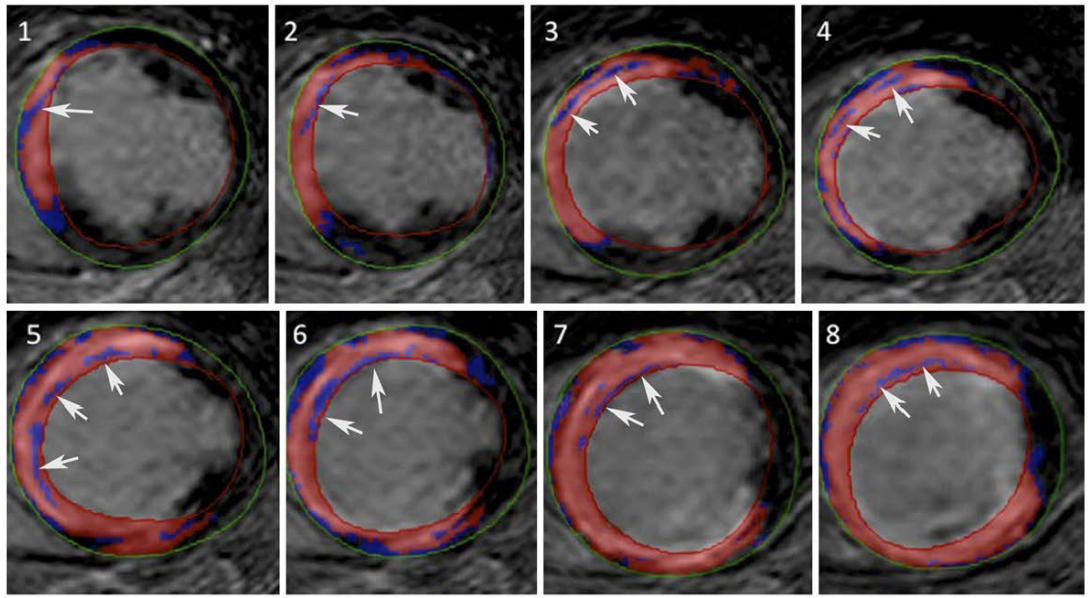

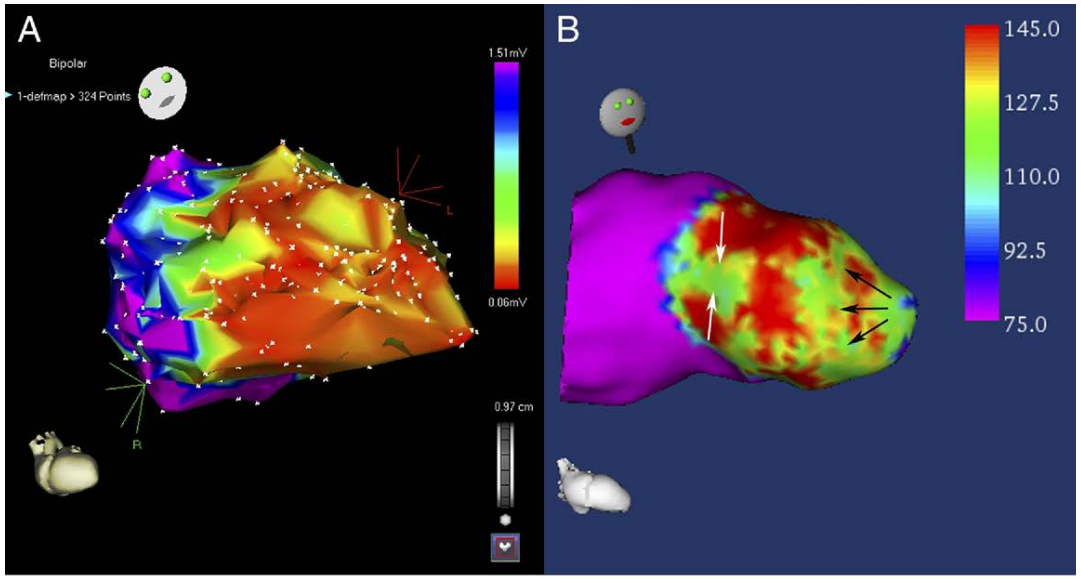

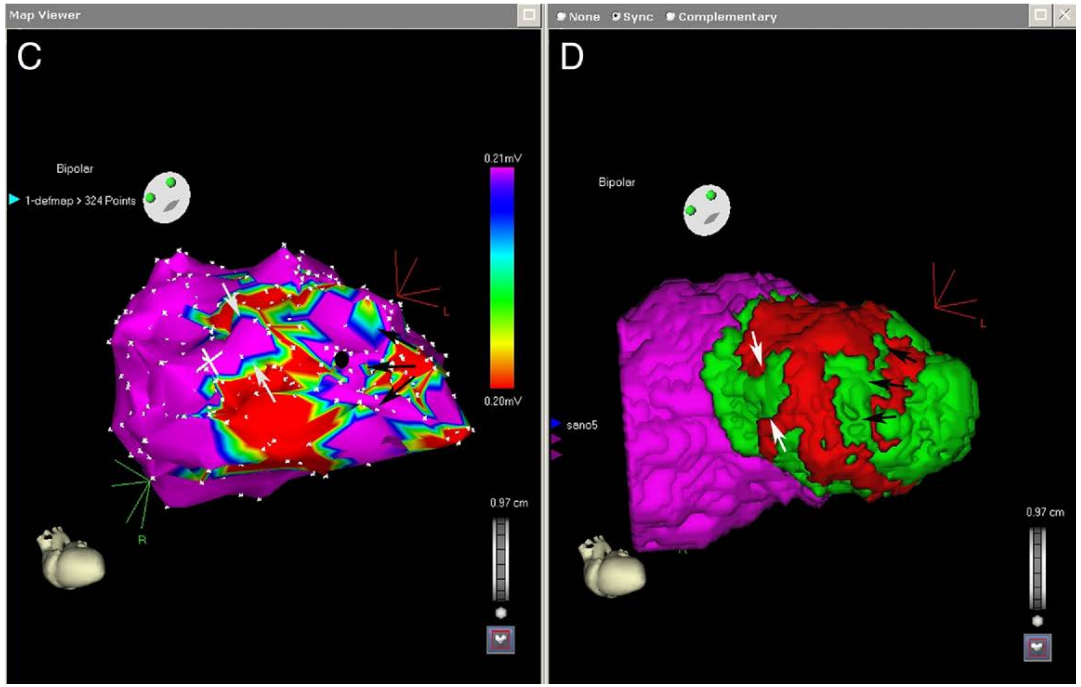

Perez-David et al. JACC 2011;184-94

Original Article

Three-Dimensional Architecture of Scar and Conducting Channels Based on High Resolution ce-CMR

Insights for Ventricular Tachycardia Ablation

Juan Fernández-Armenta, MD; Antonio Berruezo, MD, PhD; David Andreu, MSc; Oscar Camara, MSc, PhD; Etelvino Silva, BEng, PhD; Luis Serra, MSc, PhD; Valeria Barbarito, MSc; Luigi Carotenutto, MSc; Reinder Evertz, MD; José T. Ortiz-Pérez, MD, PhD; Teresa María De Caralt, MD, PhD; Rosario Jesús Perea, MD, PhD; Marta Sitges, MD, PhD; Lluis Mont, MD, PhD; Alejandro Frangi, MSc, PhD; Josep Brugada, MD, PhD

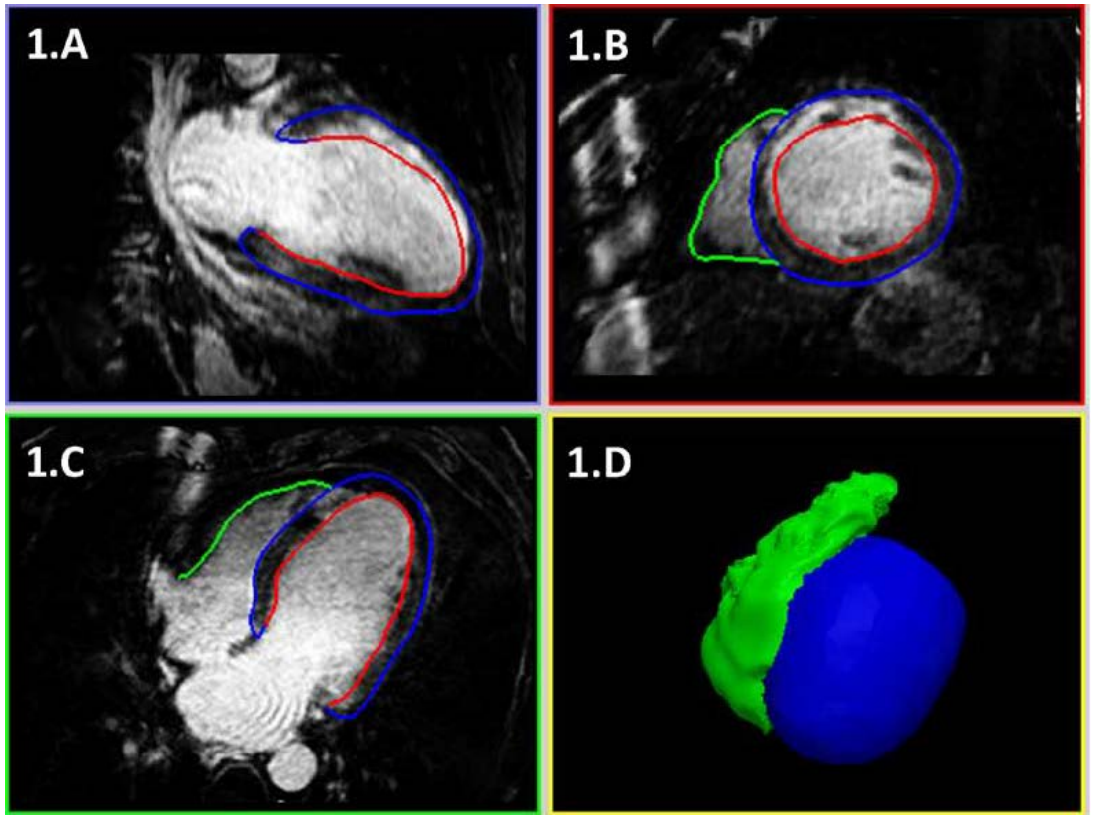

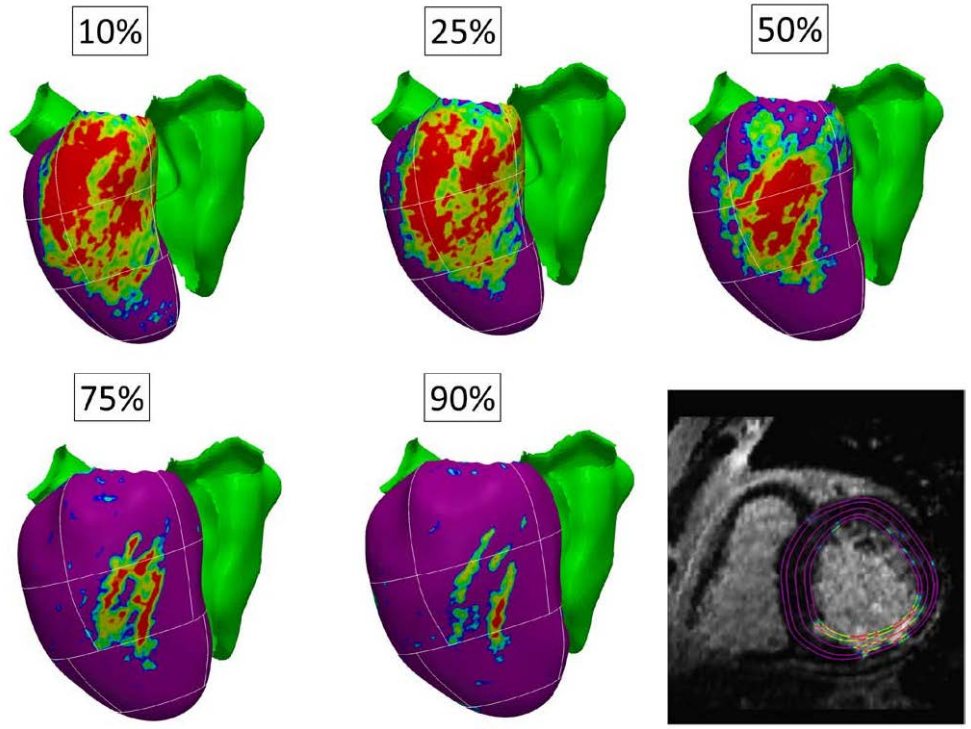

Table 3. Comparison Between CCs on EAM and BZ Channels on ce-CMR

BZ Channel ce-CMR	EAM Matching
10% shell	20/25 (80%)
25% shell	8/9 (89%)
10+25% shells	28/34 (82%)
Endocardial CC EAM	**Ce-CMR matching**
Voltage CC	16/23 (70%)
Late potential CC	12/33 (36%)
All CC	28/56 (50%)

Fernandez-Armenta et al. Circ Arrhythm Electrophysiol 2013;6:528-537

Journal of the American College of Cardiology
© 2008 by the American College of Cardiology Foundation
Published by Elsevier Inc.

Vol. 52, No. 10, 2008
ISSN 0735-1097/08/$34.00
doi:10.1016/j.jacc.2008.05.038

Cardiac Imaging

Electroanatomic Characterization of Post-Infarct Scars

Comparison With 3-Dimensional Myocardial Scar Reconstruction Based on Magnetic Resonance Imaging

Andrei Codreanu, MD,*§ Freddy Odille, MS,§ Etienne Aliot, MD,* Pierre-Yves Marie, MD, PHD,†‖
Isabelle Magnin-Poull, MD,* Marius Andronache, MD,* Damien Mandry, MD,‡
Wassila Djaballah, MD,†§ Denis Régent, MD,‡§ Jacques Felblinger, PHD,§
Christian de Chillou, MD, PHD*§

Nancy, France

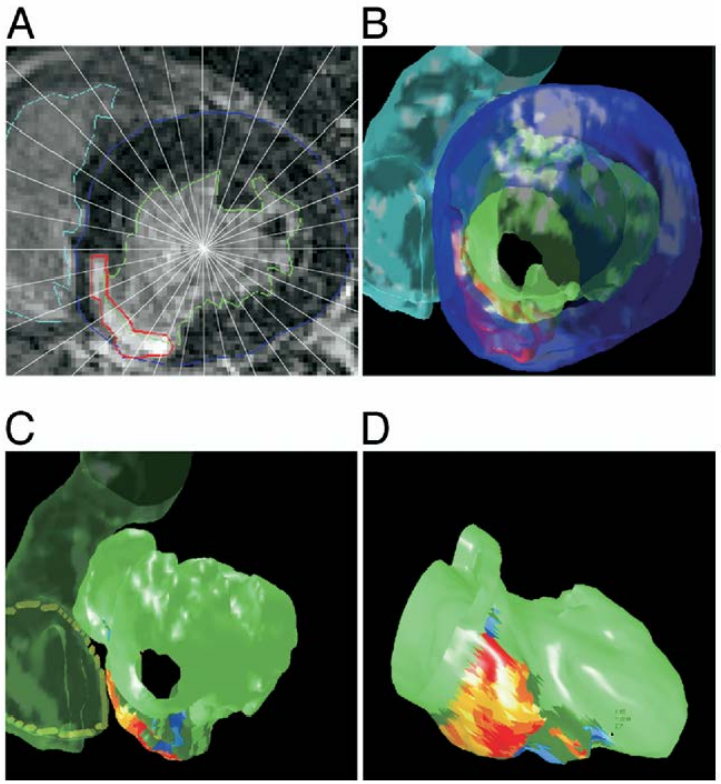

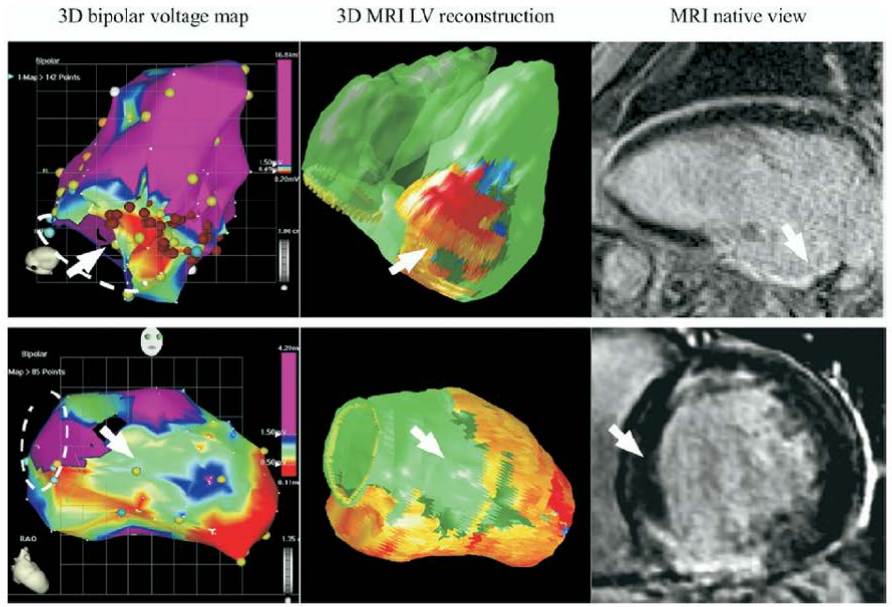

Figure 2 Mismatch in Scar Delineation Between CARTO Bipolar Maps and MRI Shells

(Left) CARTO bipolar maps; **(middle)** MRI shells; **(right)** native MRI images. The **top row** shows underestimated inferior wall scar on the CARTO map. The **bottom row** shows LV septal scar on the CARTO map not confirmed by MRI. On **each panel**, the **arrows** show the mismatch zone. The **dotted lines** represent the mitral annulus plane. 3D = 3-dimensional; other abbreviations as in Figure 1.

- A matching process allocated any CARTO EAM point to its corresponding position on the MRI-reconstructed LV endocardial shell.
- Electrogram (EGM) characteristics were evaluated in relation to scar data (intramural location & transmural extent).
- A spiky EGM morphology, reduced unipolar or bipolar EGM voltage amplitude (6.52 and 1.54 mV), longer bipolar EGM duration (56 ms) independently correlated with the presence of scar.

Andrei Codreanu et al. JACC 2008;52:839-42

Preprocedural magnetic resonance imaging for image-guided catheter ablation of scar-related ventricular tachycardia

Qian Tao · Sebastiaan R. D. Piers · Hildo J. Lamb · Katja Zeppenfeld · Rob J. van der Geest

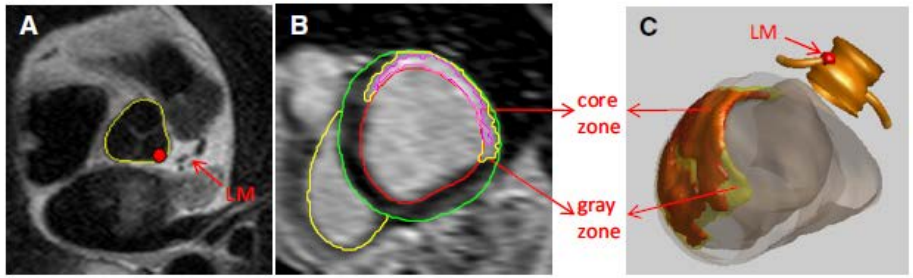

Fig. 2 The semi-automated image analysis of the MRI sequences. **a** The image analysis on the BBTSE sequence for aorta and LM identification. **b** The image analysis on the LGE sequence for ventricle contour and scar core zone (*magenta*) and gray zone (*yellow*) identification. **c** 3D reconstruction of the heart anatomy scar substrate, in standard posterior anterior (PA) view, with the meshes indicating the core zone and *yellow* meshes indicating gray zone

Fig. 3 The effect of inter-scan registration. **a** The MRI scan volume for aorta (BBTSE, *red color*) and LV (LGE, *blue color*). **b** The aorta contours from the BBTSE projected onto an image slice within the LGE. **c** The same contour after inter-scan registration

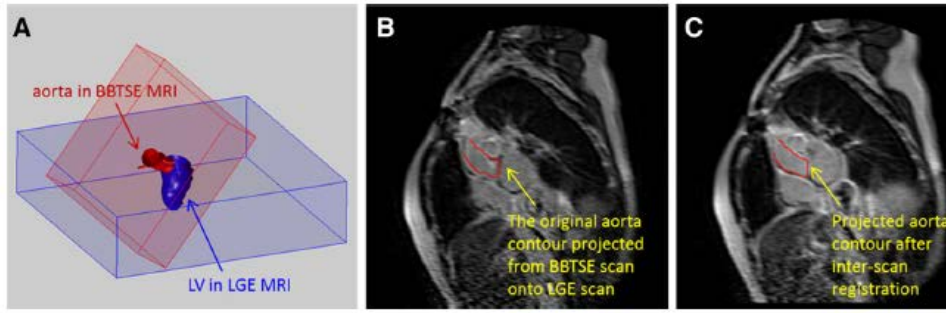

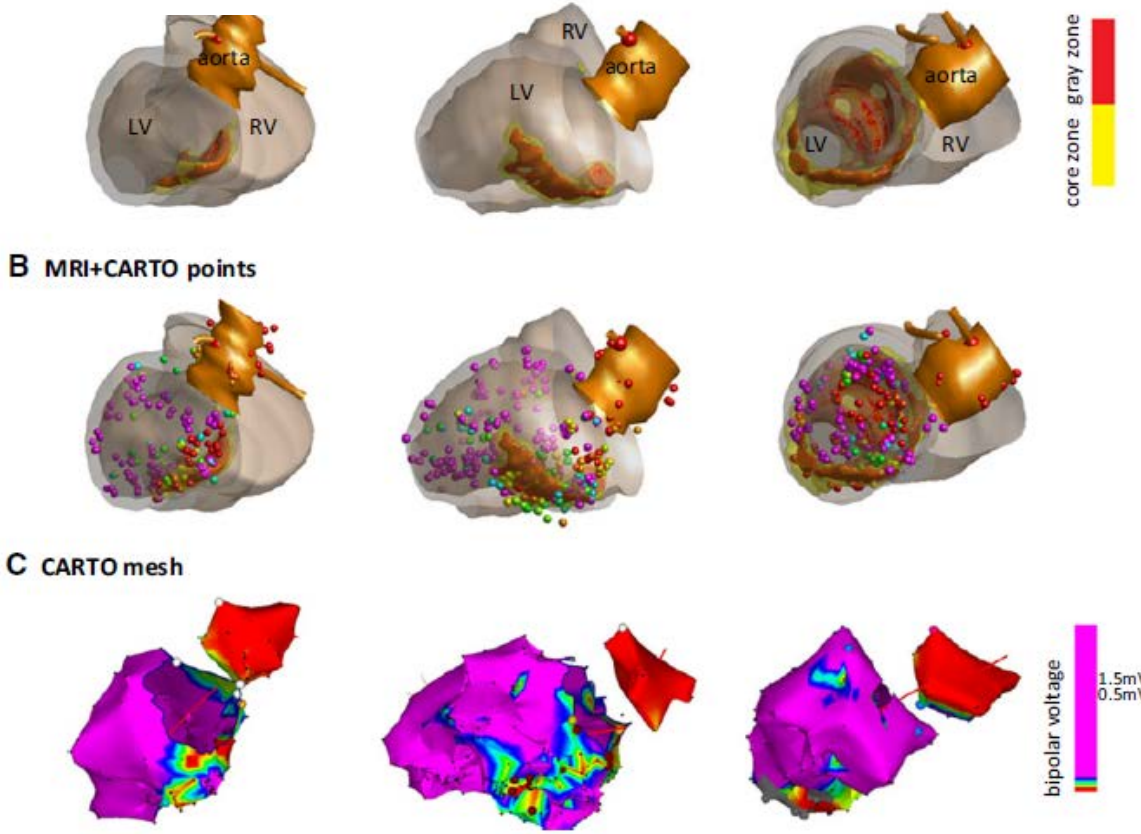

Qian Tao et al. Int J Cardiovasc Imaging 2015;31:369-377

Head-to-head comparison of contrast-enhanced magnetic resonance imaging and electroanatomical voltage mapping to assess post-infarct scar characteristics in patients with ventricular tachycardias: real-time image integration and reversed registration

Adrianus P. Wijnmaalen[1], Rob J. van der Geest[2], Carine F.B. van Huls van Taxis[1], Hans-Marc J. Siebelink[1], Lucia J.M. Kroft[3], Jeroen J. Bax[1], Johan H.C. Reiber[2], Martin J. Schalij[1], and Katja Zeppenfeld[1]*

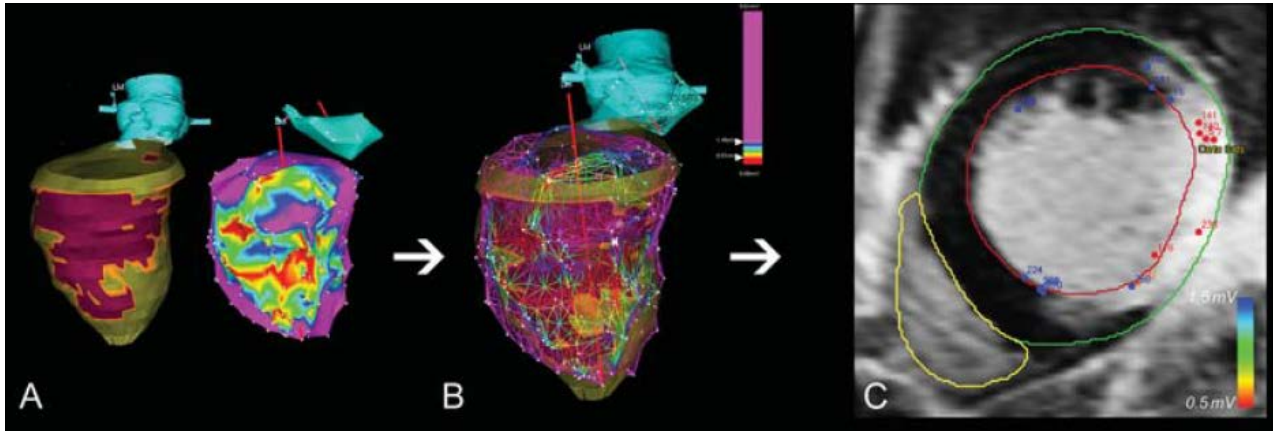

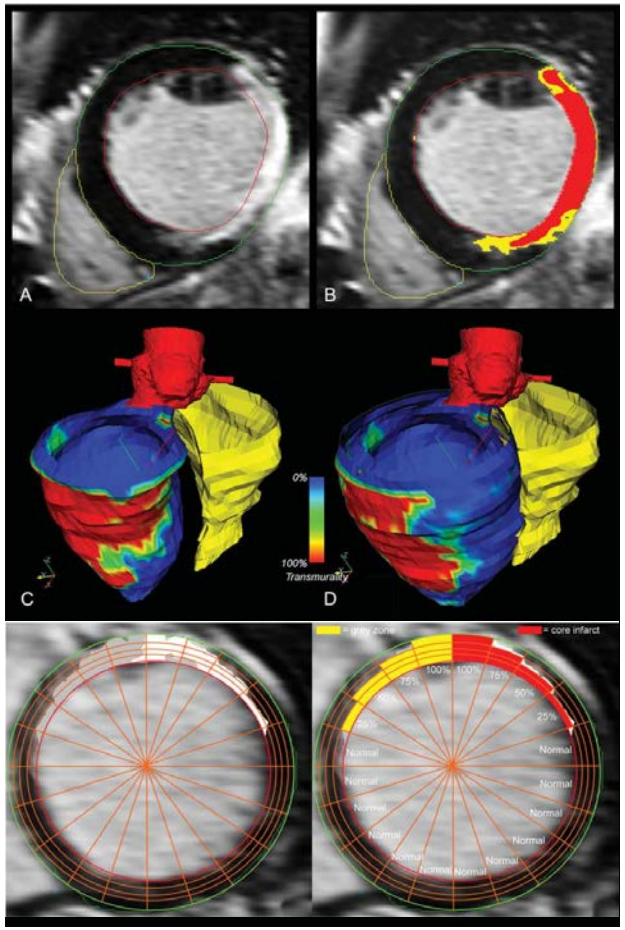

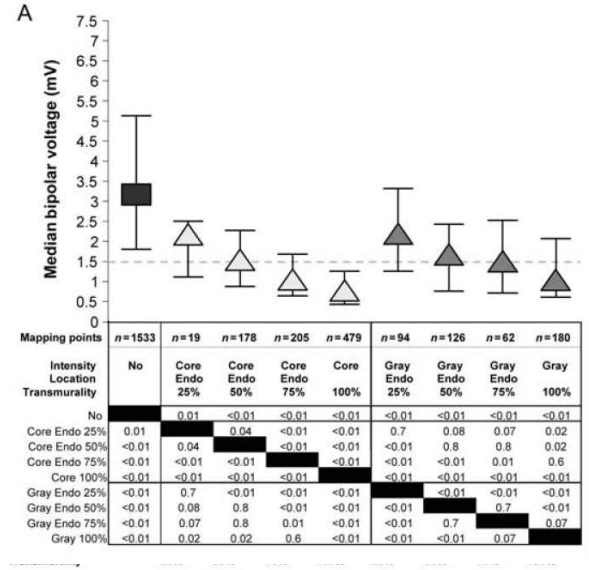

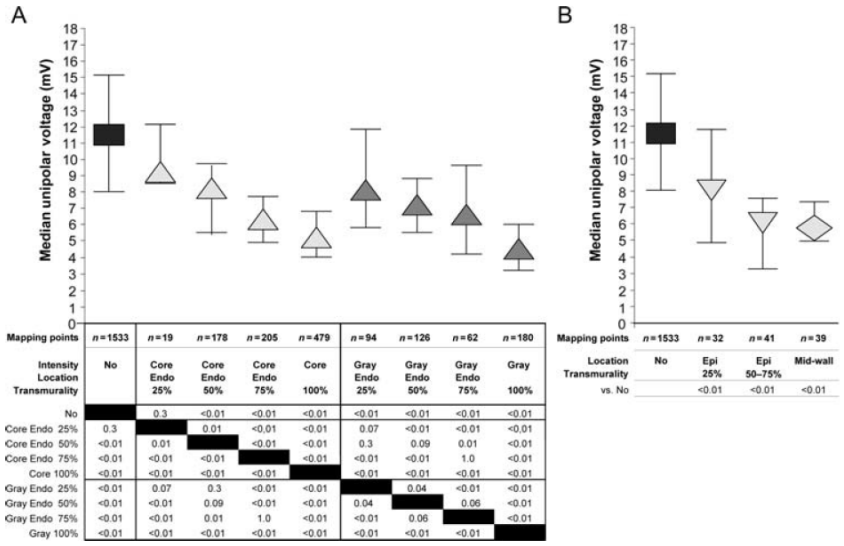

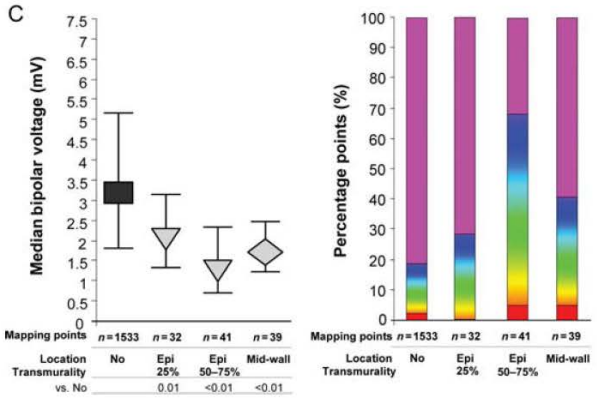

- Local bipolar & unipolar voltages decreased with increasing scar transmurality and were influenced by scar heterogeneity.
- In 3 patients, the exit site during VT or best pace map matching site was at a normal voltage site. However, at these sites, LGE-CMR identified subendocardial septal or intramural inferoseptal scar.

Wijnmaalen et al. Eur. Heart J. 2011;32:104-114

Original Article

Impact of Nonischemic Scar Features on Local Ventricular Electrograms and Scar-Related Ventricular Tachycardia Circuits in Patients With Nonischemic Cardiomyopathy

Takeshi Sasaki, MD, PhD; Christopher F. Miller, MS; Rozann Hansford, RN, MPH; Vadim Zipunnikov, PhD; Menekhem M. Zviman, PhD; Joseph E. Marine, MD; David Spragg, MD; Alan Cheng, MD; Harikrishna Tandri, MD; Sunil Sinha, MD; Aravindan Kolandaivelu, MD; Stefan L. Zimmerman, MD; David A. Bluemke, MD, PhD; Gordon F. Tomaselli, MD; Ronald D. Berger, MD, PhD; Henry R. Halperin, MD; Hugh Calkins, MD; Saman Nazarian, MD, PhD

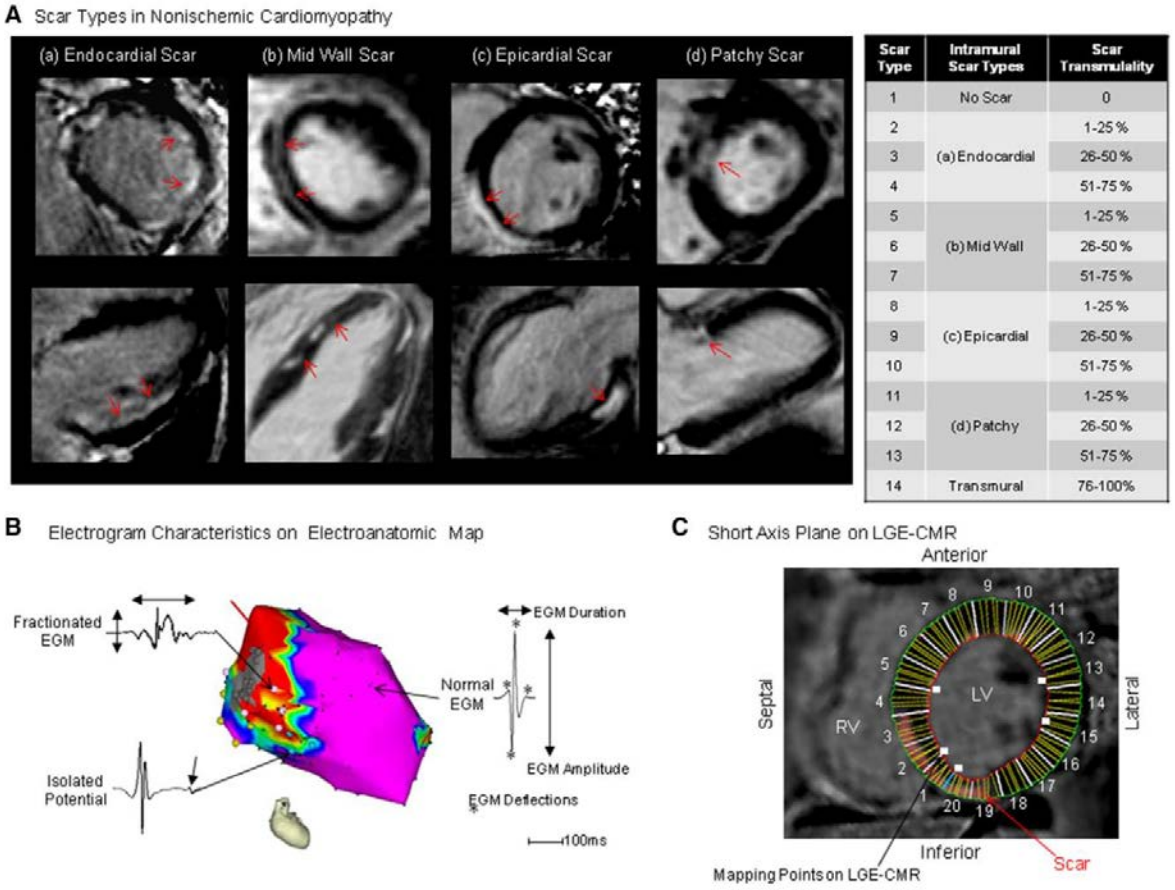

Scar Type	Intramural Scar Types	Scar Transmulality
1	No Scar	0
2	(a) Endocardial	1-25%
3		26-50%
4		51-75%
5	(b) Mid Wall	1-25%
6		26-50%
7		51-75%
8	(c) Epicardial	1-25%
9		26-50%
10		51-75%
11	(d) Patchy	1-25%
12		26-50%
13		51-75%
14	Transmural	76-100%

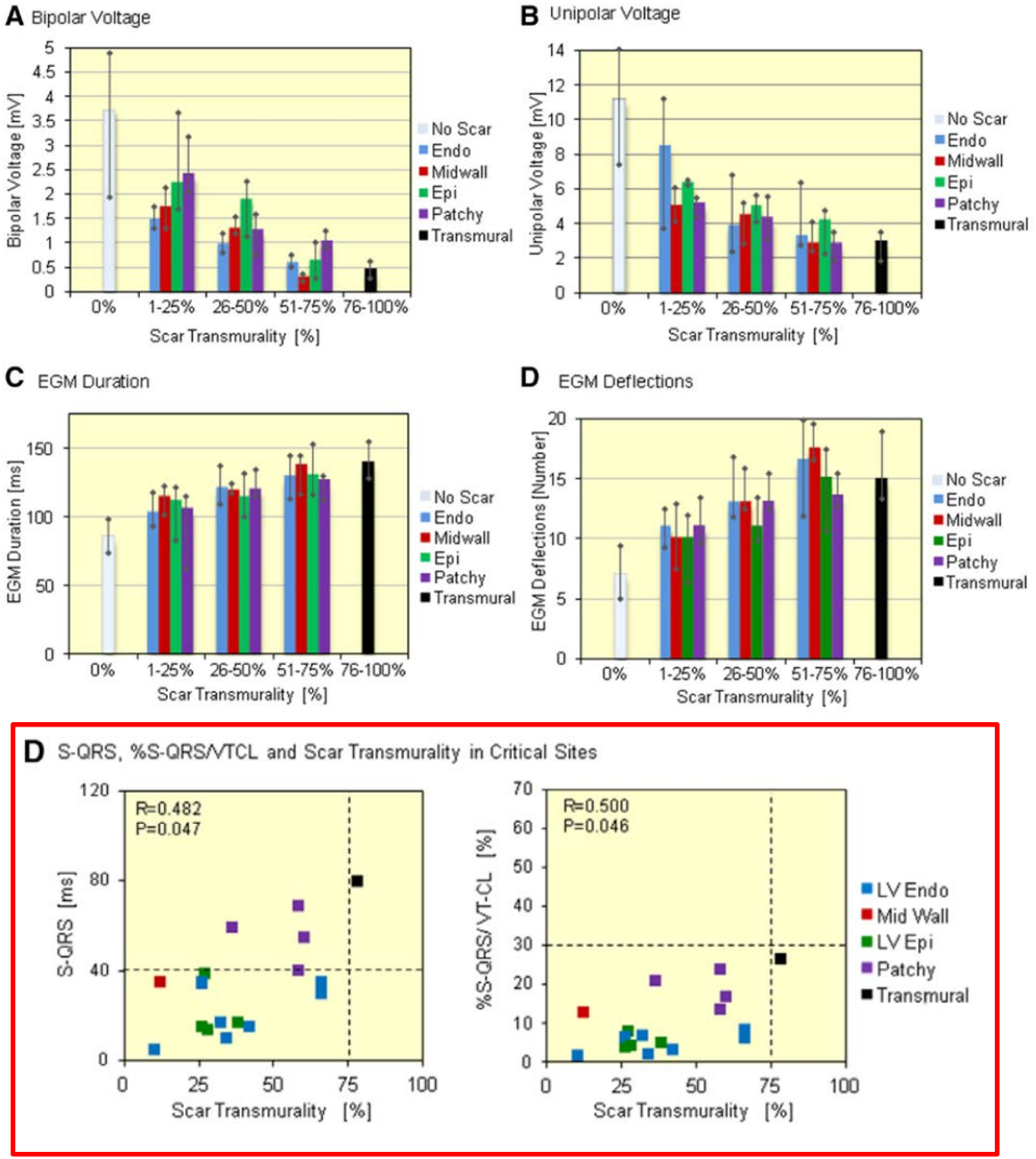

Sasaki et al. Circ Arrhythm Electrophysiol. 2013;6:139-1147

Association of LGE characteristics & wall thickness on CMR with endocardial & epicardial EGM features and paced QRS duration in Nonischemic CMP

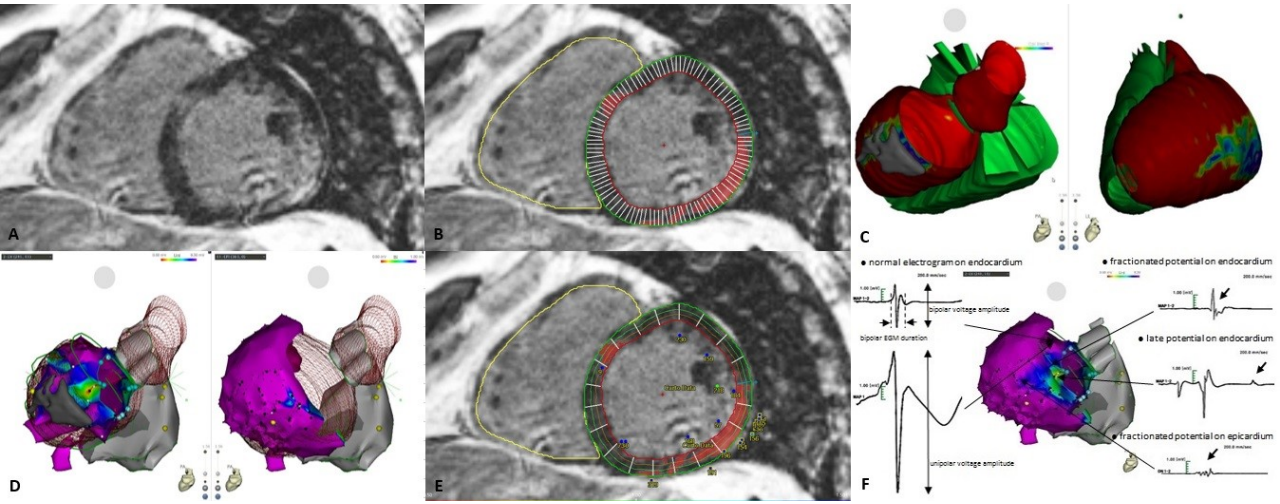

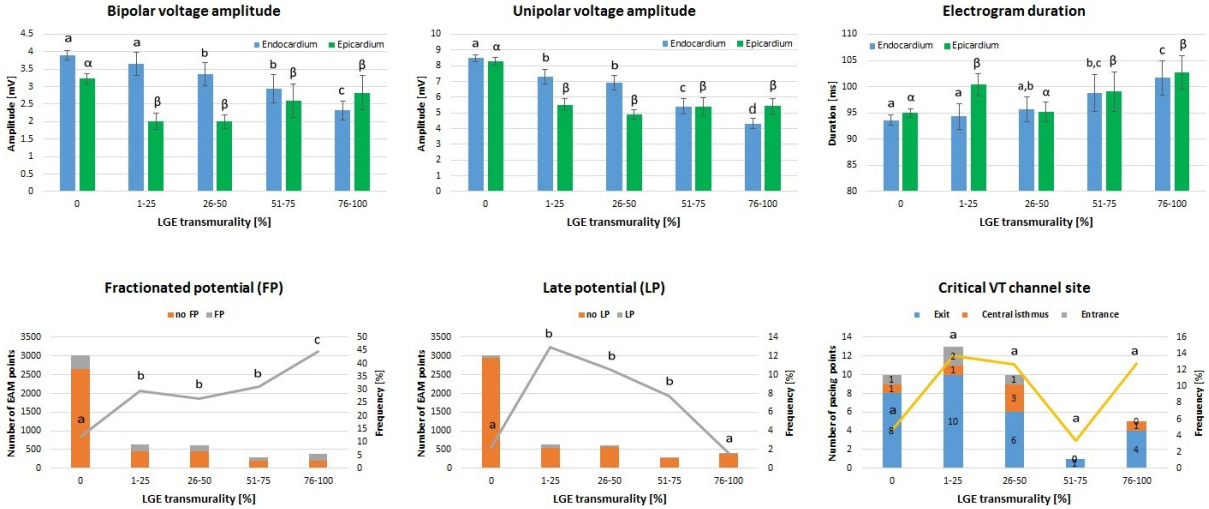

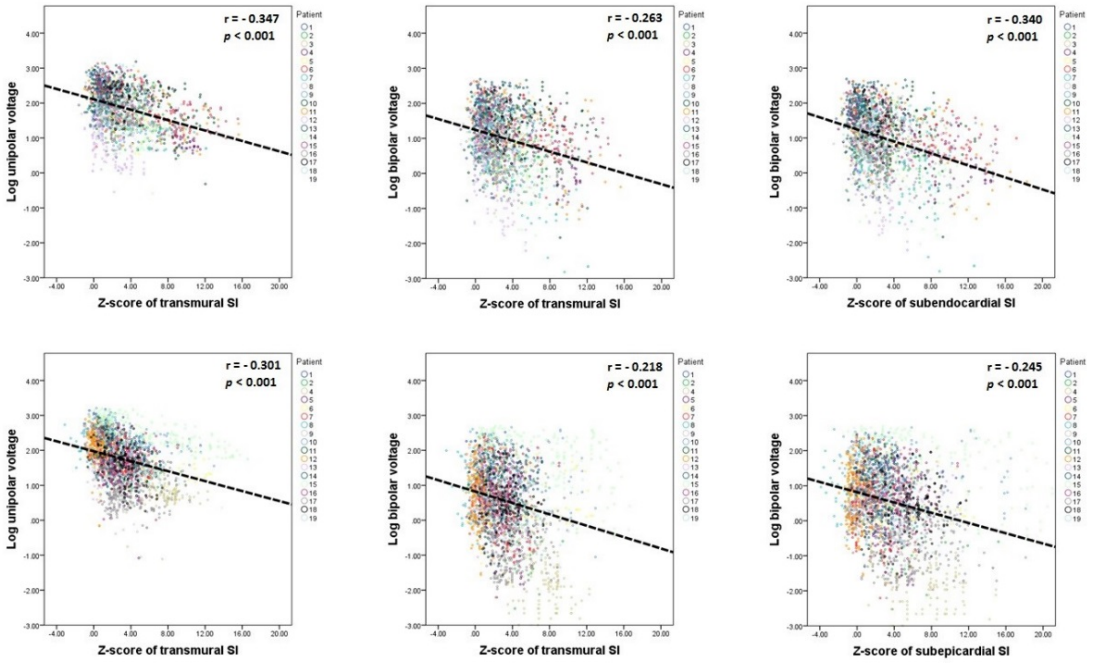

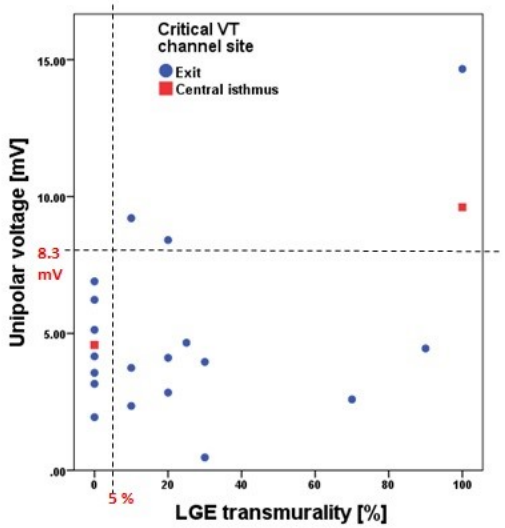

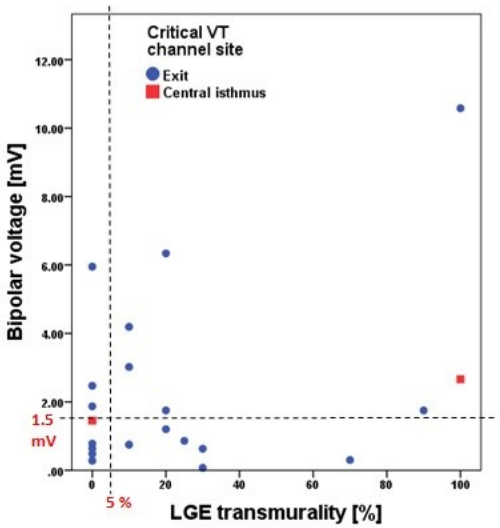

Jaeseok Park & Saman Nazarian et al. (submitted)

3D delayed-enhanced magnetic resonance sequences improve conducting channel delineation prior to ventricular tachycardia ablation

David Andreu[1], Jose T. Ortiz-Pérez[1], Juan Fernández-Armenta[1], Esther Guiu[1], Juan Acosta[1], Susanna Prat-González[1], Teresa M. De Caralt[2], Rosario J. Perea[2], César Garrido[2], Lluis Mont[1], Josep Brugada[1], and Antonio Berruezo[1]*

Table 2 Comparison between the three sequences studied

	2D-GRE	2D-SSFP	3D-GRE	2D-GRE vs. 2D-SSFP (*P* value)	2D-GRE vs. 3D-GRE (*P* value)	2D-SSFP vs. 3D-GRE (*P* value)
Myocardial fibrosis mass (g)	16.70 ± 10.89	17.65 ± 10.70	17.18 ± 9.32	$P = 0.168$	$P = 0.689$	$P = 0.641$
Core mass (g)	7.48 ± 6.68	8.26 ± 5.69	6.26 ± 4.37	$P = 0.280$	$P = 0.522$	$P = 0.007$
BZ mass (g)	9.22 ± 5.97	9.39 ± 6.33	10.92 ± 5.98	$P = 0.815$	$P = 0.028$	$P = 0.040$
Acquisition time (min)	11.64 ± 4.28	1.06 ± 0.64	16.43 ± 7.19	$P < 0.001$	$P = 0.008$	$P < 0.001$
Segmentation and processing time (min)	1.85 ± 0.38	1.70 ± 0.42	9.01 ± 2.83	$P = 0.002$	$P < 0.001$	$P < 0.001$

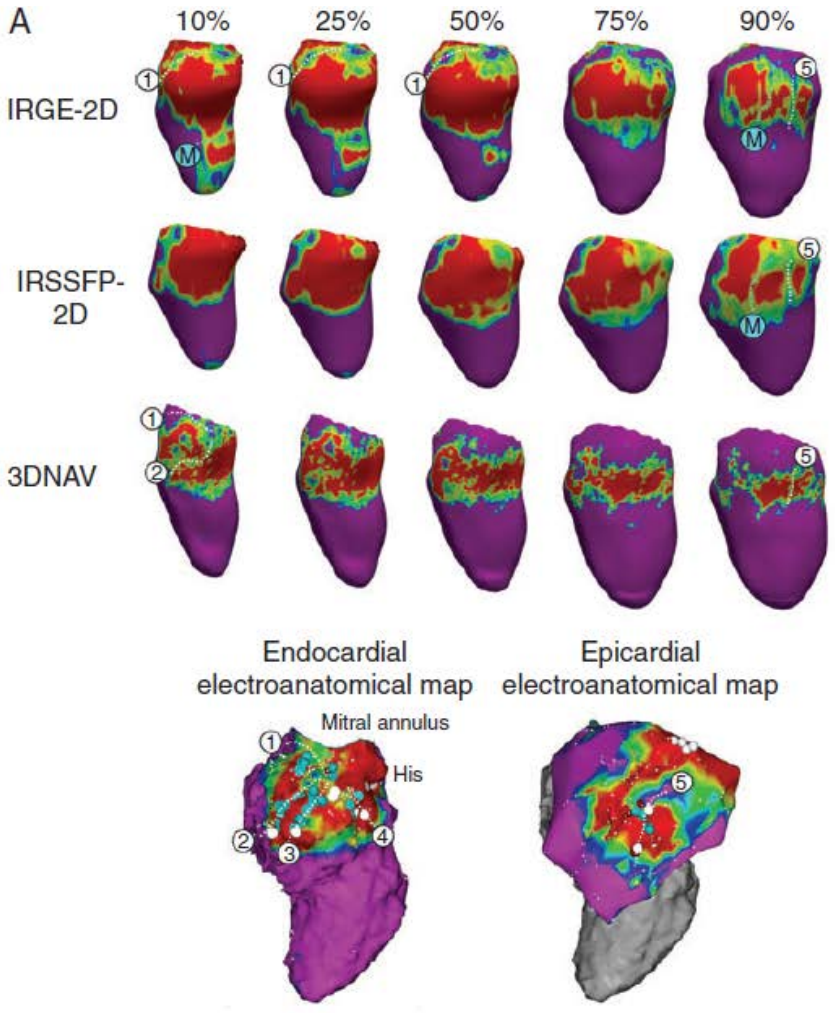

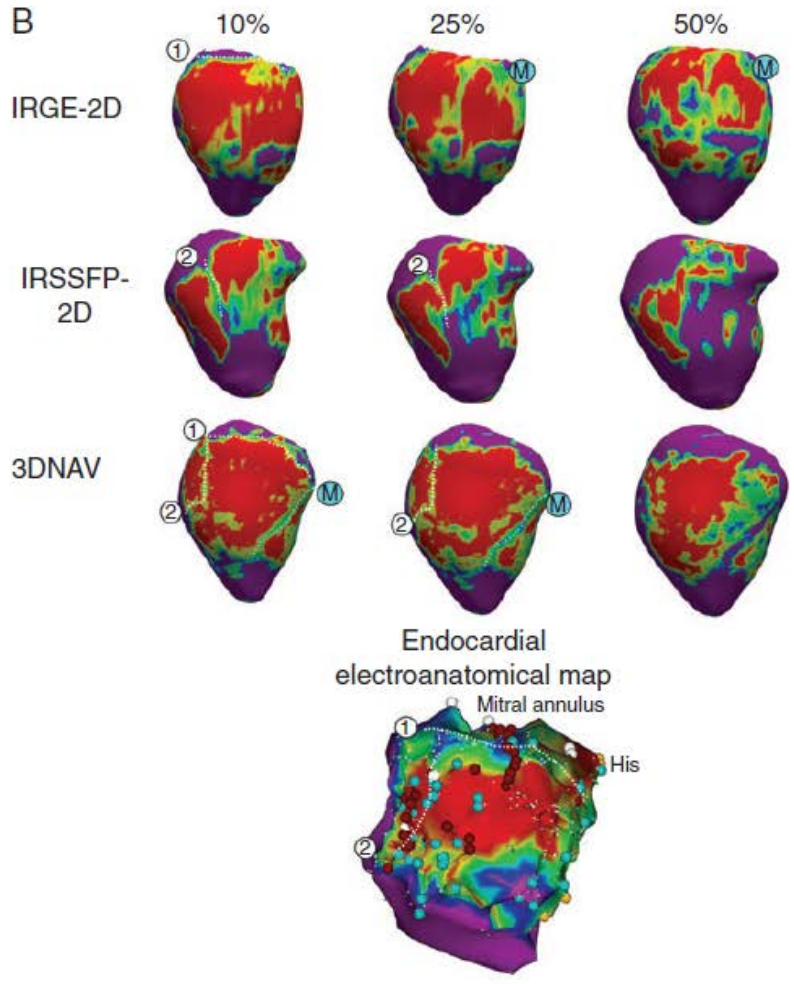

Andreu et al. Europace. 2015;17:938-945

Integration of Merged Delayed-Enhanced Magnetic Resonance Imaging and Multidetector Computed Tomography for the Guidance of Ventricular Tachycardia Ablation: A Pilot Study

HUBERT COCHET, M.D.,*,‡ YUKI KOMATSU, M.D.,†,‡ FREDERIC SACHER, M.D.,†,‡ AMIR SHERWAN JADIDI, M.D.,†,‡ DANIEL SCHERR, M.D.,†,‡ MATTHIEU RIFFAUD, M.D.,* NICOLAS DERVAL, M.D.,†,‡ ASHOK SHAH, M.D.,†,‡ LAURENT ROTEN, M.D,†,‡ PATRIZIO PASCALE, M.D.,†,‡ JATIN RELAN, PH.D.,§ MAXIME SERMESANT, PH.D.,§ NICHOLAS AYACHE, PH.D.,§ MICHEL MONTAUDON, M.D., PH.D.,*,‡ FRANÇOIS LAURENT, M.D.,*,‡ MÉLÈZE HOCINI, M.D.,†,‡ MICHEL HAÏSSAGUERRE, M.D.,†, and PIERRE JAÏS, M.D., PH.D.†,‡

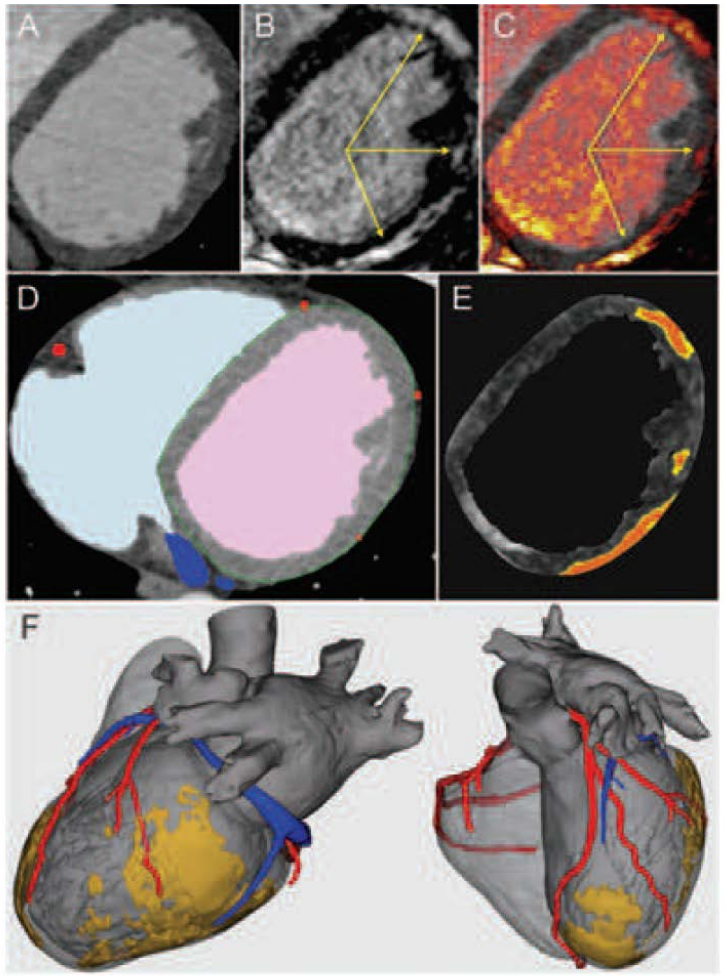

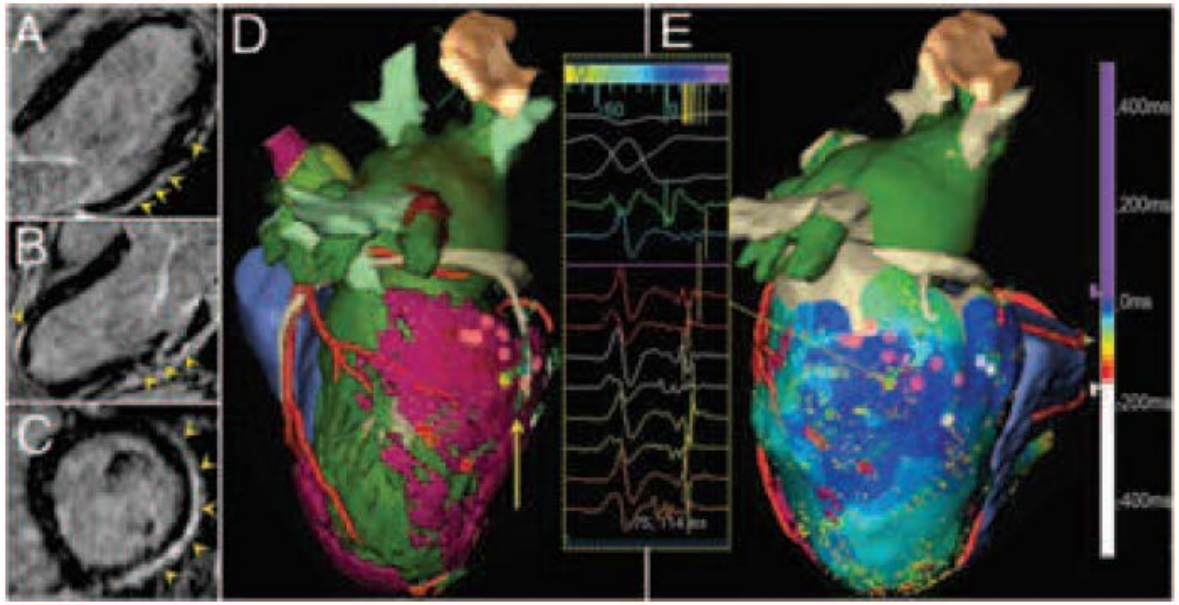

TABLE 3

Distribution of LAVA According to Substrate at Imaging

Patient	Aetiology	No. of LAVA Sites	Low Voltage	MR scarw + GZ	CT Thinning	Any Substrate at Imaging
1	ICM	86	80 (93%)	81 (94%)	72 (84%)	81 (94%)
2	ICM	24	24 (100%)	24 (100%)	19 (79%)	24 (100%)
3	ICM	16	14 (87%)	16 (100%)	11 (69%)	16 (100%)
4	NICM	40	36 (90%)	–	25 (63%)	25 (63%)
5	NICM	31	29 (93%)	26 (84%)	26 (84%)	26 (84%)
6	NICM	0	–	–	–	–
7	Myocarditis	34	28 (82%)	33 (97%)	–	33 (97%)
8	Myocarditis	35	24 (68%)	32 (92%)	–	32 (92%)
9	Idiopathic VT	0	–	–	–	–
	Total	266	235 / 266 (88 ± 10%)	212 / 226 (95 ± 6%)	153 / 197 (76 ± 9%)	237 / 266 (90 ± 13%)

Cochet et al. JCE. 2013;24:419-426

51 years old male: history of NICM, BiV ICD. Referred for recurrent VTs on amiodarone. Subendocardial scar in lat & inf walls between base-mid LV.

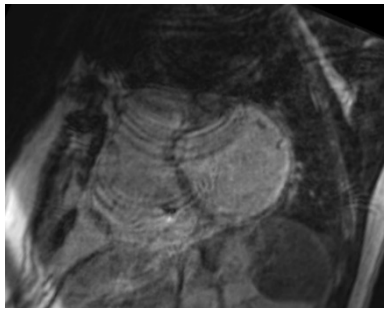

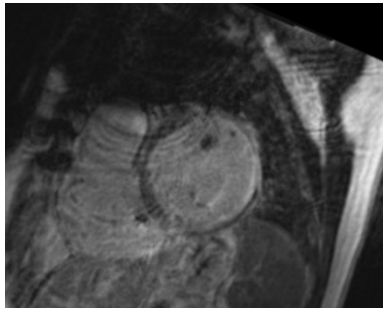

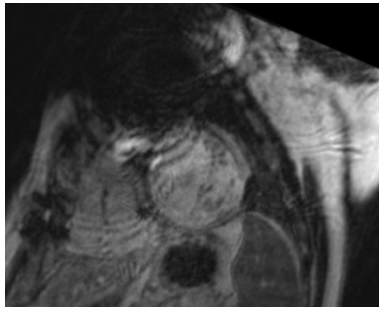

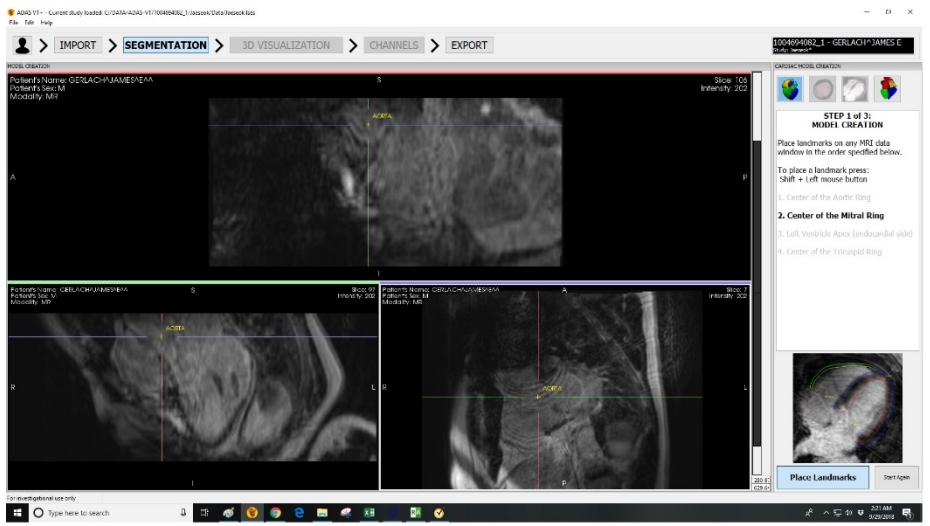

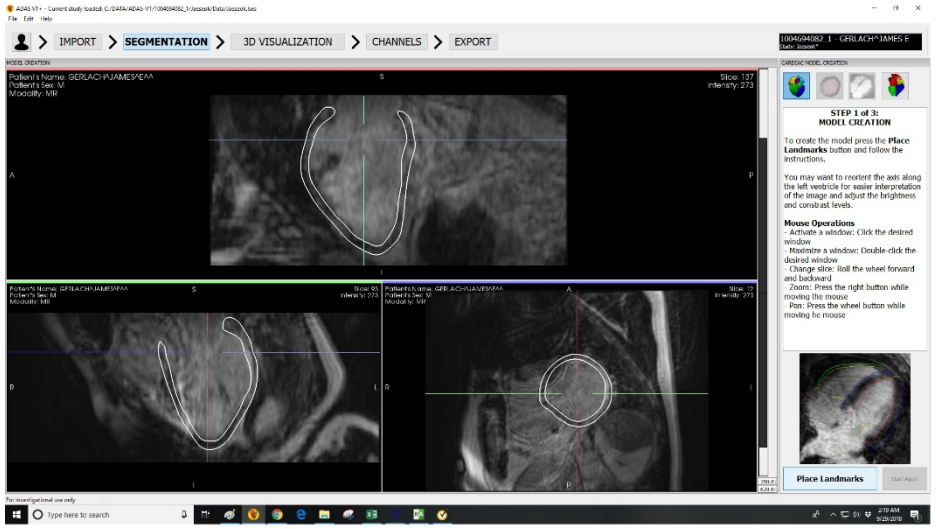

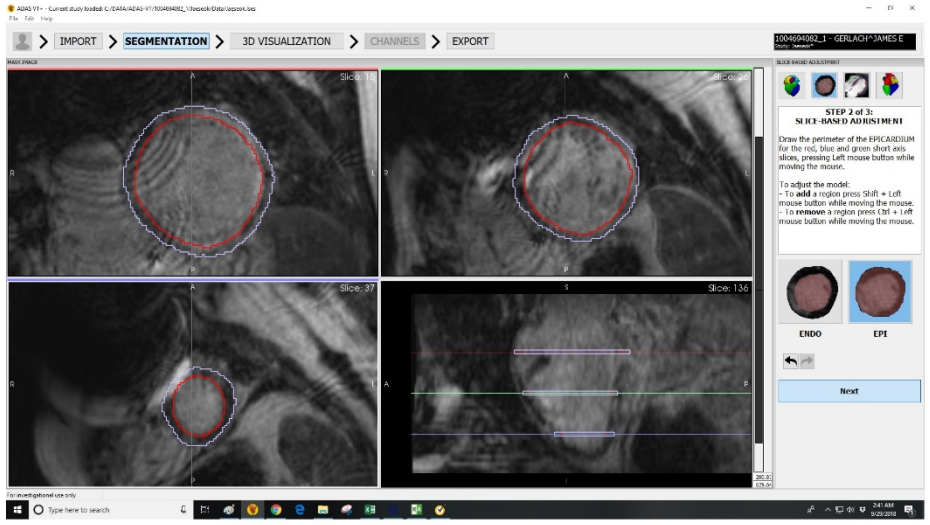

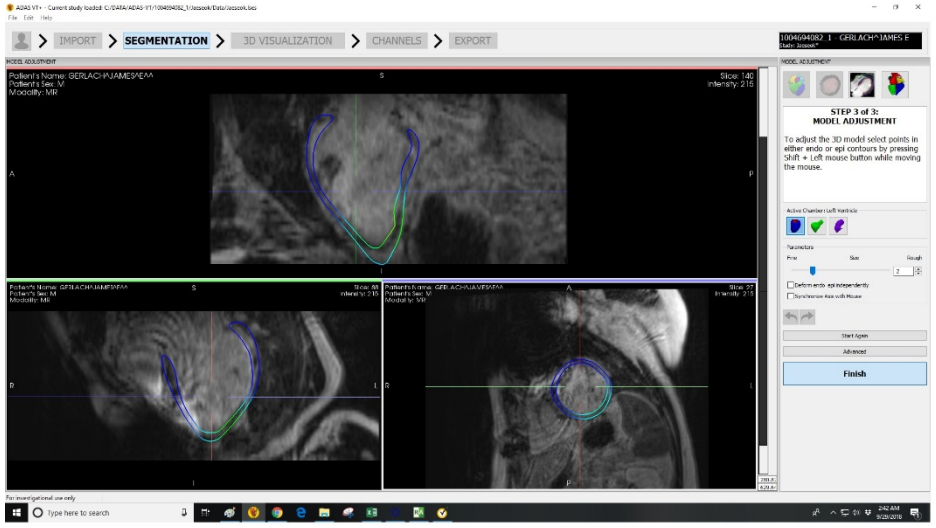

Courtesy of S. Nazarian

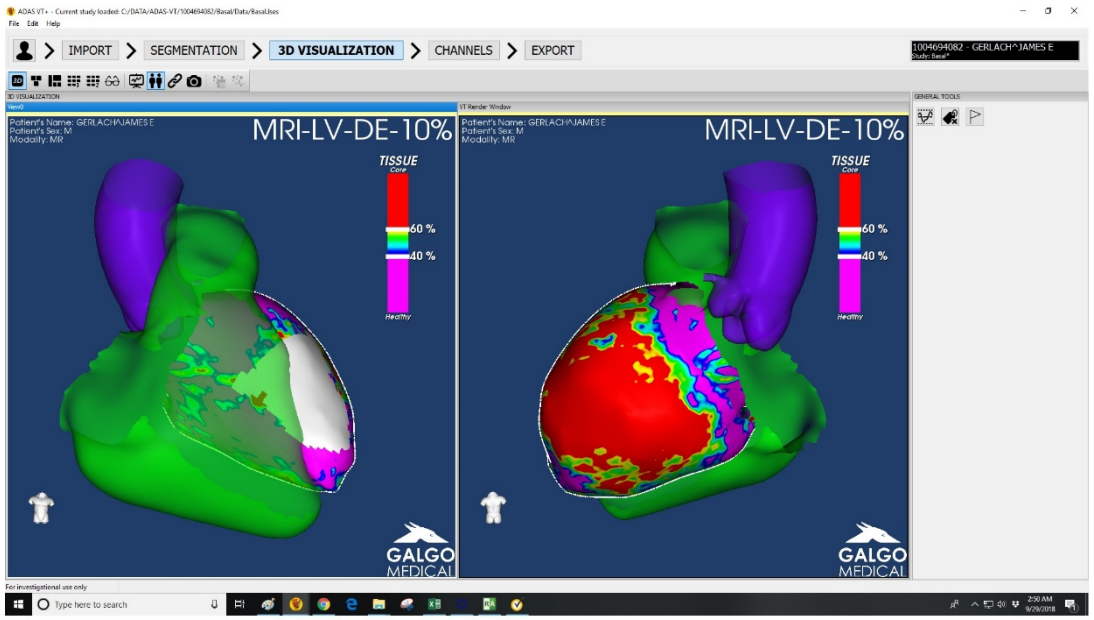

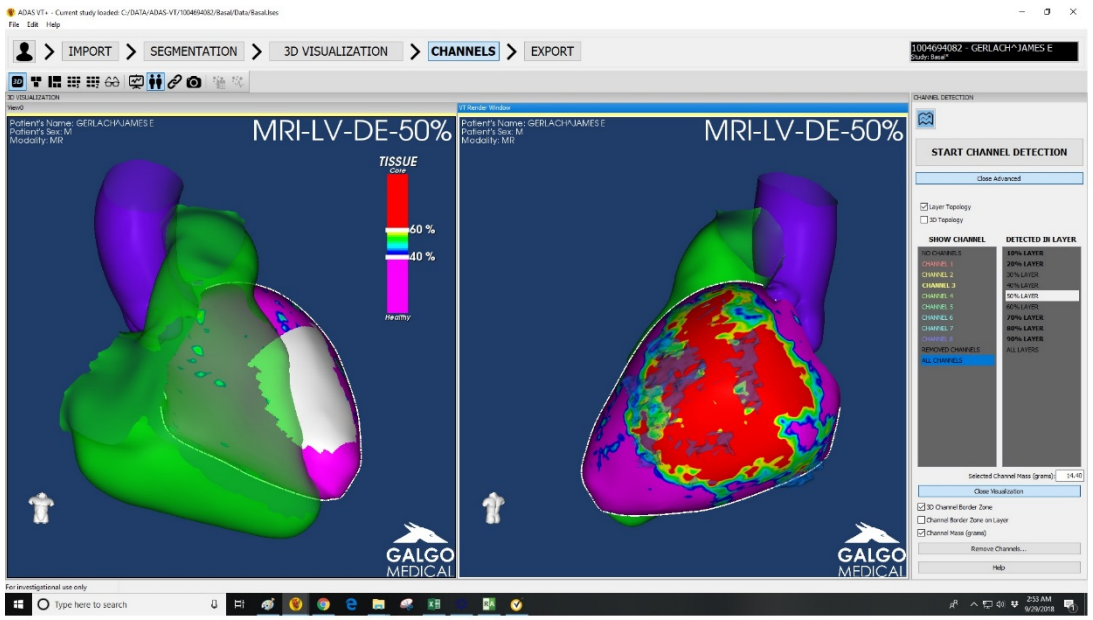

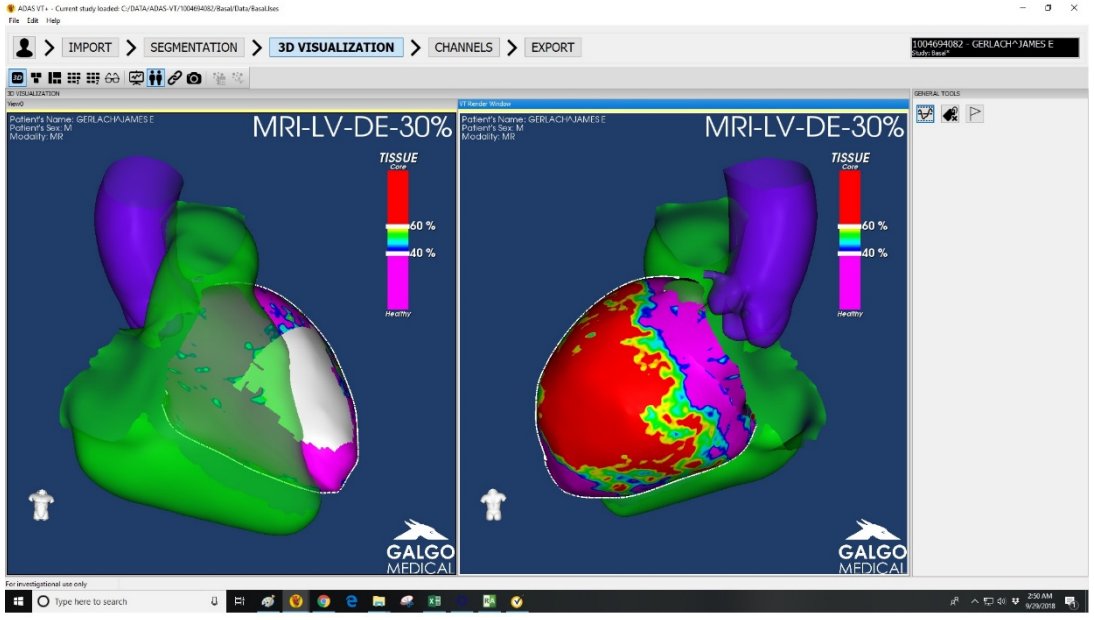

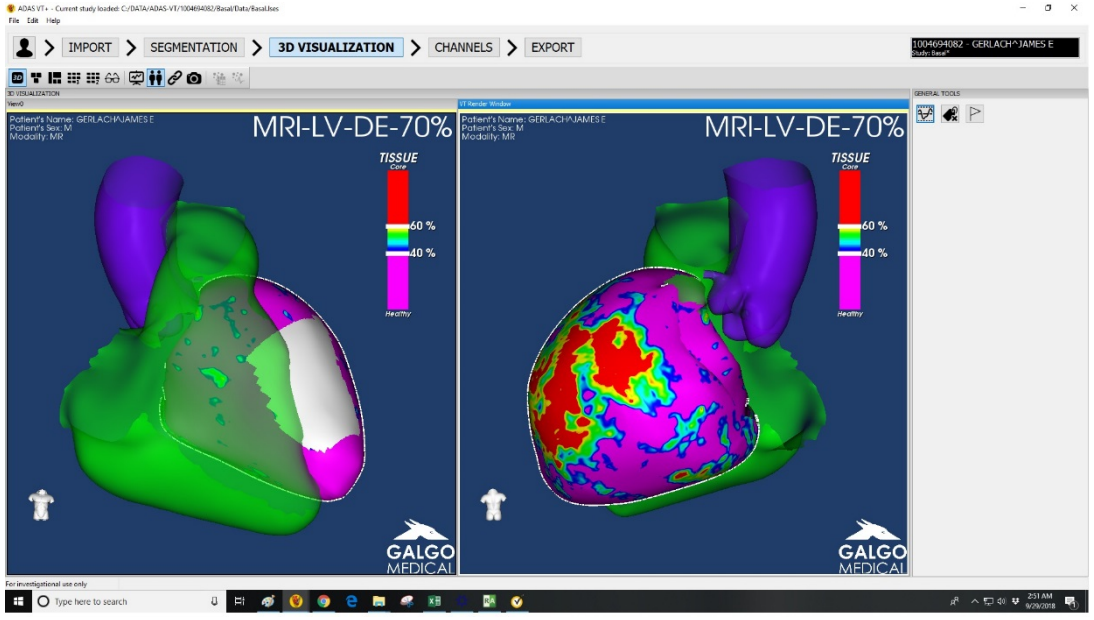

Courtesy of S. Nazarian

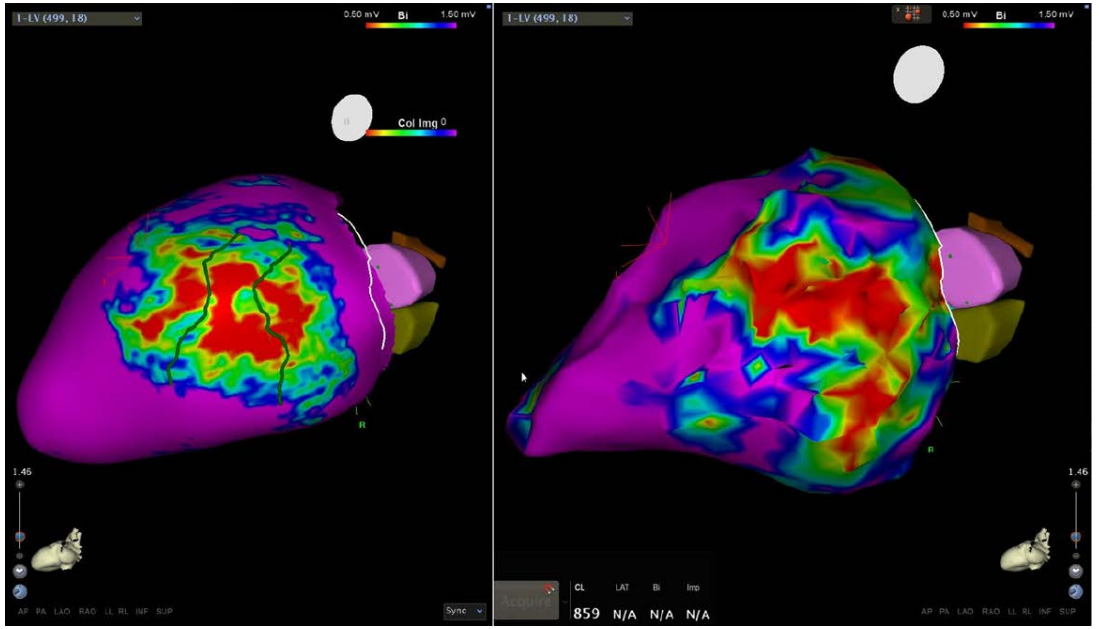

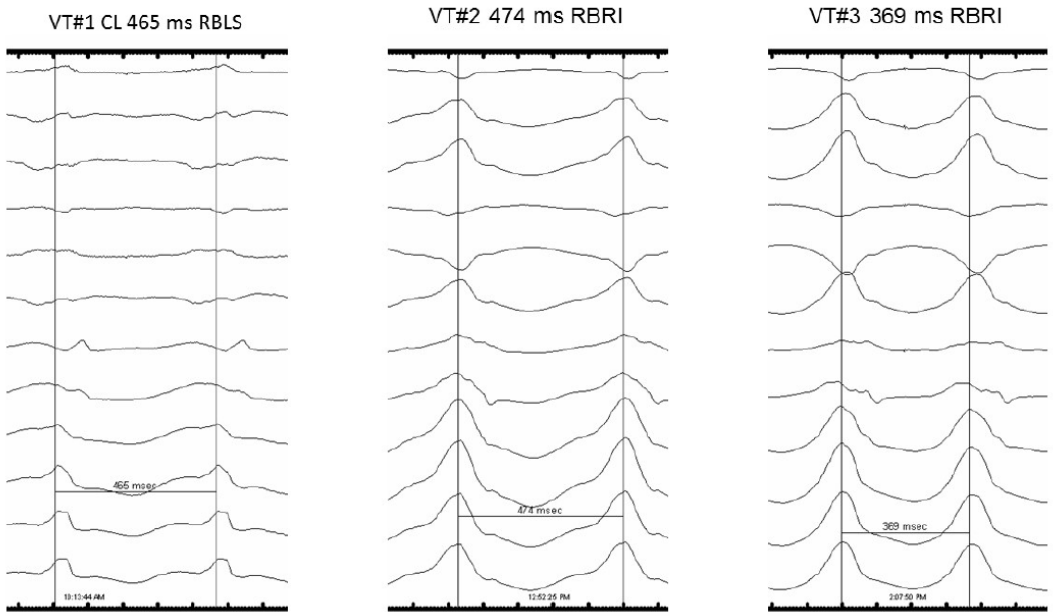

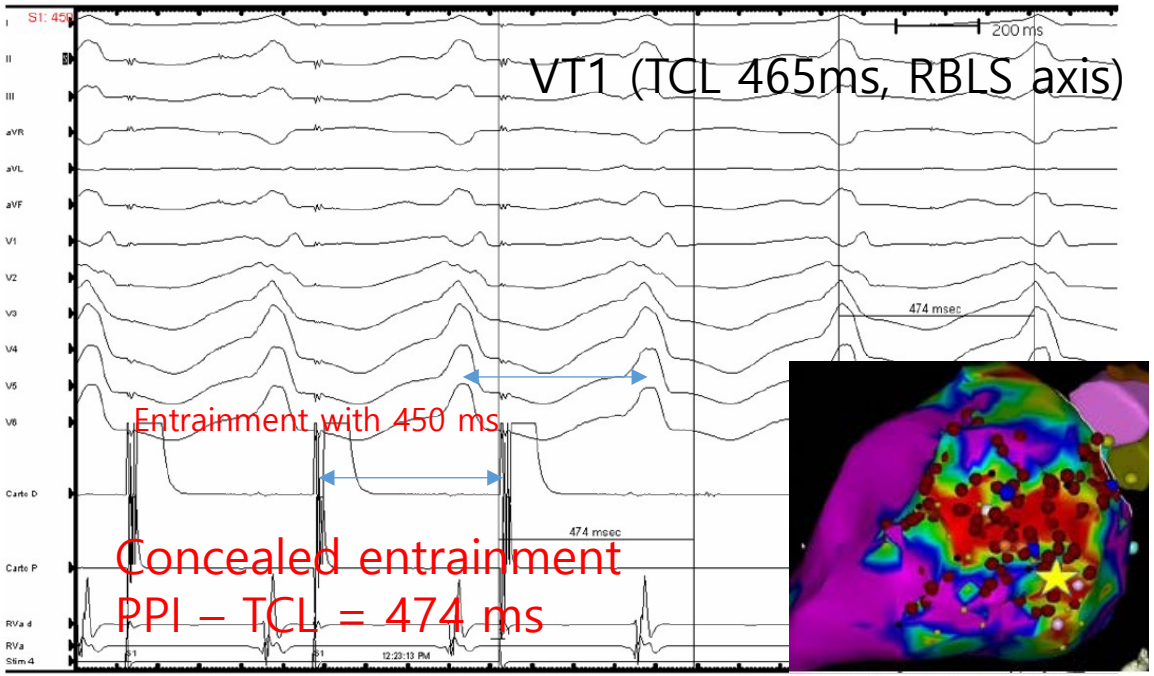

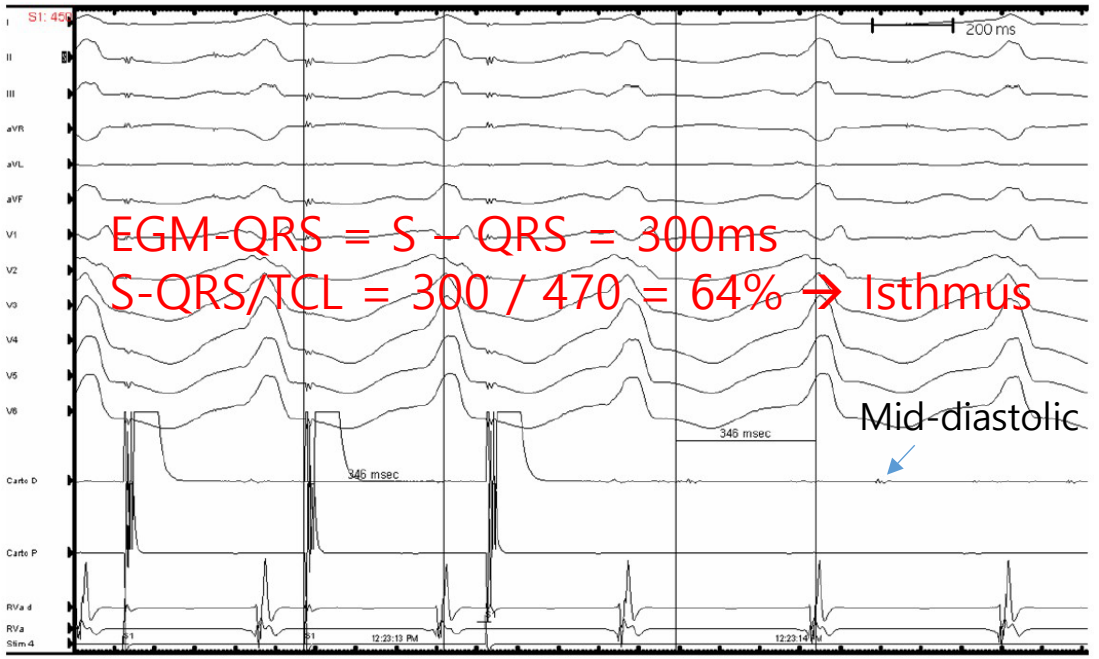

Courtesy of S. Nazarian

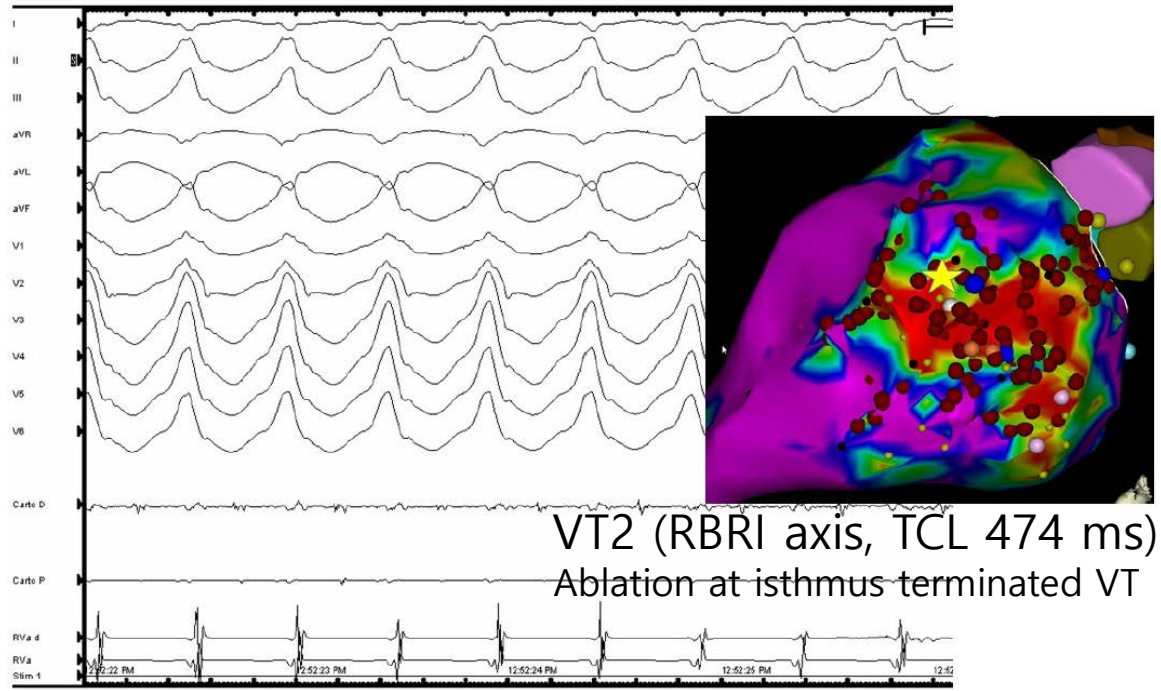

VT2 (RBRI axis, TCL 474 ms)

Ablation at isthmus terminated VT

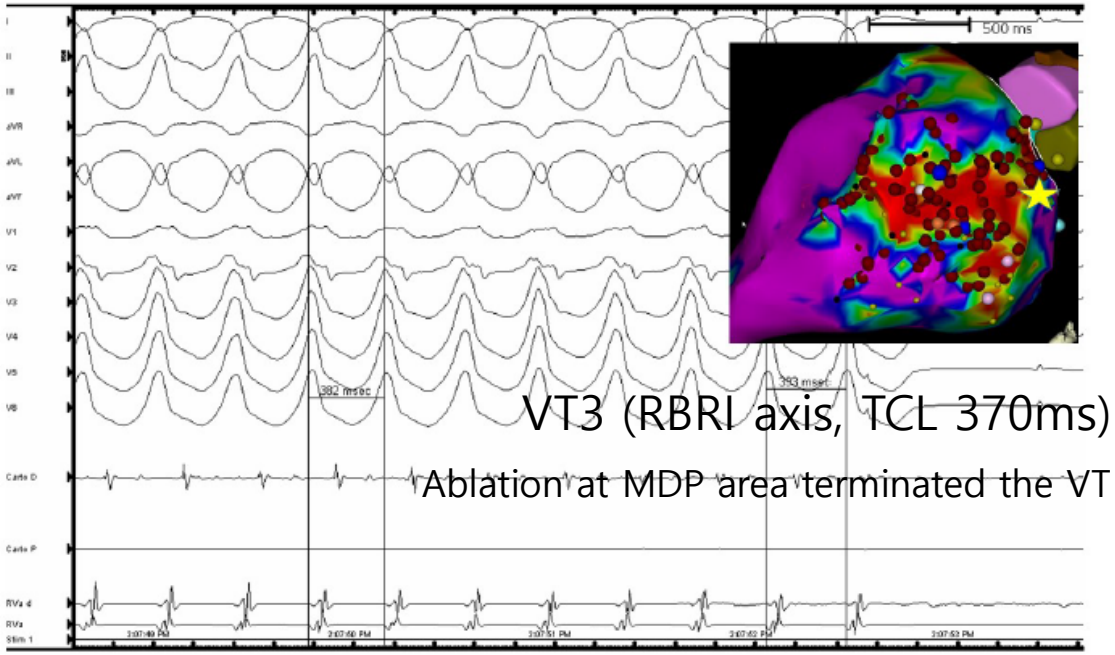

VT3 (RBRI axis, TCL 370ms)

Ablation at MDP area terminated the VT

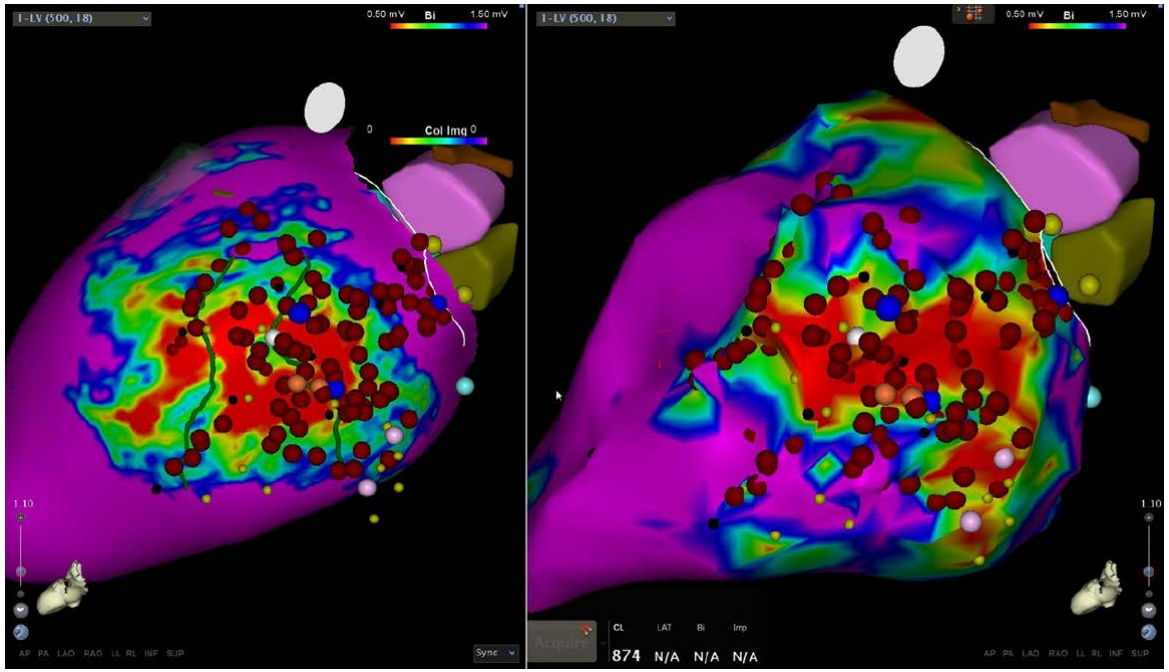

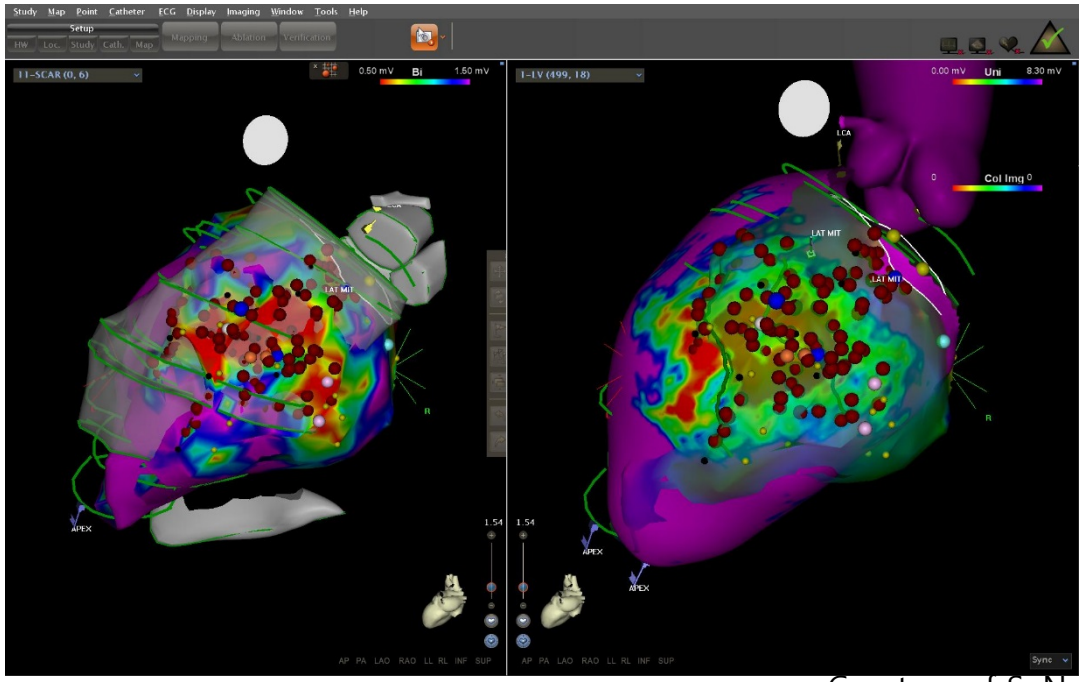

Courtesy of S. Nazarian

Association of regional epicardial RV electrogram voltage amplitude & LGE distribution on CMR in ARVC

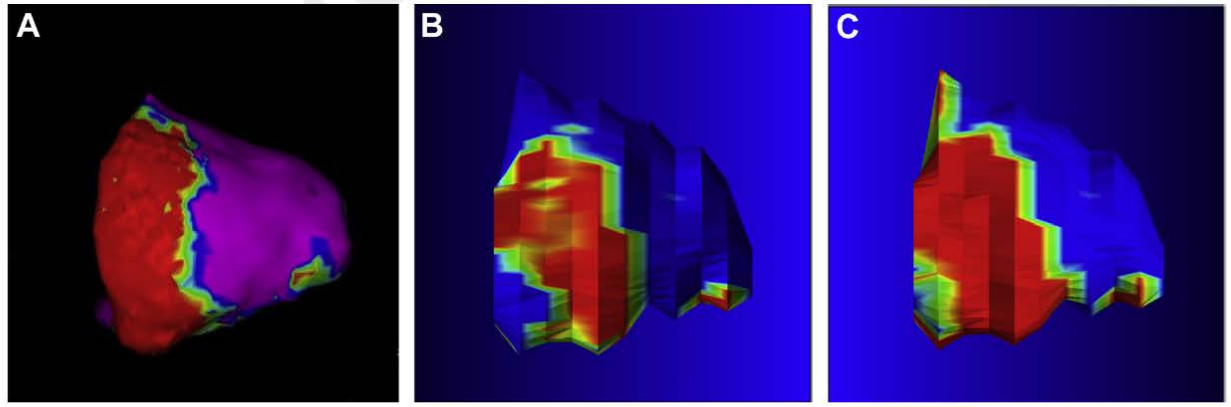

Figure 3 Comparison of bipolar electrogram map with image-predicted scar distribution. **A:** Bipolar electrogram map (0.5–1.0 mV). **B:** SI z-scores based data in the study. **C:** Commonly applied threshold of 6 SD > mean used for quantification of scar in NICM.

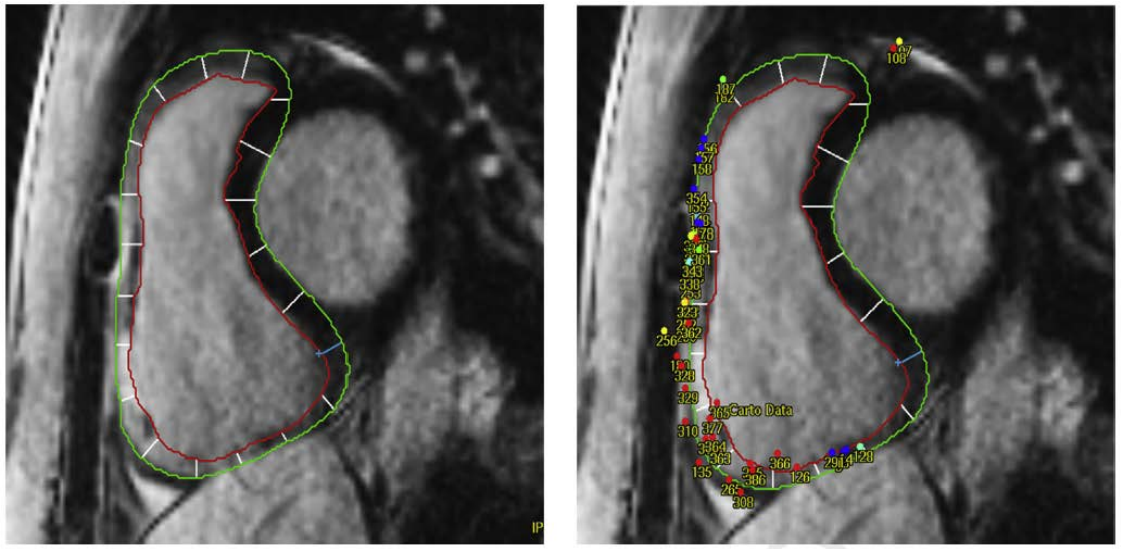

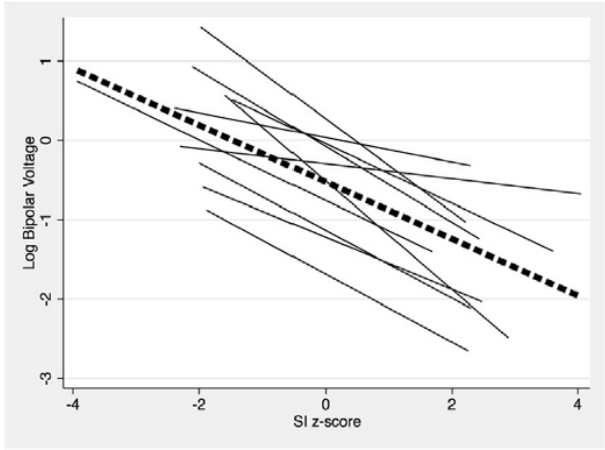

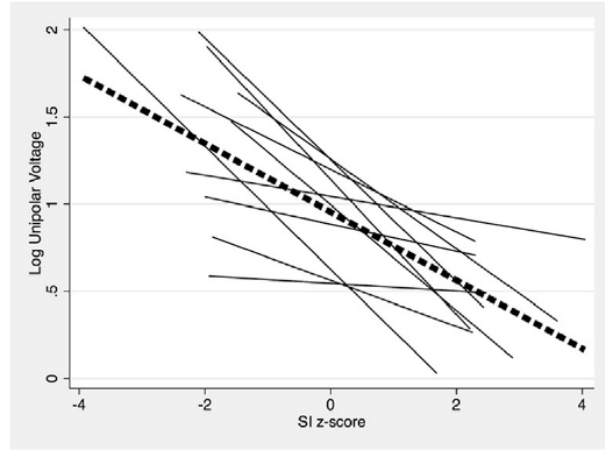

Shuanglun Xie & Saman Nazarian et al. Heart Rhythm 2018 (In Press)

73 years old male: referred for ablation of recurrent VT despite sotalol. Subendocardial scar in lateral & inferior walls between base-mid LV.

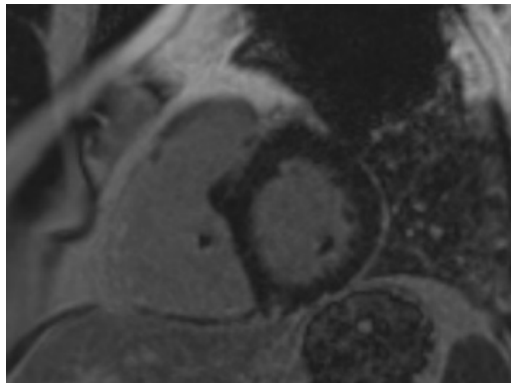

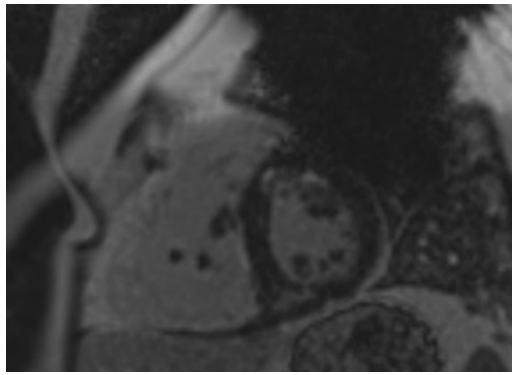

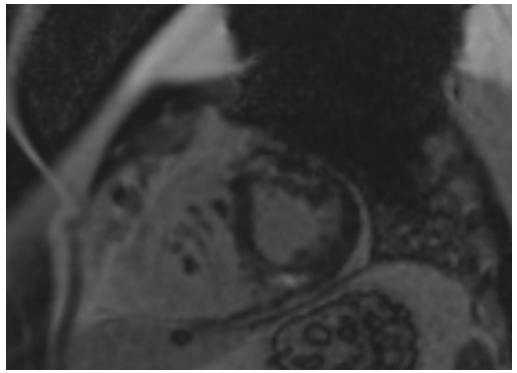

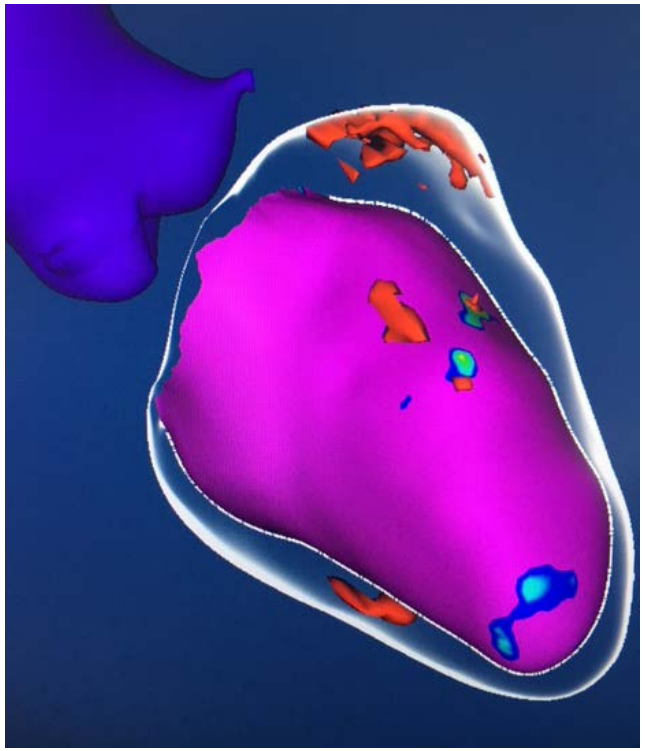

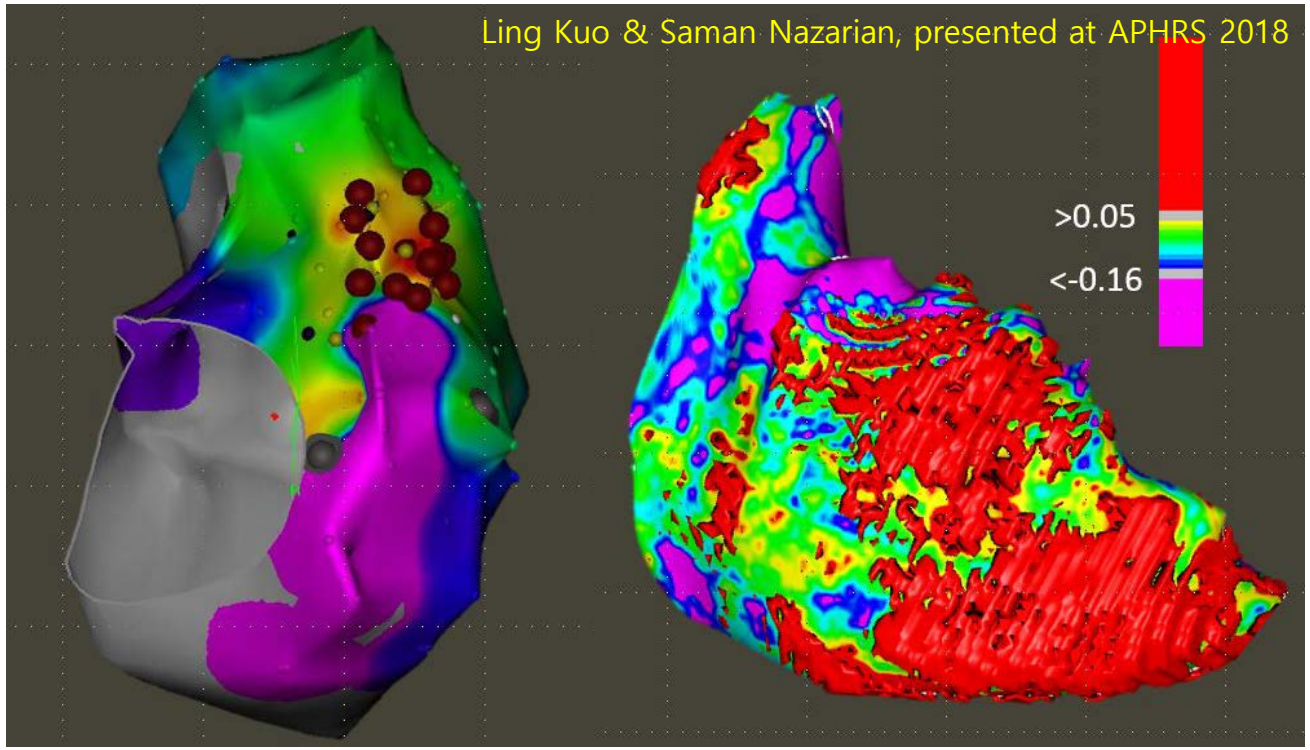

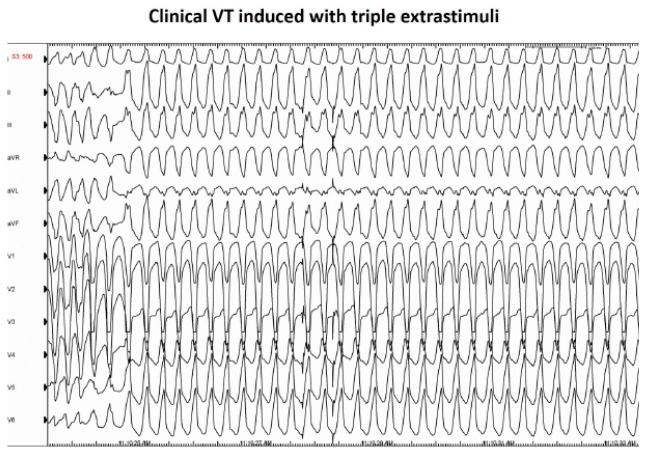

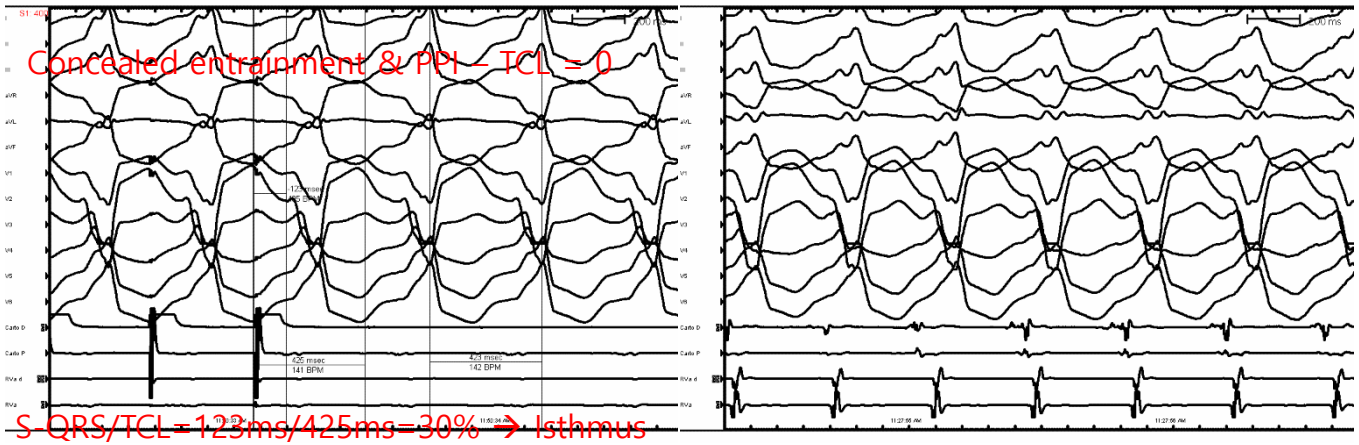

Standard Ablation Versus Magnetic Resonance Imaging–Guided Ablation in the Treatment of Ventricular Tachycardia

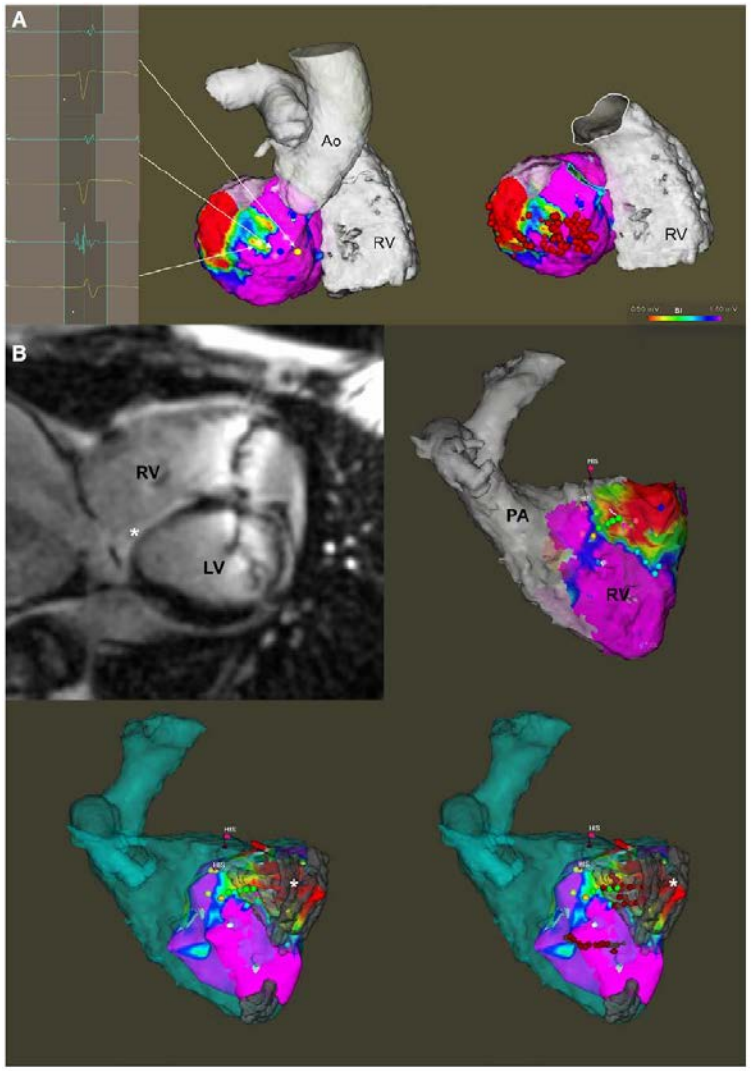

- In the scar integration group, all patients with inducible VTs had evidence of LGE on MRI, and ablation within or at the border of LGE sites terminated the VT.
- Procedural, fluoroscopy, and ablation times, as well as ablation burden, were similar in both study arms ($P>0.05$).
- Acute procedural success(clinical VT termination or non-inducibility) achieved in all patients.
- During median follow-up of 38.5 interquartile range (26–53) months, 16 (73%) patients had VT recurrence (7 in study group vs. 9 controls.
- After adjusting for age, sex, cardiac substrate, epicardial ablation, and LVEF, MRI-guided ablation was associated with reduced VT recurrence during follow-up (HR, 0.12; 95% confidence interval, 0.02–0.75; $P=0.023$).

Zghaib et al. Circ Arrhythm Electrophysiol 2018 Jan;11(1)

Take home messages

- LGE-CMR can detect and quantify myocardial scar tissue accurately.
- LGE-CMR can identify complex 3D scar structure including scar intramural location, scar transmurality, and scar heterogeneity.
- Conducting channels detected by LGE-CMR is useful in VT ablation.
- Integration of CMR-derived scar map with EAVM for VT ablation is feasible.
- LGE-CMR can provide supplementary substrate information for VT ablation.

Philadelphia, PA

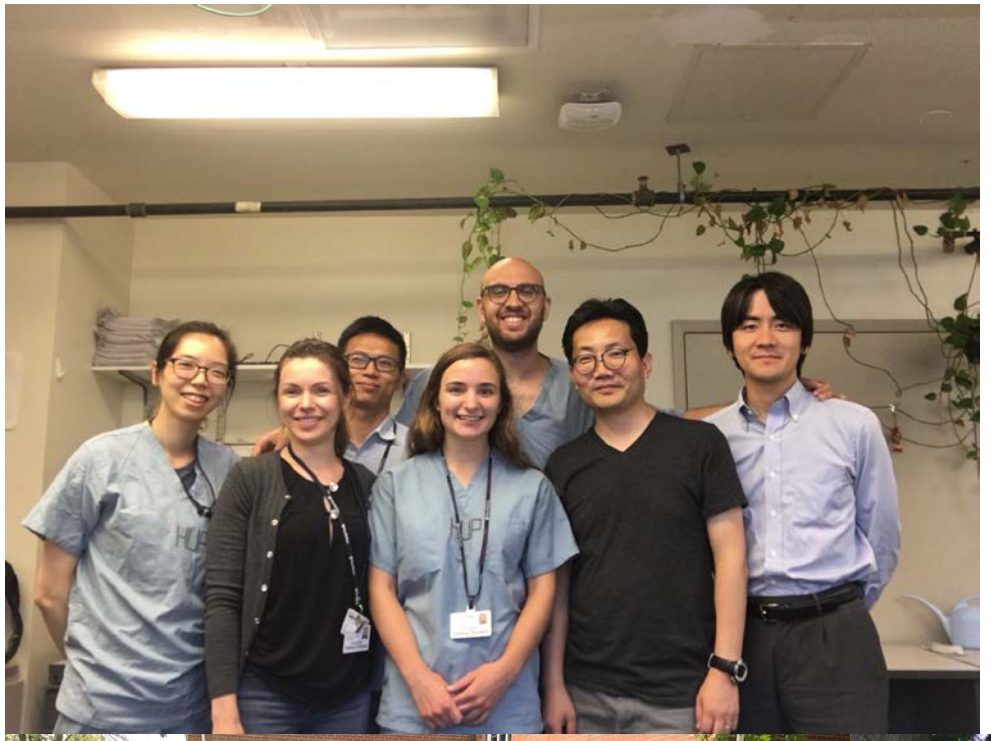

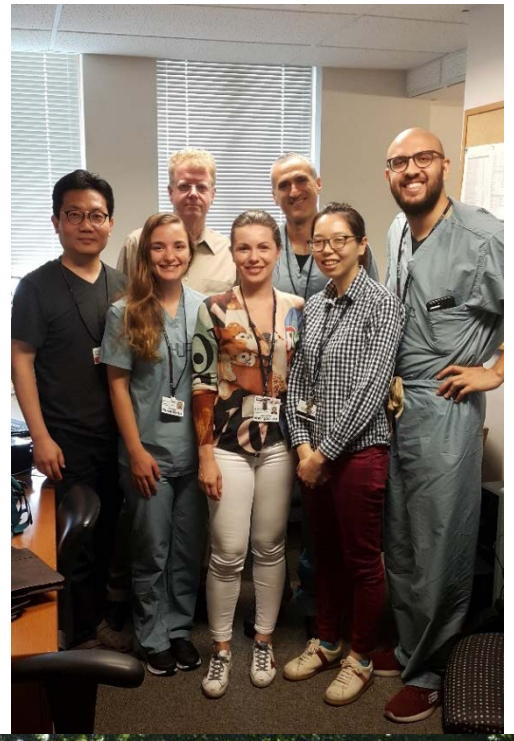


APHRS
2018

Cape May

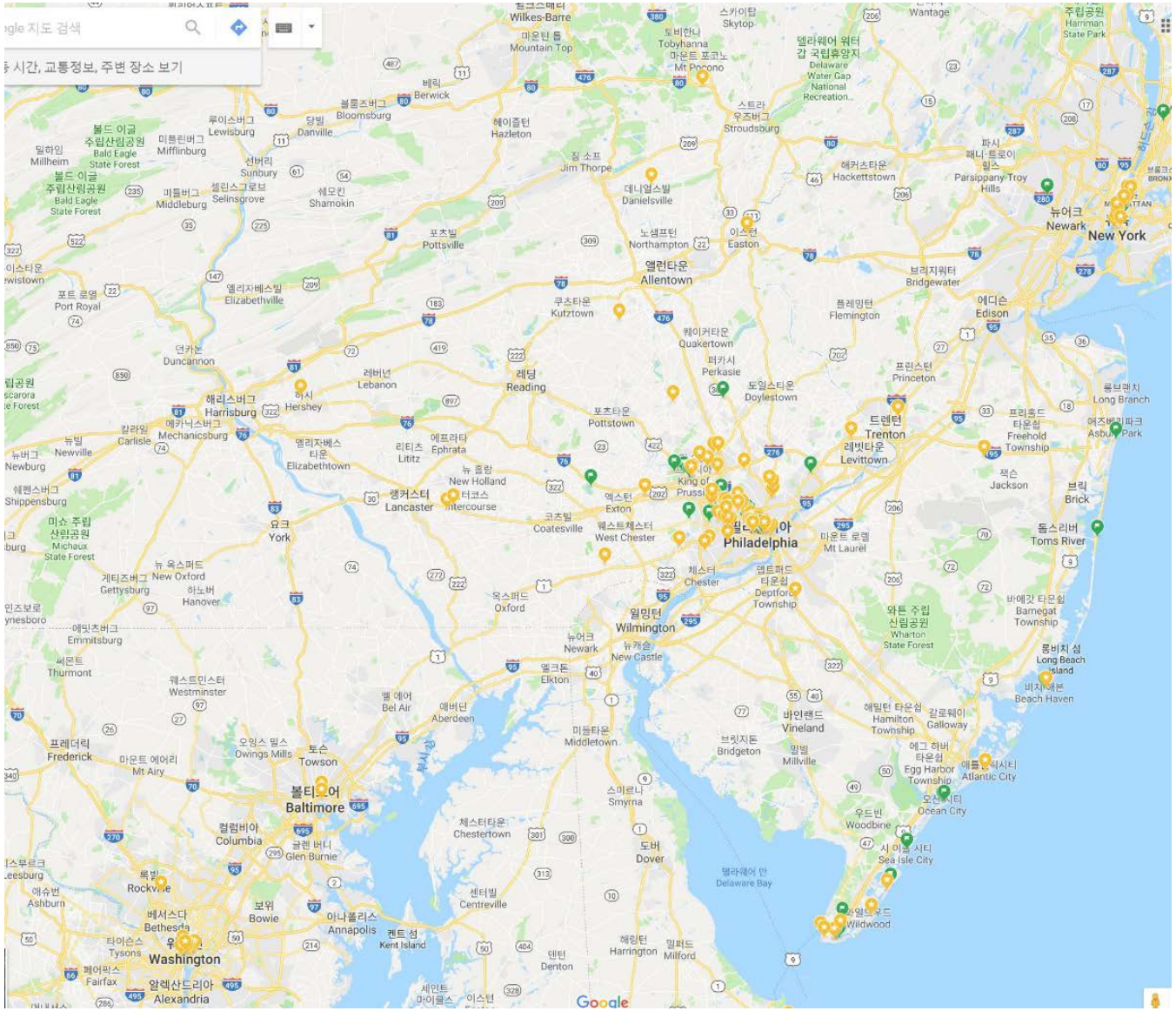
Philadelphia
Baltimore
Washington
Wilmington
Atlantic City
Ocean City
Wildwood
Cape May
Lancaster
Trenton
New York
Newark
Google


Concrete Ship
Cape May
Lighthouse
CAPE MAY POINT
STATE PARK


CAPE MAY


Thank you for
your attention
SE
JONG